CANADIAN THESES ON MICROFICHE

THESES CANADIENNES SUR MICROFICHE

I.S.B.N.

National Library of Canada
Collections Development Branch

Canadian Theses on
Microfiche Service

Ottawa, Canada
K1A 0N4

Bibliothèque nationale du Canada
Direction du développement des collections

Service des thèses canadiennes
sur microfiche

NOTICE

The quality of this microfiche is heavily dependent upon the quality of the original thesis submitted for microfilming. Every effort has been made to ensure the highest quality of reproduction possible.

If pages are missing, contact the university which granted the degree.

Some pages may have indistinct print especially if the original pages were typed with a poor typewriter ribbon or if the university sent us a poor photocopy.

Previously copyrighted materials (journal articles, published tests, etc.) are not filmed.

Reproduction in full or in part of this film is governed by the Canadian Copyright Act, R.S.C. 1970, c. C-30. Please read the authorization forms which accompany this thesis.

THIS DISSERTATION
HAS BEEN MICROFILMED
EXACTLY AS RECEIVED

AVIS

La qualité de cette microfiche dépend grandement de la qualité de la thèse soumise au microfilmage. Nous avons tout fait pour assurer une qualité supérieure de reproduction.

S'il manque des pages, veuillez communiquer avec l'université qui a conféré le grade.

La qualité d'impression de certaines pages peut laisser à désirer, surtout si les pages originales ont été dactylographiées à l'aide d'un ruban usé ou si l'université nous a fait parvenir une photocopie de mauvaise qualité.

Les documents qui font déjà l'objet d'un droit d'auteur (articles de revue, examens publiés, etc.) ne sont pas microfilmés.

La reproduction, même partielle, de ce microfilm est soumise à la Loi canadienne sur le droit d'auteur, SRC 1970, c. C-30. Veuillez prendre connaissance des formules d'autorisation qui accompagnent cette thèse.

LA THÈSE A ÉTÉ
MICROFILMÉE TELLE QUE
NOUS L'AVONS REÇUE

NL-339 (r. 82/08)

Canada

DISPROPORTIONATION OF PROPYLENE OVER TUNGSTEN OXIDE CATALYST

by

Jamal Adli Anabtawi

A thesis submitted to the School of Graduate Studies in partial fulfillment of the requirements for the Ph.D. degree in Chemical Engineering

UNIVERSITY OF OTTAWA
OTTAWA, CANADA, 1981

ACKNOWLEDGEMENTS

The author wishes to express his sincere appreciation and gratitude to Dr. R.S. Mann, who directed this research, for his patience and encouragement throughout the course of this investigation and his help in the preparation of this thesis.

The author is much indebted to Dr. F.D.F. Talbot, for providing the facilities of the department for this research and other members of the teaching staff of the department for their valuable discussions and suggestions, to Mr. G. Gasperetti for his technical assistance and to acknowledge Dr. K.C. Khulbe for helpful discussions during the course of this investigation.

Finally, the author would like to thank his wife, Rafia, for her patience and encouragement throughout this investigation.

TABLE OF CONTENTS

Page

Page

LIST OF TABLES

LIST OF FIGURES

ABSTRACT

The vapor phase disproportionation of propylene was studied over tungsten oxide catalyst in an isothermal integral flow reactor at 4.403 atm between 140 to 490°C and space time (W/F) 7.88 g.cat-hr/g.mol. The effect of the supporting material, tungsten oxide concentration and activation procedure, oxide catalyst for propylene disproportionation activity was studied. A catalyst containing 10 wt% WO_3/γ- Alumina was found to be most active.

It was suggested that WO_3/silica-alumina consists of two types of active sites. One site is active at lower temperatures (≈160°C) and the other one at higher temperatures (≈350°C). The different supports were shown to have a pronounced effect on the activity and selectivity of the catalyst. A 10 wt% WO_3 supported on γ-alumina was active at temperatures 230°C lower than that supported on silica gel. It was observed that the conversion of propylene increased with the increase in the concentration of tungsten oxide on γ- alumina. The active phase of the catalyst for the disproportionation reaction was found to be $Al_2(WO_4)_3$.

The kinetics of propylene disproportionation over a 10 wt% WO_3/γ-alumina was investigated in the temperature range 180-300°C and pressures between 3.041 to 7.124 atm. The effect of various process variables, namely reaction temperature, initial pressure of propylene and the product distribution was determined.

The products and reactants were analyzed by gas chromatography.

While the conversion of propylene increased with increase in reaction temperature and W/F ratio, selectivity decreased due to isomerization of 2-butene to 1-butene.

Out of the several mechanisms proposed for the disproportionation of propylene over WO_3/γ-alumina catalyst, the experimental data was well correlated by assuming that a Langmuir-Hinshelwood, dual-site surface reaction was the rate controlling step in the reaction mechanism. The rate of reaction is given by the following expression

$$r = \frac{k\,(P_p^2 - P_E\,P_B\,/\,K)}{(1 + K_pP_p + K_EP_E + K_BP_B)^2}$$

The mechanism parameters and their temperature dependence were calculated from the experimental data using a non-linear least-squares technique. An apparent activation energy of 5.06 kcal/mol was obtained over a 10 wt % WO_3/γ-alumina catalyst. The present data supports the four-center mechanism and a quasi-cyclobutane intermediate.

I. INTRODUCTION

Heterogeneous catalytic reactions play an important role in today's chemical industry by providing new and efficient pathways for chemical syntheses which are economically attractive. Because of the ability of catalysts to significantly modify the economics of chemical syntheses, considerable amount of research activity has been directed towards discovering new catalysts or improving existing catalysts.

The demand for ethylene as a raw material in the chemical industry continues to increase at a rapid rate. However, as the production of ethylene increases so does the production of by-products such as propylene and butenes. While butenes continue to be in demand due to the growing elastomer industry and by gasoline producers, propylene threatens to remain surplus on a worldwide basis. Disproportionation reactions provide the basis for new petrochemical processes which can interconvert commodity olefins, e.g. propylene, into more useful products.

A commercial application of olefin disproportionation, called the Triolefin Process, has been used to convert propylene into ethylene and butene (1,2). Other applications of Triolefin process include : The synthesis of detergent-range linear olefins from

propylene (3,4), the incorporation of Triolefin process with naphtha cracking to increase ethylene and butadiene yield (5), and with olefin-paraffin alkylation to increase octane rating of gasoline (6). Laboratory development of the Triolefin process technology for synthesizing isoamylene, and intermediate in poly-isoprene production, was reported by Banks and Regier (7).

The commercial future of olefin disproportionation technology is strongly linked to the economics of the petrochemical industry and is highly sensitive to the relative costs of feedstocks and products. Currently the economics of many applications of disproportionation technology are only marginal. However, the decreasing supply of available feedstocks as well as any number of possible changes in the international chemical market place could rapidly alter this situation.

The commercial future of olefin disproportionation has attracted researchers in this field. In an extensive program, Heckelsberg et al. (8) produced a large list of disproportionation catalysts including transition metal oxides, carbonyls, and metal sulfides on various supports. The effect of various effects on catalyst activity and selectivity and temperature dependence were investigated. Several patents and some publications mention the disproportionation of olefins.

However, not much is mentioned by way of describing the catalysts used or the mechanism of reaction.

Much of the disproportionation data in the literature are for the conversion of propylene. This is because of the convenience of propylene as a test reactant for catalytic studies and because many of the commercial applications of disproportionation involve propylene feed. In the absence of catalyst, propylene disproportionation reaction is very difficult to proceed and requires very large activation energy. Propylene disproportionation catalysts lower this energy barrier and provide pathways for the reaction. The optimum catalyst for disproportionation should give high activity, selectivity, resistance to poisons and a stable activity.

Tungsten oxide catalysts on silica have been studied in detail. However, they show activity only at high temperature, exhibit an induction period (up to 24 hours) before reaching steady-state activity (37) and show interpahse mass transfer effects caused by a heterogeneous surface.

Studies have shown that tungsten oxide supported on alumina shows activity for disproportionation at 200-300°C lower than those supported on silica gel (45).

Tungsten oxide supported on-alumina was investigated

for its disproportionation activity for propylene. The effect of temperature, concentration of WO_3, initial pressure of propylene, and support material on the distribution of products, isomerization activity and selectivity were studied.

In order to adopt a process with optimum performance, it is desirable to have reliable kinetic expression for the main reaction as well as any important secondary reactions. Furthermore, kinetic studies aid the determination of the reaction mechanism, which can be the basis for suggested improvement of catalysts as well as add to the general knowledge of catalysis.

Since the kinetic study is a fair method of learning the characteristics of a reaction , the kinetics of the disproportionation of propylene over tungsten oxide supported on γ- alumina catalyst was studied to postulate a reaction mechanism and a rate equation. The properties of WO_3/γ-alumina were compared with other disproportionation catalysts for activity, selectivity, isomerization activity, active sites, mechanism and rate equation.

THE OBJECTIVES OF THE PRESENT WORK.

- To design and construct an apparatus to investigate the catalytic disproportionation of propylene under controlled condition (Pressures, temperature and space time)

- To calibrate analytical equipment (rotameters, pressure gauges, thermocouples and chromatograph)

- To study the effect of tungsten oxide content, support type and activation procedure for a tungsten oxide catalyst on the activity for propylene disproportionation and product distribution.

- To establish the reactor operating conditions to eliminate the effect of interphase and interparticle mass transfer in all subsequent experiments.

- To study the effect of process variables (P,T,W/F) on conversion and product distribution over a 10wt% $WO_3/\gamma\text{-}Al_2O_3$ catalyst.

- To establish a rate expression based upon the rate controlling mechanism step and postulate a reaction mechanism for the catalytic disproportionation of propylene which would satisfactorily represent the data.

II. LITERATURE SURVEY

A. Disproportionation of Olefins

The disproportion of propylene was first encountered by Schneider and Frolich (9) in 1931 during the non-catalytic pyrolysis of propylene at 725°C and 0.2 atm, when 48% of the reacting propylene disproportionated to ethylene and butenes. However, it was not until the discovery of heterogeneous and homogeneous catalysts, which can promote the reaction at much lower temperature and minimize side reactions, that the application of the disproportionation reaction could be considered.

Banks and Bailey (18) reported in 1964 that linear olefins could be catalytically converted with high selectivity into equimolar shorter and longer chains. The reaction described (18) was of the type:

$$2C_n H_{2n} \rightleftharpoons C_{(n-a)} H_{2(n-a)} + C_{(n+a)} H_{2(n+a)} \quad (2-1)$$

where $n \geq 3$ and $n-a \geq 2$, and was referred to by the authors as olefin disproportionation.

During the past two decades, olefin disproportionation has received increasing attention, including commercialization. The literature contains a large number of patents and publica-

tions related to the subject. The literature can be classified into the following:

1 - Reviews and catalogues on, and related to, this topic (4,10,11,12,13).

2 - Industrialization and new processes (1,2,14,15,16,17).

3 - Investigation of new catalysts and selectivity improvement (8,18-23).

4 - Study of mechanism of disproportionation (24-31).

5 - Study of kinetics of the reaction (31-39).

6 - Investigation of the structure and active sites (40-47).

The present review includes a summary of the published literature on heterogeneous catalysts for disproportionation of olefins. Emphasis is placed on the reaction kinetics, the effect of several variables on selectivity of these catalysts; the mechanism of reaction, evidence regarding the influence of the catalyst active sites on conversion and selectivity, and the break-in phenomena.

Some of the solid catalysts used for disproportionation reaction are those derived from oxides, carbonyls, or sulfides of molybdenum, tungsten or rhenium supported on a high surface area materials such as silica, alumina or phosphates. Generally, heterogeneous catalysts require activation before use. Many of

the metal oxide catalyst need to be heated in a stream of inert gas or dry air to temperatures of 600 °C. It is believed that the high temperatures cause chemical interaction between the oxide and support, and also desorb polar material which may poison the catalyst surface (16).

B. Several Effects on Activity and Selectivity of Disproportionation Catalysts

In a new catalytic process (18), linear olefins (three to eight carbon atoms) were converted to homologs of shorter and longer chains. The disproportionation reaction was observed first on catalysts containing molybdenum and tungsten hexacarbonyl on alumina. Conversion ranged from 10-60% for disproportionation of propylene, 1-butene, 1-pentene and hexene in a continuous flow system over $Mo(CO)_6/\gamma\text{-}Al_2O_3$ catalyst in a fixed bed reactor at 120°C and 21.4 atm. Tungsten hexacarbonyl on alumina showed lower activity than $Mo(CO)_6/\gamma\text{-}Al_2O_3$ under the same condition. Banks and Bailey (18) investigated the disproportionation of propylene over a commercial cobalt molybdate on alumina catalyst in a temperature range 93-299°C and 31.6 atm. The rates of conversion, double bond isomerization and product distribution were studied as a function of temperature. The effect of space velocity at 163°C and 31.6 atm with propylene-propane feed containing 60 and 99% propylene was investigated. Propylene conversion decreased with increase in

space velocity, while the presence of propane in the feed acted as a diluent.

The effect of molybdenum oxide content of an alumina supported catalyst in the range 0-13.2% has been studied (18). Propylene conversions were highest with 7-12% molybdena catalyst. The effect of temprature, space velocity and the presence of other olefin on disproportionation of propylene were also examined. Although this investigation was carried out in 1964, it explains the effect of several parameters on disproportionation of olefins. However, the study does not cover the mechanism of reaction or the active sites reponsible for the activity of the catalyst.

Heckelsberg et al. (16) have reported that tungsten oxide on silica catalyst apparently have more desirable properties for olefin disproportionation than do molybdena-alumina catalysts. They studied the effect of temperature, pressure, space velocity and the tungsten oxide concentration on propylene conversion over a catalyst containing tungsten oxide supported on silica has been carried out in an integral flow reactor. Conversion of propylene increased when the temperature increased from 232 to 377°C at 31.6 atm. Pressure had a similar effect on conversion in the range of 1 to 31.6 atm and at 260°C. The increase in space velocity from 20 to 80 WHSV decreased conversion levels from 45.5 to 41.8%

when carried out at 31.6 atm and 399°C. The effect of WO_3 concentration on conversion was studied in the range from 1 to 75% at 260°C, 31.6 atm and a space velocity of 40 WHSV. A catalyst containing 10% WO_3 supported on silica was most active. The investigation of Heckelsberg et al. (16) showed that air, water, acetone, carbon monoxide, and methanol in the feed act like temporary poisons. These compounds decreased catalytic activity of tungsten oxide, but on the introduction of pure feed the original activity was restored.

The disproportionation of propylene over molybdenum hexacarbonyl on several supports (SiO_2, Al_2O_3, SiO_2-Al_2O_3) has been investigated by Smith et al. (48) in a static system at 25°C and a pressure of 0.033 atm. The catalytic activity was found to depend markedly on the temperature of degasification and activation. The role of the support in the catalyst was found to be two fold, to disperse the molybdenum hexacarbonyl, and to assist oxidation of the molybdenum to form the active species. Maximum activity on any support was achieved when both of these conditions were optimized.

Bradshaw and his coworkers (25) studied the catalytic disproportionation of n-butenes on a commercial cobalt molybdate on γ-alumina over a temperature range 122 to 245°C and at atmospheric pressure. Much of this work was concerned with the

disproportionation of 1-butene and 2-butene. Using a feed of 1-butene, the expected products from disproportionation reaction were ethylene and 3-hexene. Their data showed a large percentage of propylene and n-pentenes. This was easily explained by the isomerization of 1-butene to 2-butene. Isomerization was found to take place on acidic active sites of the catalyst surface. The effect of space velocity and temperature on product distribution has been studied. The results of their investigation showed that by suitable choice of temperature and space velocity or by careful poisoning of the catalyst with sodium ions, the selectivity to certain pairs of olefin could be raised to a higher value. Bradshaw et al. (25) showed that disproportionation of olefins is accompanied by isomerization, which is the main route for the production of a wide spectum of by-products. Therefore, in order to have a good disproportionation catalyst the side reactions should be minimized by reducing the rate of isomerization.

The effect of addition of Tl,Na,K,Rb,and Cs to molybdenum oxide/γ-alumina on the selective disproportionation of olefins was investigated by Kobylinski and Swift (19). Disproportionation of 1-butene and 1-octene was carried out in a continuous flow system over a catalyst containing 13 wt% $MoO_3/\gamma\text{-}Al_2O_3$ at atmospheric pressure and temperature between 120-140^{o}C. The experimental data

showed that the addition of 2% thallium increased the selectivity of 1-butene to ethylene and 3-hexene from 22 to 81%. While the selectivity of 1-octene to ethylene and 7-tetradecene increased from 17.9 to 89%. The greatest percentage gain in the selectivity was obtained between 0.5 to 2.0% thallium to MoO_3 on alumina, however, the conversion declined linearly over the range studied. The effect of temperature on selectivity showed a decline with increasing temperature in the range from 120 to 260°C. The authors explained this decline with temperature to be due to higher activation energy for isomerization than for disproportionation. This was verified by the increase in the percentage of 2-butene in the recovered butenes from the disproportionation of 1-butene with increasing reaction temperature. Several metal ions were evaluated while attempting to improve selectivity over MoO_3/γ-alumina (19). However it was concluded that only thallium or Group Ia and IIa metals could improve selectivity.

In a subsequent paper, Kobylinski and Swift (20) investigated the effect of pretreating MoO_3/γ-Al_2O_3 with various olefins to enhance selective disproportionation of 1-octene. Treatment of a 10wt% MoO_3/γ-Al_2O_3 catalyst at temperatures from 195-235°C with olefins resulted in an increase in selectivity caused by deposition of a residue on the catalyst. It was proposed that this residue enhanced olefin disproportionation

selectivity by a similar mechanism proposed for a similar enhancement caused by adding a large polarizable cation such as K, Cs, Rb, and Tl to the catalyst.

The effect of pressure on the activity of a MoO_3/γ-Al_2O_3 catalyst for disproportionation of olefin was studied by Sadesawa et al. (49). The activity and selectivity for propylene disproportionation was studied in the pressure range from 1.033 to 134.32 atm. The selectivity to ethylene and butenes decreased while the amount of polymer formed over the catalyst increased with the reaction pressure. The authors concluded that degradation of the catalytic activity resulted from the polymer formed over the catalyst. They reported that the catalyst life of MoO_3/γ-Al_2O_3 was increased in the presence of solvents and that n- heptane was the most effective. This indicated that the catalyst surface was kept clean in the presence of solvents. However, the maximum conversion was not affected by the reaction pressure.

The disproportionation of propylene in the gas and liquid phases over a MoO_3/γ -Al_2O_3 catalyst was studied by Ogata and Kamiya (22). All experiments in the gas phase were carried out in a flow system with a fixed catalyst bed under atmospheric pressure and temperatures between 0 to 85°C. The product

distribution showed that larger amounts of ethylene than butene resulted during the initial period of reaction stream and a period of 9 hours was required until equal amounts came out. The authors reported that the catalyst activity decreased rapidly with reaction time and that the activity, selectivity and deactivation improved by utilizing regenerated catalysts. The selectivity to ethylene and butene decreased with temperature increase, which proved that the activation energy for double-bond shift was higher than that of disproportionation. The activation energy for propylene disproportionation was calculated as 5.0 kcal/mol over the temperature range from 0 to 50°C. Experimental results of the disproportionation of propylene over MoO_3/Al_2O_3 in the liquid phase showed the catalyst to be efficient at low temperature because of its selectivity and durability.

Sadesawa et al. (50) investigated the disproportionation of propylene in a fixed bed flow system over a MoO_3/SiO_2 catalyst treated with HCl and NH_4OH in the temperature range 350-600°C under atmospheric pressure. The activity of the catalyst extracted with NH_4OH remained constant for a long time since most MoO_3 was removed from the catalyst surface. This gave rise to an increase in the selectivity for disproportionation of propylene to ethylene and butene and decrease in selectivity for hydrogenation, isomerization and polymerization. The catalyst

showed a higher activity when treated with hydrogen than the one treated by nitrogen gas. The authors observed an increase in catalytic activity of molybdenum oxide catalyst with the oxidation state of molybdenum (V).

Carrier effects of supported molybdenum oxide catalyst on disproportionation of propylene have been investigated by Nakamura and Echigoya (51) at 150°C and 0.4 atm. Results showed that the activity increased in the following order:

$MoO_3/TiO_2 > MoO_3/Al_2O_3 > MoO_3/SiO_2 > MoO_3/MgO > MoO_3/ThO_2$

The activities of catalysts were correlated with ESR intensities of Mo^{+5} and the amount of CO adsorbed. A linear relationship between the adsorption of CO and activities was obtained. The relationship between the acidity of the carrier and the activity of MoO_3/Al_2O_3 was explained by assuming that propylene was adsorbed on these acidic centers of alumina and reduced the catalyst to produce new active centers. However, the acidic sites were not the active centers for disproportionation and do not participate in the reaction.

Yamaguchi et al. (52) investigated the isomerization of 1-butene and cyclopropane and the disproportionation of 1-butene, propylene and ethylene over tungsten oxide on different supports. The reactions were carried out by using a closed recirculation system at 100°C and under 0.132 atm. Variation of WO_3 content in

a TiO_2 supported catalyst showed that a 5 mol % content of WO_3 increased the activity for isomerization of 1-butene and the formation of isobutene from propylene. The order of activity for various supported catalyst for disproportionation of propylene was:

$$WO_3/TiO_2 > WO_3/ZrO_2 > WO_3/Al_2O_3 > WO_3/SiO_2 > WO_3/MgO = WO_3 = 0$$

C. Kinetics of Propylene Disproportionation

Begley and Wilson (32) conducted a kinetic study of propylene disproportionation over a 9 wt% WO_3/SiO_2. In their study an integral reactor was used to collect data over a pressure range from 2.0 to 62.2 atm and temperatures between 316 to 441°C. The data obtained in this study was used to examine the models of two possible mechanisms for propylene disproportionation. These two models were: 1) Langmuir-Hinshelwood, a second order reaction, which hypothesizes the reaction between two absorbed molecules and 2) Rideal, a second order reaction, which is based on the hypothesis of the interaction of an obsorbed molecule and a gas phase molecule.

The investigators rejected the Langmuir-Hinshelwood model because the rate constant for the model should have approached a limiting value as pressure was increased and the surface sites became saturated with propylene.

Rate constants for the Rideal model, however, were found to be represented by a common correlating line with some considerable deviation in some cases. These deviations were explained due to differences in the catalyst surface conditions due to differences in conversion levels or in the amount of adsorbed poisons on the catalyst which were not removed in the pretreatment. These variations were also attributed to possible variation in temperature settings. Their experimental results did indicate surface coverage to be independent of pressure over the pressure range 21.4 to 62.2 atm.

Based on the experimental data, the effectiveness factor for the catalyst particles used (1/8" extrudate) was found to be near unity, indicating that pore diffusion was not the rate controlling step. Also, the mass transfer rate from the bulk of the gas stream to the external catalyst particle surface was found not to be significant.

Begley and Wilson (32) used two feeds of propylene. One feed contained 35% propane and 65% propylene while the other feed contained more than 99% propylene. The ratio of adsorption coefficient calculated from their data indicates that propane is more strongly absorbed than propylene. This result is contrary to established knowledge on relative absorption of the two compounds

The explanation offered was the possibility that a slight difference existed in the poison level of the two feeds.

It seems that the results obtained by Begley and Wilson (32) might have been governed by mass transfer effects (film diffusion), and it can be easily shown that first-order kinetics are to be expected if external mass transfer is the rate determining step. This objection is supported by recent results of Moffat et al. (30,31) who observed severe interphase mass transfer limitation for the same catalytic system, inspite of calculation which predicted that mass transfer rate to be several orders of magnitude greater than the observed rate. As a possible explanation for this discrepancy, it was suggested that the reaction occurs on a small number of very active site areas which are widely separated on the catalyst surface. The activities of these sites are limited by localized interface diffusional effects. However, a high activation energy was found, while in the case of limitation by mass transfer a very low apparent activation energy is to be expected. According to Moffat et al. (30,31) this high activation energy is due to the fact that the surface of the catalyst is heterogeneous.

Lewis and Willis (35,36) investigated propylene disproportionation over a commercial catalyst containing 3.5 wt.% CoO and 10 wt.% MoO_3 on alumina support. Initial rates were measured

between 121 and 205°C, in a pressure range from 1 to 9 atm in a differential fixed bed reactor. While a number of Hougen and Watson type rate expressions were considered, only the dual-site mechanism (Langmuir-Hinshelwood) proved successful in correlating the experimental data. The mechanism which assumes a surface reaction betwen two adsorbed propylene molecules as the controlling step was given by:

$$r = \frac{k(P_p^2 - P_E P_B/K)}{(1+K_E P_E + K_B P_B + K_p P_p)2} \qquad (2\text{-}2)$$

where P_p, P_E and P_B are partial pressures of propylene, ethylene and butene and K_p, K_E and K_B are adsorption contants of propylene, ethylene and butene respectively.

Equation (2-2) was reduced to the initial rate form

$$r = kP_p^2/(1+K_p P_p)^2 \qquad (2\text{-}3)$$

The values of k and K_p were determined from equation (2-3) by linear least squares treatment of the initial data at each temperature . These values were used as initial estimates and the values of K_E and K_B assumed equal to that of propylene. The Gaussian non-linear least squares technique was used to evaluate the rate and adsorption constants in equation (2-2).

The kinetics of propylene disproportionation over a

cobalt molybdate on alumina has been investigated by Moffat and Clark (30). The study was carried out in an integral flow reactor at 121-205°C and pressures of 1.36 to 5.44 atm. While studying the effect of temperature from 82 to 260°C on conversion of propylene at constant space velocity and pressure, the investigators noted a rate maximum at a temperature (T_{max}), which was followed by an increasing rapid rate of catalyst decay as the temperature was raised further. When a given catalyst sample was subjected to three heating-cooling cycles at constant space velocity and pressure, the authors noted an irreversible loss of catalyst activity. They concluded that there was a reversible deactivation of sites superimposed upon the irreversible poisoning of the sites. Two mechanistic models (Rideal and Langmuir-Hinshelwood) were used to correlate the experimental data. It was concluded that Langmuir-Hinshelwood model applied to the heterogeneous surface and was found consistent with a) the observed general kinetics of the disproportionation of propylene below T_{max}, b) the observed rate-temperature maximum, c) the decrease of T_{max} with decrease in pressure and d) the decrease in T_{max} with decreasing catalyst activity.

Moffat and Clark (31) have confirmed the kinetics observed by Lewis and Wills (36). However, they found that Langmuir-Hinshelwood model was also applicable under integral

conditions. They observed an increase in conversion to a maximum at a T_{max}, followed by a decrease in conversion as the temperature increased. This phenomena has also been observed by Banks and Bailey (18) and Bradshaw et al. (25). Moffat and Clark (31) disagree with Bradshaw et al. who suggested that these rate maxima are caused by irreversible poisoning of the catalyst sites.

Takahashi (39) investigated the kinetics of propylene disproportionation in a closed circulating reactor at temperatures between 40-170°C and in a pressure range 0.105 to 0.368 atm. The experimental data obtained over a 9 wt% MoO_3/γ-Al_2O_3 and 14.5 wt% WO_3/γ-Al_2O_3 catalysts were well correlated by a rate expression based upon a dual-site Langmuir-Hinshelwood mechanism. However, the adsorption of propylene on a 5.1 wt% WO_3/SiO_2 catalyst obeys the Freunlich equation rather than Langmuir isotherm. The apparent activation energies for the surface reaction were evaluated to be 5.15 kcal mol on MoO_3/Al_2O_3, 14.8 kcal/mol on the WO_3/Al_2O_3 and 11.5 kcal/mol on WO_3/SiO_2.

The kinetics of propylene disproportionation has been investigated by Davie et al. (33) on a catalyst containing 5 wt% molybdenum hexacarbonyl supported on alumina. In their investigation, they studied the effect of changing the initial pressure of propylene on the initial rate of disproportionation

in a static system at temperatures between 0 to 80°C, and over a pressure range from 0.005 to 0.197 atm. They found that the initial rate is an assymptotic value of 3.5×10^{-6} mol/L-min as the initial pressure of propylene increased. Initial rate data showed that the rate contolling step is a surface reaction between two adjacently adsorbed propylene molecules (Langmuir-Hinshelwood mechanism). The energy of activation for propylene disproportionation was found to be 7.286 kcal/mol.

Luckner et al. (37) obtained kinetic data for the disproportionation of propylene over a commercial catalyst containing 10% WO_3 on silica. Initial rate data were measured at 399 to 454°C and at pressures ranging from 1 to 9 atm in a near differential fixed bed reactor. The authors chose such reactor operating conditions that mass transfer effects would be negligible.

The complete rate equations for Langmuir-Hinshelwood and Rideal mechanisms were used, and initial assumptions of near zero partial pressures of products were applied. The initial rate data was tested by both models. Model discrimination between two rival models which has been reviewed by Kittrell (98) suggests a quantitative method based on examining the linearized forms of the two rival models. Using this criterion the authors found the Langmuir-Hinshelwood form to correlate the data better.

A second qualitative criterion is that the rate and adsorption constants estimated usig these linearized form should be positive. The Langmuir-Hinshelwood form, correlated that data with positive rate and adsorption constants at each temperature studied. The apparent activation energy for the surface reaction was calculated to be 24.73 kcal/mol.

Hattikudur and Thodos (34) used a catalyst similar to that used by Luckner et al (37) to disproportionate propylene and establish a kinetic model. In their study, reaction rate data from both differential and integral bed were collected over a pressure range from 2.2 to 69.0 atm and at temperatures between 343 and 454°C. The investigators found that external diffusion and pore diffusion effects became negligible when the flow rates were kept higher than 2.4 mol/hr and particle sizes kept below -20+30 mesh (718μ).

Both the single-site mechanism (Rideal) and the dual-site mechanism (Langmuir-Hinshelwood) were considered. Initial rate data obtained in a differential reactor indicated that the actual rate-contolling step involves a Langmuir-Hinshelwood type mechanism.

The authors did integral bed studies at temperatures between 343 and 426°C and pressures up to 36.4 atm. These studies constituted runs in which the catalyst weight 0.1 to 2.0 grams and

conversion ranged from 8% up to equilibrium. The rate constant, adsorption constants of reactants and products and equilibrium constants were given as a function of temperature. These relationships were used to predict space time, W/F, for the integral bed data and compared to experimental W/F. This comparison resulted in an average deviation of 8.8% for 56 data points.

D. Break-in Phenomena in Propylene Disproportionation

During the initial contacting of WO_3 on silica catalyst with propylene, significant increase in disproportionation activity was observed to periods of up to 24 hours. Luckner and Wills (38) used a fixed bed differential reactor to perform a quantitative study of break-in phenomena exhibited by a 10% WO_3/silica catalyst. The rate of approach to steady state activity (K_s) was found to depend on both temperature and pressure according to the equation:

$$K_s = 1.993 \times 10^{12} \exp(-47.2/RT) P_p$$

The authors reported that prior reduction of the catalyst from WO_3 to WO_2 in hydrogen at 600°C substantially increased the rate of the catalyst break-in but did not eliminate the catalyst break-in phenomenon. They found that the steady-state activity of a catalyst could be largely destroyed by a simple purge of the system with helium for 3 hours. Upon re-introduction of propylene, the activity of the catalyst was greatly reduced and another break-in period was observed,

although the break-in rate was greater than that for a freshly activated catalyst.

Studies by Pennella et al. (43) have shown that the activity of a tungsten oxide/silica catalyst can be quickly and dramatically increased by dosing the reactant olefin with certain compounds, most notably polyenes (i.e.1,5 cycloocta-diene). The experimental runs were carried out at atmospheric pressure and at 21.4 atm and temperatures between 400-500°C. It was proposed that the dosing gas bonds to the tungsten and alters the bonds between tungsten and olefin in a manner that activates previously inactive sites. They further suggested that normal break-in may be due to a similar process in which ligands are slowly formed from reaction products (44). In these studies the effects were temporary and continuous dosing was necessary to maintain high activity.

Other suggestions have been put forth to explain the break-in effects. Strong adsorption of olefins during initial contacting has been observed in a pulse dosing of a fresh activated catalyst (37). This has suggested the formation of high molecular weight organic species on the surface which might be responsible for the increasing activity during the break-in period. Another possibility that has been discussed is the slow formation of oxygen vacancies through the reduction of the

oxide surface by the olefin with the possibility of such vacancies enhancing catalyst activity. (43).

Wills et al. (54) investigated the mechanism of break-in of the disproportionation of propylene over WO_3/SiO_2 catalyst. The investigators showed that rapid, though temporary, increase in activity up to 300% of steady-state is observed during break-in following the dosing of the propylene feed with ammonia and primary amines (53,54). Upon reaching steady-state, cooling followed by reheating or short purges with helium caused the relaxation of break-in.

The authors concluded that the break-in process has a large activation energy while the relaxation process has a low activation energy. They suggested that the overall break-in phenomenon was due to surface defects formation, possibly through chemical reduction, balanced by diffusion of those defects to the bulk.

Recently, the effect of various changes in reaction conditions on the break-in behavior and activity of WO_3/SiO_2 catalyst in propylene disproportionation has been studied by Gangwal et al. (55). Their results indicate that the maintenance of full catalytic activity requires both temperature and propylene flow to be maintained, and that the increase in reaction

rate during break-in is due to a decrease in the activation energy of the reaction, or to an increase in the number of active sites on the catalyst, or to a combination of both.

E. Active Sites for Catalytic Disproportionation

A critical problem to a full understanding of the disproportionation process is the knowledge of the actual catalytic species. Such information is difficult to obtain since the catalyst is activated in situ. In general, for a metal to function as a catalyst it must possess the proper distribution of energy levels and vacant coordination sites. These ends can be achieved by a change in formal oxidation state, number and nature of ligands, complex geometry or combination of all three. In the case of disproportionation catalyst many authors have attempted to understand the nature of the active sites and improve their catalytic properties by determining the effect of various ligands, and ions on activity and selectivity.

Tungsten oxide catalysts supported on silica gel have been used widely for disproportionation reactions. Many authors have attempted to study these catalysts in order to understand their structure and improve their selectivity towards the main products (45).

Results from investigation of the disproportionation of propylene over a WO_3/SiO_2 catalyst in a fixed-bed flow reactor

are worth mentioning (37). A significant increase in the activity of the fresh catalyst was observed during the first few hours after the propylene flow was started. During this period the color of the catalyst changed from pale yellow (characteristics of stoichiometric WO_3) to blue violet (characteristics of substoichiometric WO_3 with an O/W atom of 2.95 or less) (56).

Luckner and Wills (37) suggested that propylene reduces the catalyst to form active sites. The observation that pretreatment of the catalyst with reducing gas such as hydrogen or carbon monoxide, gave an increase in initial activity and resulted in a blue colored catalyst, supports this interpretation. It was suggested that in its active form tungsten oxide is actually a slightly reduced oxide such as $W_{20}O_{58}$. In view of the XRD results, Kerkhof et al.(41) concluded that in a fresh catalyst at least two tungsten species exist, WO_3 crystallite and a hardly reducible material. After use, two species, WO_3 crystallite and $W_{20}O_{58}$ were identified. For higher WO_3 content the authors (41) found that WO_2 is formed in the first few minutes. This is because large amounts of water formed from the intermediate.

Pennella and Banks (43) have found that the activity of the WO_3/SiO_2 catalyst can be significantly improved by adding small amounts of polyolefins to the propylene feed. The authors conclu-

ded that such addition could activate sites which could not be activated by propylene. Similar observation was reported by Gangwal and Wills (53) when ammonia and certain amines were dosed into the propylene feed. The increase in activity was observed during break-in as well as with fully active catalyst. These effects were temporary in nature since the catalyst activity returned to its original value when these additions were stopped.

Molybdenum oxide supported on silica shows limited activity when activated in nitrogen atmosphere. This activity increased significantly when the catalyst is reduced with hydrogen (50, 51). Sadesawa et al. (50) observed an increase in activity and selectivity when the catalyst was treated with aqueous ammonia. While Nakamura et al (51) observed that the activities of catalysts were correlated with ESR intensities of Mo^{+5} and the amount of CO adsorbed. The results confirmed that the active centers may be dispersed lower Mo ion rather than Mo^{+5}.

Molybdenium oxide on alumina catalyst has been studied by Nakamura et al. (51). The authors found a relationship between the acidity of the carrier and the activity of MoO_3/Al_2O_3. They assumed that propylene was adsorbed on the acidic centers of alumina and reduced the catalyst to produce fresh active centers, however, the acidic sites were not the active centers and did not

participate in the reaction. Giordano et al. (57) studied the structure and the catalytic activity of MoO_3/γ-Al_2O_3 containing 10-15% MoO_3. They presented evidence indicating that dimeric Mo(V) configuration of bis-molybdenyl type is active in the reaction. The disproportionation activity was shown to be related to the presence of Mo(V) species originating from the reduction of oxomolybdenum species.

The results of stork et al. (45) reported the existence of $Al_2(MoO_4)_3$ on a catalyst containing MoO_3/γ-Al_2O_3. In the formation of $Al_2(MoO_4)_3$, Mo^{+6} ions change from octahedral to tetrahedral coordination. (59). The occurrence of small MoO_3 crystallite, however, could not be entirely ruled out.

Kerkhof et al. (41), studied the relationship between carrier and oxide for WO_3/SiO_2 and WO_3/γ-Al_2O_3 and concluded that surface compounds are formed on silica as well as on alumina. However, the interaction between alumina and the oxide is stronger, resulting in better dispersion and the formation of a surface compound ($Al_2(WO_4)_3$).

A number of oxidic tungsten compounds have been tested for propylene disproportionation activity by Stork and Pott (48). The authors observed a remarkable agreement between WO_3/γ-Al_2O_3 and $Al_2(WO_4)_3$. It was concluded that at 550°C, in calcined

$WO_3/\gamma\text{-}Al_2O_3$ $Al_2(WO_4)_3$ is formed.

de Vries et al (47) studied the nature of active sites on alumina supported tungsten oxide catalyst. They assumed that the active sites are formed on lattice defects which are statistically distributed over the surface and are easier to reduce than the unperturbed surface sites.

Recently, Thomas et al. (58) confirmed the formation of $Al_2(WO_4)_3$ on $WO_3/\gamma\text{-}Al_2O_3$ by Raman spectroscopy and X-ray diffraction, but no crystallite WO_3 was observed.

F. Mechanism for Propylene Disproportionation

In the absence of a catlyst, olefin disproportionation reactions are "symmetry forbidden" and require very large activation energies. Olefin disproportionation catalysts lower this energy barrier and provide "symmetry allowed" pathways for the reaction. The means by which a given catalyst performs this task has been the subject of a great deal of speculation from which many proposed mechanisms have evolved.

Bradshaw et al. (25) were the first to publish a four-center type mechanism to explain olefin disproportionation. They conducted experiments on the disproportionation of 1-butene using cobalt molybdate catalyst at different temperatures and space velocities. The clue to the mechanism came from the observation that the selectivity to ethylene and 3-hexene varied inversely with

the isomerization of 1-butene to 2-butene. The effect of double bond isomerization and selectivity to ethylene and 3-hexene was further demonstrated with a series of cobalt molybdate catalysts treated with various amounts of $NaHCO_3$ to poison the isomerization sites. These workers suggested that the reaction occurs via "quasi cyclobutane" intermediate formed by the correct alignment of the carbon atoms at the double bonds of the two reaction olefins. Applied to 1-butene, the reaction was pictured as follows:

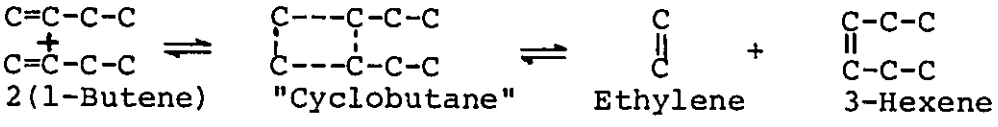

(2-5)

The reaction between ethylene and 2-butene and with ethylene and 4-methyl-2-pentene provided additional support and demonstrated that the disproportionation reaction was reversible.

Calderon et al. (62) proposed a similar mechanism for olefin disproportionation catalyzed by the homogeneous complex obtained from the interaction of WCl_6, C_2H_5OH and $C_2H_5AlCl_2$. They pictured a transalkylidenation reaction as follows:

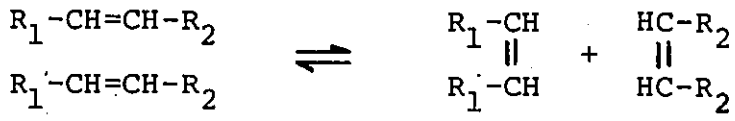

(2-6)

In another publication, Calderon and Co-workers (98) showed the intermediate as

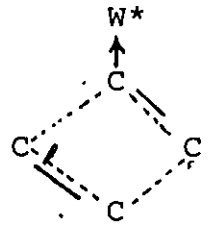

where W* is the transition metal atom plus the remaining ligands.

Mol et al. (62) proposed that a four-center intermediate forms with the abstraction of two hydrogen atoms by the catalyst, so that a cyclobutadiene intermediate is formed instead of the cyclobutane structure.

The experiments of Calderon et al. (26) with butene plus deuterated butene would appear to rule out the mechanism suggested by earlier workers (62). Further experiements by Crain (63) also indicated that the cyclobutadiene intermediate was not likely to occur. Crain studied the reaction of 2,3 dimethyl-2-butene and ethylene over molybdena/alumina catalyst treated with KOH and obtained isobutene as the only product. The cyclobutadiene intermediate would require the migration of 2 methyl groups and 2 hydrogen atoms to the catalyst and their return to the same carbon atoms. The author could not detect propylene, n-butenes or methylbutenes in the product and concluded the possibility of a cyclobutadiene as an intermediate to be remote.

Banks and Bailey (24) noted the occurrence of disproportionation, isomerization and polymerization over similar catalysts or simultaneously over the same catalyst which suggested a similarity of mechanism. They proposed that the ability of the catalyst to shift hydrogen atoms is the key factor in determining the reaction course. They concluded that disproportionation occurs when two molecules are adsorbed with the formation of a

four-center complex and then desorbed with the breakage of two opposite bonds without hydrogen shift. Polymerization occurs when two molecules are adsorbed with the formation of four-center complex and then are desorbed with the breakage of one bond and a hydrogen shift. Skeletal isomerization occurs when one molecule is adsorbed with the formation of a four-center complex and is then desorbed with the breakage of one bond and a hydrogen shift.

Studies on the mechanism of disproportionation using deuterated propylene have been reported by several investigators (27,29,62). Clark and Cook (27) disproportionated [1-^{14}C] propylene and [2-^{14}C] propylene over a Cobalt molybdate catalyst. At 60^{o}C their results were consistent with the four-center mechanism. However at temperatures above 60^{o}C, double bond isomerization activity became a factor and up to 160^{o}C, nearly one half the [1-^{14}C] propylene was isomerized to [3-^{14}C] propylene prior to disproportionation.

Woody et al. (29) studied the disproportionation of [1-^{14}C] propylene over a Cobalt molybdate catalyst at 149°C and 177^{o}C. Their results were in agreement with Clark and Cook (27).

Recently, Mol et al. reacted propylene labeled with [^{14}C] in each of the three positions over rhenium oxide/alumina catalyst at moderate temperatures (62,64). The data were extrapolated to zero contact time to eliminate the influence of isomer-

ization reactions. In the disproportionation of [2-^{14}C] propylene the ethylene formed showed no radioactivity, in contrast with butenes, which showed a specific radioactivity twice as high as that of the starting material. Experiments have indicated that cyclobutane structure plays a part in the reaction mechanism (24,25).

Some of the investigators have concluded that the reaction proceed by a single step process possibly involving a metal carbene intermediate. Yamaguchi (52) observed the formation of i-butene during the disproportionation reaction of propylene over WO_3/TiO_2. Production of propylene was also found in the reaction of ethylene over the same catalyst. Because of the formation of i-butene from propylene and propylene from ethylene, the authors suggested that the reaction proceeds via carbene intermediate (52). The mechanism explains the various side reaction that occurs on disproportionation catalyst (dimerization, isomerization, Polymerization and disproportionation).

III. EXPERIMENTAL

The following section consists of the plan of investigation, experimental apparatus and calibration, operation procedures, and information concerning the type of reactor used and the design of the reactor. Included also is a description of preparation, activation and characterization of the catalyst.

A. Plan of Experimentation

The overall approach to the experimental work was to design and construct a reaction system and to investigate the catalytic disproportionation of propylene under various conditions. In somewhat more detail, the plan consisted of calibration of analytical equipment, preliminary studies to determine appropriate operating conditions and collection of integral conversion data.

1. Comparison of Integral and Differential Reactors

Kinetic data for catalytic systems are best obtained in a flow reactor. Any change in the catalytic activity can be detected and corrected for in a flow reactor. Flow reactor may be either integral or differential depending upon the degree of conversion allowed to take place in the reactor. Conversion is limited in a differential reactor, but may be complete in an integral reactor.

The chief advantage of the differential reactors is that it measures rate directly. Since most catalytic kinetic equations are in terms of rate the experimental data can be used directly to check these equations. One disadvantage is that because of small conversions involved, the analysis must be extremely accurate. Another disadvantage is that although initial rates can be determined easily enough by using pure feed, rates corresponding to volume element other than the initial rates would require the use of feeds consisting of he same mixture of reactants and products that corresponds to the desired value of conversion. This would be virtually impossible in a system that involves many side or secondary reactions.

The method often used in experimental kinetic work is the integral reactor study. The advantage is that chemical analysis need not be so rigorous for a reasonable degree of accuracy in the total conversion. Also, in each case the feed may be pure reactant (except in recycle studies). The main disadvantage of intergral reactor is that the rate is not mearued directly. The rate is the slope of the tangent to the conversion versus W/F curve. Therefore, it is the slope rather than the value of the ordinate that determines the rate equation. Any slight scattering of the experimental points would have a great effect upon the slope. The rate equation which can be integrated and the data can be expressed in W/F as a function of conversion.

However, it is much more difficult to integrate the rate equations.

Another disadvantage of the integral reactor is that the portion of the conversion vs W/F curve which is most important in determining the mechanism is at low values of W/F. Yet this is the portion where the accuracy of analysis becomes increasingly important since the conversion is low. In this study, conversions were measured at low W/F in order to get an accurate slope.

2. Criteria for Selection and Design of Reactor

Based upon considerations such as those described in the previous section an integral reactor was selected for this reaction. The conversion, rate and equilibrium constants of the rate equation are usually sensitive to temprature and pressure. Therefore, during a test the temperature and pressure should be kept constant. Temperature variation could be observed traversely as well as longitudinally in a reactor. Several methods are widely used to minimize reactor temperature gradients. In our investigation the reactor was surrounded by a steel metal cylinder. The heat was supplied to the outer cylinder by two layers of heating wires wrapped around the cylinder then to the

Schematic Diagram of Experimental Apparatus

Symbol	Item
AUX	Other gases used for calibration
B	Bubble Soap Meter
F	Filter
FC	Flow Controller
GC	Gas Chromatograph
IR	Integral Reactor
NV	Needle Valve
P	Pressure gauges
PC	Pressure Controller
R	Rotameters
SV	Gas Sampling valve
TC	Thermocouple
TG	Pressure Test gauge
W	Wet Test Meter

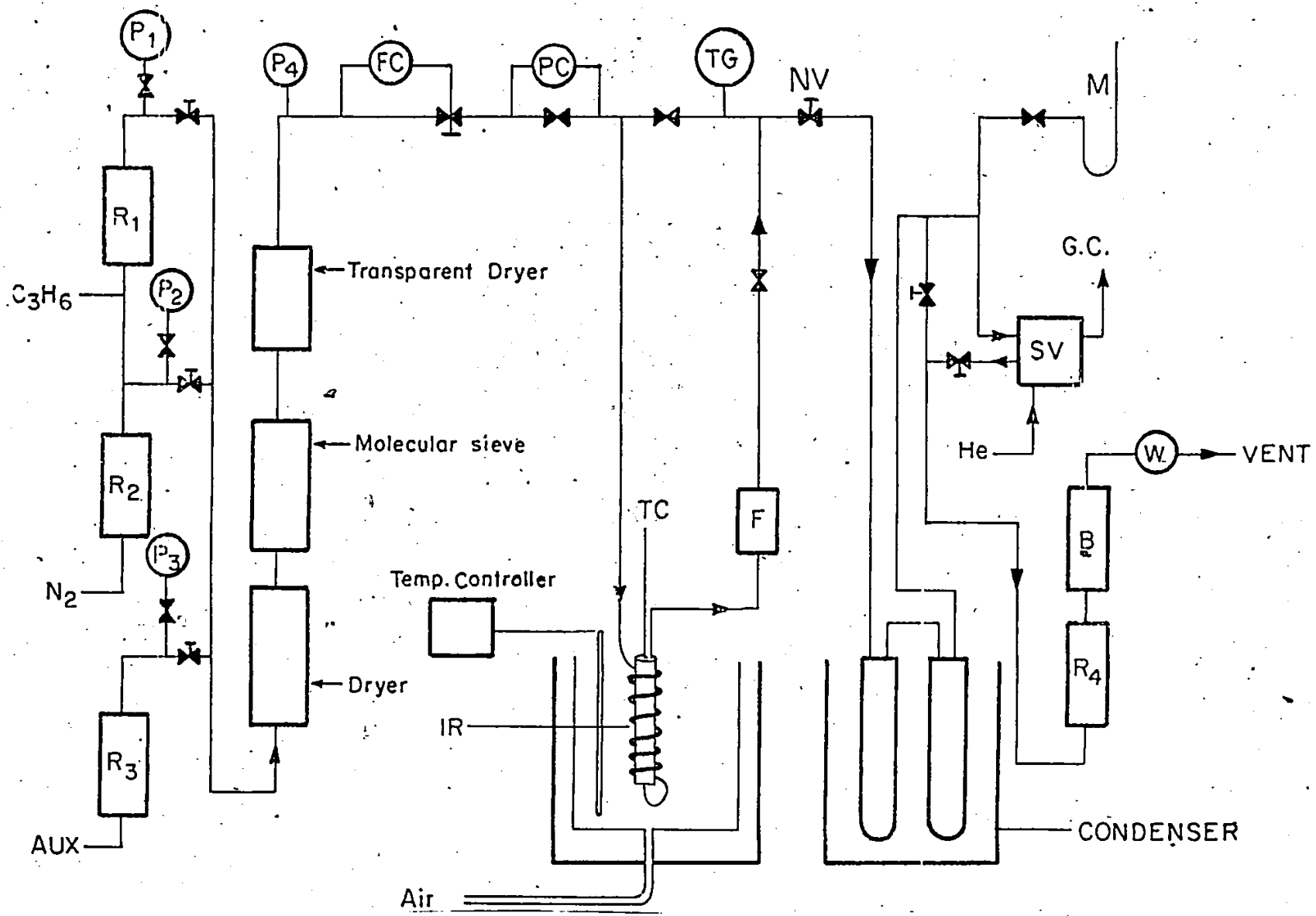

Figure 3-1 Schematic Diagram of The Experimental Apparatus.

reactor by a fluidized sand bed. The high heat transfer rate and large mass of the cylinder cause a better distribution of heat.

It is important that the reactants be brought up to the reaction temperature before entering the catalyst bed. This was achieved with a spiral preheater and introducing the reactants from the bottom of the reactor.

The feedrate and pressure were maintained at a constant value during a test by using a constant upstream reference differential flow controller, and a Nupro-needle valve respectively.

B. Experimental Equipment

The Disproportionation of propylene was carried out in a fixed bed integral reactor. The experimental equipment used in this investigation was designed to operate at controlled temperature and pressure. A schematic diagram of the apparatus is shown in Figure (3-1).

The apparatus may be divided into three sections: (1) feed section (2) reactor assembly and (3) product analysis unit.

1. Feed Section

This section consisted of six gas streams. Two gas streams supplied helium as a carrier gas to the reference and

sample chromatographic columns. Helium was obtained from a high pressure cylinder through a two stage pressure regulator and then through rotameters (tube and float 601, Matheson Co.). The gas streams were carried via 1/4" O.D. copper tubing. The third stream, which carried air to the fluidize sand bed, was made of 1/4" O.D. copper tubing covered with heating tape.

Prior to entering the reactor, all streams passed through two dryers containing Drierite and Molecular sieve 5X respectively, to remove moisture from the feed. A transparent plexiglass dryer containing indicating Drierite was also used to indicate moisture in the feed. A Brooks differential type flow controller, was used to keep a steady flow to the reactor. A pressure line regulator was used to keep a constant pressure to the reactor. The fourth stream which carried nitrogen in a 1/8" O.D. stainless steel tubing was obtained from a high pressure cylinder through a two stage pressure regulator and then through a rotameter (tube and float 601, Matheson Co.). An auxiliary stream which could carry (ethylene or butenes) for calibration purposes, consisted of a 1/8" O.D. stainless steel tubing and a flowmeter (tube and float 601, Matheson Co.). Propylene was obtained from a high pressure cylinder (136 psig) through a two stage pressure regulator (model 975-0451) obtained from Matheson Company. Propylene could be obtained up to a pressure of 130 psig.

2. Reactor Assembly

The reactant line was connected to a Swagelock "T" connection. While one branch led to the reactor through a preheater the other by-passed the reactor and preheater for calibration purposes. The preheater was made of 6 feet long 1/8" O.D. stainless steel tubing which was wound around the reactor. The reactants were preheated to the reaction temperature and entered from the bottom of the reactor. Details of preheater and reactor are given in Figure (3-2).

The reactor was made of 8 x 1/2" O.D. 316 stainless steel tube. A porous stainless steel plate (supplied by Pall-Trinity Micro Corp., Cortland, N.Y.) was inserted at the bottom of the reactor tube. The Grade D plate had a mean pore size of 65 microns, a normal thickness of 1/16" and produced a pressure drop of approximately 0.1 psig per 180 cfm/ft^2. An autoclave reducer was welded below the porous plate and connected to the feed line from the preheater.

The top of the reactor was connected to a Swagelock "T" connector (SS-400-3) through a 1/2" to 1/4" reducer union (SS-810-6-4), supplied by Ottawa Valve and Fitting Co.). A stainless steel thermocouple type J (supplied by Honeywell Co.) was inserted through the upper opening of the "T". The lower end of the thermocouple was kept 1/2" from the porous plate in

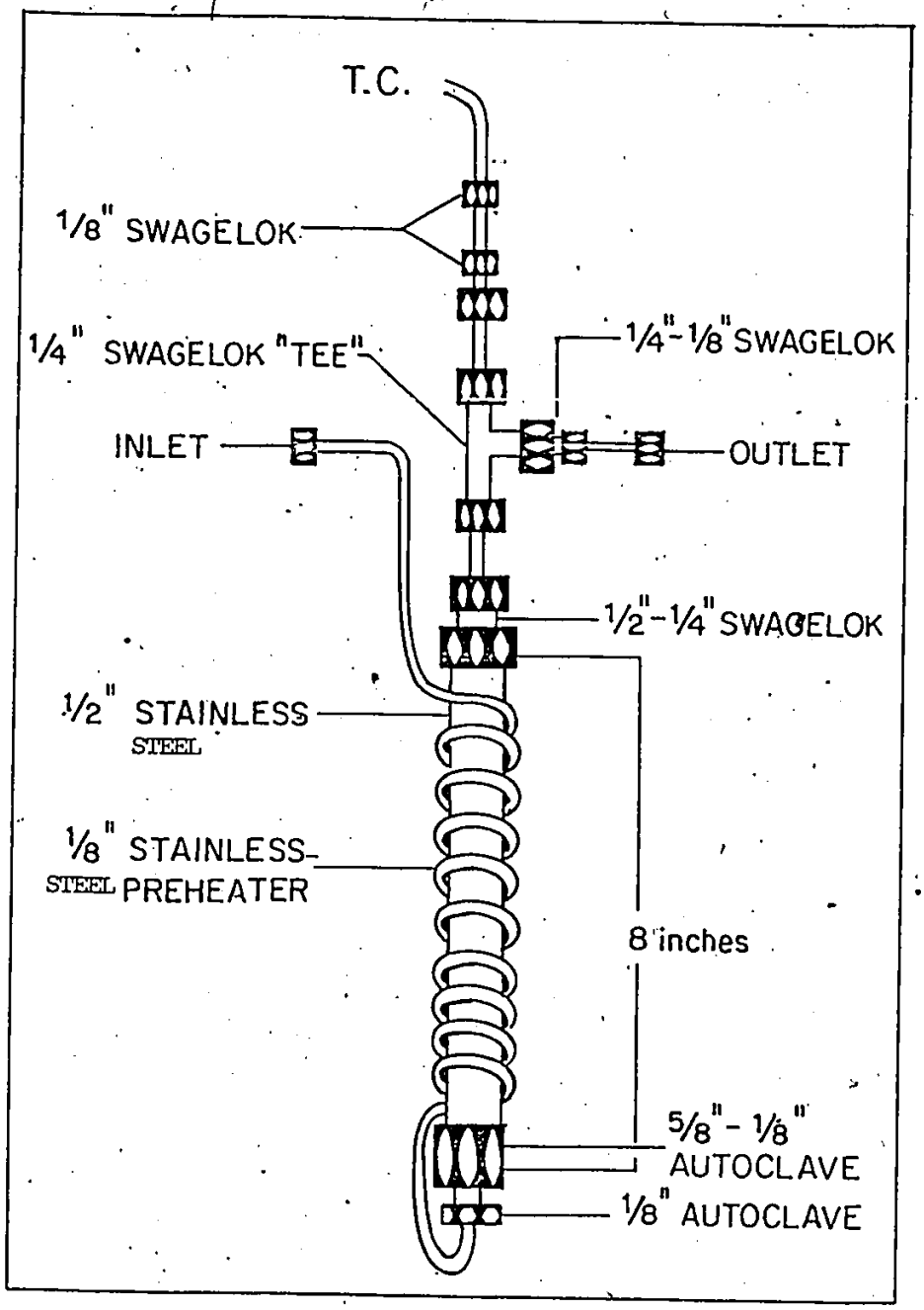

Figure 3-2 Schematic Diagram of the Reactor

contact with the catalyst bed. The thermocouple was connected to a potentiometer (supplied by Leeds and Northup Co.) for measuring the temperature during the reaction. A second thermocouple type "K" (supplied by Honeywell Co.) was placed in the fluidized sand bed and connected to a Honeywell Pyro-Vane temperature controller. The temperature controller was used with a transducerin such a way that the output signal from the thermocouple (type K) was measured by the controller which activated the relay to maintain constant temperature at the set point. The controller when coupled with a variable transformer could maintain the reactor temperature to within $\pm$ 2^{o}C. The reactor and reactants preheaters were kept immersed in a constant temperature fluidized bed. The container for the fluidized bed was made from a 6" O.D. and 1/4" thickness steel cylinder. A porous stainless steel plate (Pall Trinity Micro Corp., Cartland, New York) was inserted at the bottom and further welded to a reducing cone with 1/2" pipe. Clean sand 40-60 mesh size was used as the fluidizing mediumand was placed in the container on top of the porous plate. The reactor was held upright in the center of the bed, while the vessel was almost completely filled with sand. Sufficient flow of air was passed to keep the sand fluidized and to obtain a uniform temperature. The tube carrying the air was wrapped with a 5 feet heating tape to reduce temperature

fluctuations. For heating the reactor, two layers of ceram-A-flex heating wire (Chemical Rubber Co., Cleveland, Ohio) with a resistance of about 50 ohms was wrapped around the steel cylinder. A paste of asbestos power mixed with water was applied to the wires for insulation and to fix the wires in position. The first heating wire was connected to the temperature controller. The second heating wire was connected to a 10-ampere powerstat (Fisher Scientific Co.) which was adjusted to a sufficient power to maintain the reactor temperature slightly below the required temperature set on the temperature contoller. This reduced the heating load in the controller circuit (inner heating wire) and made more precise control of the reaction temperature possible. The reactor and fluidized bed were placed in an outer steel cylinder 12 inches in diameter, placed on piece of asbestos plate, in the center of which a hole was provided for air line to fluidize the bed. The annular space between the steel cylinder and the bed was packed with insulating asbestos powder. The surface of the outer cylinder was coated with a layer of fiber glass and asbestos cloth 4" thick for further insulation. The top of the fluidized sand bed was covered with an asbestos plate in order to reduce the temperature variation caused by radiation.

3. Product Analysis Unit

The product analysis unit consisted of a liquid trap, two condensers, gas sampling valve, rotameter, wet test meter, gas chromatograph, integrator, and recorder. The pressure in the reactor was maintained constant by combination of a constant upstream reference differential flow controller (Brooks Instrument Div.), a pressure line regulator (Matheson Co.), and a Nupro-needle valve. By adjusting the micrometer needle valve and the differential flow controller resistance valve, very accurate flow and pressure settings could be maintained easily. The product stream from the reactor was filtered by a high purity stainless steel filter (Matheson Co.) and kept above 45°C by heating the 1/8" O.D. stainless steel tubing by a heating tape controlled by a power-stat (Fisher Scientific). The product stream was condensed in a two stage condensing tube immersed in an ice-bath flask. This was done to ensure condensation of olefins higher than four carbon atoms.

A high-temperature gas sampling valve (Chromatographic Specialities Ltd.) was used to inject samples of the product stream to the gas chromatograph to be analyzed. The gas sampling valve had 8 ports. While the carrier gas (helium) continuously passed through the first loop (0.70 cm^3), the product stream passed through the other loop (0.70 cm^3). When the sampling

valve was turned on, the flow of the product stream and the carrier gas was switched. A product sample from the sample loop was flushed by helium to the chromatographic column for separation. The pressure on the sample loop was kept constant at each injection to make sure that a constant volume was injected each time. This was done by adjusting the flow before and after the gas sampling valve. The product stream after leaving the gas sampling valve was passed through a rotaméter (tube and float series 602, Matheson Co.) and a wet test meter.

A Gow-Mac W 2X hot wire 333 mount, made of rhenium-tungsten, in a temperature regulated four elements macro cell (Model TR-III AWX) was used to analyze the products separated by the column. The detector temperature was controlled by a Fenwal thermoswitch with an adjustable range from ambient to 205°C. Two cartridge heaters were connected in series with a thermoswitch and the temperature of the unit could be varied by turning on adjustable screw at the bottom of the case, one revolution for every 32°C rise in temperature and vice-versa. The temperature of the detector was kept at 70°C. Direct current for the detector was supplied by a Gow-Mac Cell Model 405-C.

Chromatographic columns were kept in a water bath, the temperature of which was maintained at 30°C. The temperature of the bath was maintained constant by a thermo-regulator having

a controlled deviation within ± 0.05°C. The bath, 10" x 10" O.D. (Pyrex-Corning Glass Works) was well insulated with asbestos cement and glass wool to reduce the heat losses to the surrounding.

The output signal (in millivolts) from the detector was transferred to an integrator (Hewlett-Packard) where the area of the peaks were calculated. The signal was then transmitted to a chart recorder (Fisher Scientific Co.).

C. Experimental Procedure

1. Calibration of Equipment

Description of the procedures used for calibrating various pieces of equipment and procedures for operation of the catalytic reactor and experimental runs and analyses are given in detail in the following sections.

(i) Calibration of Flowmeters

Flow measurements during this study were made with Matheson 601 or 602 tube rotameters. The rotameters were calibrated with air at atmospheric pressure and 25°C. The volumetric flow rates were checked by both the soap bubble method and a wet test meter (supplied by Precision Scientific Co.) The rotameters then were calibrated for propylene at 25°C and one

atmosphere. However, the overall equipment design required that certain rotameters be calibrated at pressures higher than one atmosphere. In the assembled equipment a rotameter (R1) was placed before the reactor. This meant that this rotameter was functioning at the pressure of the reactor. Downstream from the reactor was another rotameter (R4) functioning under atmospheric pressure. Pure propylene was fed to the reactor, without reaction, at various pressures to be used during reaction studies. The rotameter was thus calibrated at various pressures against the rotameter downstream at atmospheric pressure. Calibration curves of R4 at atmospheric pressure and R1 at 3.041, 4.403, 5.703 and 7.124 atm are shown in Figure (8-1) and (8-2) respectively and given in Appendix (B).

(ii) Calibration of Thermocouples

The thermocouples were calibrated by inserting them in the fluidized bed furnace with an AST M Thermometer (100-600°C attached to it. During calibration, a potentiometer was used to read voltages corresponding to each temperature measured. The reference junction was placed in a Dewar flask filled with crushed ice for all calibrations and during equipment operation. A calibration curve of temperature against millivolts is shown in Figure (8-3), Appendix (B).

(iii) Calibration of Pressure Gauges

These were calibrated against a stainless steel test gauge. Gauges being calibrated were placed in a system pressurized with nitrogen and connected to the Test gauge (Previously calibrated by Matheson company). The test gauge was used to read the reaction pressure. A calibration curve is given in given in Figure (8-4), Appendix (B).

(iv) Calibration of Chromatograph

All olefins produced by disproportionation of propylene were analyzed by gas chromatography. The chromatograph detector was calibrated for ethylene, propane, propylene, 1-butene, trans-2-butene, and cis-2-butene. The gas chromatograph used in this investigation, which was assembled in our department was connected to a gas sampling valve. This valve consisted chiefly of a calibrated volume sample loops of 0.70 cubic centimeter.

Pure components were used to flush the sample loop. Samples were analyzed until only the particular component was detected by the thermal detector. Then, the pressure on the sample valve monitored by a mercury U-tube manometer was set at a given value. From the pressure P_1, volume of sample loop V_1, the temperature T_1, the number of moles injected could be calculated as follows:

$$n_I = P_1 V_1 / \overline{Z}_I RT \qquad (3\text{-}1)$$

The area of the peak for component (I) was integrated by the Hewlett-Packard integrator. The thermal conductivity detector was assumed to have an output which was proportional to the number of moles of a particular compound being injected.

Mathematically: $n = f A$ (3-2)

The procedure ws repeated for several partial pressures of pure ethylene, propane, propylene, 1-butene, trans-2-butene and cis-2-butene. Using multiple linear regression, the best least squares estimates factor f of each component was determined.

To eliminate the scale of the recorder, the integrator and the constants, the proportionality factor of each component was normalized by dividing it by the propylene calibration factor, since propylene was expected to be present in every sample analyzed during this investigation.

Mathematically: $f^* = f / f$

In order to check the calibration factor of each component, the particular component and propylene were allowed to flow at a known flow rate. A sample was injected at a pressure of 1.092 atm. The molar ratio of the component-to-propylene was calculated. A plot of area ratio of component to propylene versus the molar ratio of component to propylene was prepared. Using the multiple linear regression, the best least squares estimates of f^* factor of each component was determined. Calibration curves for each component are given in Figure (8-5), Appendix (C).

Appendix (c).

A thermal conductivity detector was used in the analysis of the various components of the reaction product. A column packed within 30% Hexamethylphosphoramide coated on chromosorb P,NAW,60-80 mesh was used. Two columns, each five meters, were used in parallel to give a stable base line on the recorder. For all analyses the same control positions (as used during calibration) were maintained on the chromatograph. The detector bridge was operated at 100 milliamperes and a temperature of 70°C, column temperature at 30°C, a helium inlet pressure of 3.450 atm. at a flow rate of 60 cm^3/min.

2. Leakage Test

The system was tested at 7.124 atm for any possible leaks in the following way:

1) propylene gas at a pressure slightly higher than 7.124 atm was allowed to flow into the apparatus with the exit kept closed. If there was no leak the rotameter would show no flow. However, if a leak existed, the apparatus was checked in each section and the leak was corrected.
2) The system was pressurized up to 7.124 atm and both the inlet and outlet valves were closed. The apparatus was left for 4 hours to check for any pressure drop. If a pressure drop

was observed the procedure was repeated for each section to check for the source of the leak.

3. Operating Procedure

Details of the experimental procedure for making a run with a specified weight of fresh catalyst are described in this section.

(i) Start up

a) Test the system for any leaks by pressurizing the system with propylene at 7.124 atm.

b) Turn on departmental compressed air to fluidize the furnace bed.

c) switch heat to various heating tapes used for heating air.

d) Turn on the powerstat for direct heater and indirect heater setting the temperature at 600°C.

e) Charge the reactor with the desired weight of fresh catalyst and cover it with layers of glass wool to prevent catalyst escape from the reactor.

f) Check for leaks in the reactor by pressurizing with propylene up to 100 psig.

g) Turn the nitrogen flow at 135-150 cm^3/min at a pressure of 3.041 atm.

h) When the temperature of the sandbath stabilized at 600°C, the reactor was connected to the system to activate the catalyst for 12 hours at 600°C.

i) Cool the reactor by switching the powerstats direct and indirect heaters.

j) Open the helium cylinder valve so that a constant pressure of 3.450 atm. the flow rate was 60 cm^3/min in both columns.

k) Switch on, recorder, detector current, integrator, heater to water bath, stirrer and thermoregulator.

l) Fill Dewar flask and ice bath with crushed ice for product condensation.

(ii) Experimental Run

a) When the reaction temperature was attained, the powerstat of direct heater and indirect heater were adjusted to the appropriate voltage and temperature was allowed to stabilize.

b) The pressure of propylene was adjusted to 1.5 atm higher than the reaction pressure, and propylene was used to flush the nitrogen from the apparatus for 20 minutes.

c) Several samples of product stream were analyzed to ensure that nitrogen was completely flushed.

d) The reaction pressure and the flow rate were adjusted by controlling the differential flow controller and the needle valve at the exit of product stream.

e) The pressure on the sample valve was adjusted to 7 cm of mercury by controlling the flow to the sample valve and that by passing it.

f) Continue the run, meanwhile injecting samples every 15 minutes until steady-state was reached.

g) Shut off the propylene flow and start nitrogen flow at 135-150 cm^3/min for 1 hour, before starting another run.

h) The gas chromatograph calibration was checked periodically to assure the stability of the column and detector.

D. Preparation of Catalysts

Tungsten oxide containing catalysts supported on different material (α-alumina, γ-alumina, silica gel, silica-alumina, kesielghar and zirconium oxide) used in this study were prepared by the conventional incipient impregnation method (95).

The carrier of the required particle size was added to an aqueous solution of ammonium paratungstate $(NH_4)_6W_7O_{24}\ ^6(H_2O)$ (Supplied by ICN pharmaceutical Inc., U.S.A.). All supports were crushed to the required size and dried for three hours at 110°C before being impregnated. The mixture of support and the ammonium paratungstate solution was

stirred over-night and then slowly evaporated over a steambath. After the removal of water, the catalyst was successively heated at 1/2 hour intervals in steps of 100°C up to 600°C and calcined at 600°C overnight. All catalysts were activated in the reactor in a stream of dry nitrogen (135-150 c.c./min) at 600°C for 12 hours.

CATALYST ACTIVATION

Catalyst activation was carried out in-situ in a stream of dry propylene. The catalyst (-28+42 mesh) was dried at 100°C for 3 hours. A weighed sample was placed in the reactor. The reactor was connected to the apparatus while the temperature of the fluidized bed was held at 600°C. Nitrogen flow rate was adjusted at 135-150 cm^3/min at atmospheric pressure. The catalyst was activated in the nitrogen stream for 12 hours. Subsequently, the catalyst was cooled to the required reaction temperature, while nitrogen flow was maintained constant.

During activation of the catalyst a considerable amount of water was released. The water was noticeable in the initial period of activation. The initial activity of the catalyst was found to decrease slightly, however the decline being more noticeable at higher temperatures.

E. Reactants and Chemicals

Polymerization grade propylene gas, with a minimum purity of 99%, was used for chromatagraphic calibration purposes and in reaction studies. The gas was supplied by Matheson Co. in size 1-F cylinder at a pressure of 136 psig. Analysis of propylene gas by chromatography has shown 0.64% vol propane to be the major impurity. The gases used for calibration of the chromatagraph were 1-butene, cis-2-butene, trans-2 butene, ethylene, propane and 1,3 butadiene. All gases used in this study were dried prior to passing through the catalyst bed. Activated molecular sieve 5x and indicating drierite (10-20 mesh) used for drying purposes were supplied by Fisher Scientific Co.

Chromatographic columns packing 30% Hexamethylphosphoramide coated on chromosorb P, NAW, 60-80 mesh (catalogue no. CCP20) and copper tubing were supplied by Chromatographic Specialties Ltd.

Helium, used as carrier gas in the gas chromatographic analyses, and nitrogen used to condition the catalyst were high purity grade gases (99%) and were supplied in size L.B. cylinders by Central Oxygen Ltd.

Catalysts were prepared from ammonium paratungstate ($(NH_4)_6W_7O_{24}^6(H_2O)$), obtained from ICN pharmaceuticals, Inc., Plain view, N.Y. All supports used to prepare the catalyst, were supplied by Strem Chemicals Inc., MA, U.S.A. These supports are listed as follows.

γ-Alumina (high activity) containing 96% Al_2O_3 was obtained as 1/8" x 1/8" pellets and had a surface area of 200 m^2/g.

α-Alumina trihydrate was reported to contain 64.9% alumina, 34.7% combined water and 0.35% Na_2O.

-Silica-alumina contains 12% Al_2O_3 and 87% SiO_2 in the form of 1/8" x 1/8" pellets and reported to have a surface area of 425 m^2/g.

-Silica gel (large pores) was obtained as 8 mesh granules with a surface area of 340 m^2/g.

IV. RESULTS

The results of the experimental data collected in the previous section are presented in this section. More specifically, this section contains, the catalyst characterization studies, the effect of supporting material and oxide content of tungsten oxide catalysts for theconversion of propylene and yield of ethylene and 2-butene, the effect of temperature on conversion, yield and selectivity, product distribution and isomerization rates, the effect of space time (W/F) on conversion, yield and selectivity, and the effect of pressure on conversion and yield.

The experimental data were obtained by means of a quasi-isothermal fixed bed reactor at a pressure range of 3.041 to 7.124 atm. The steady state was inferred from the operating conditions and from product analysis. The effect of several variables, namely, the reaction temperature, T, the initial pressure of propylene $(P_p)_o$, and the space time, W/F, on the conversion of propylene, X, yield of ethylene and 2-butene were studied.

The conversion (X) was defined as the ratio of moles of propylene reacted per hour to the moles of propylene fed into the reactor per hour. The yield (Y) was expressed as the ratio of

the moles of ethylene and 2-butene formed per hour to the moles of propylene fed into the reactor per hour. The ratio of the moles of ethylene and 2-butene produced per hour to the moles of propylene reacted per hour has been defined as selectivity (S).

In order to obtain a consistent and reproducible results for disproportionation catalysts several factors should be observed. A poor reproducibility can be caused by many factors, including sensitivity of the catalyst to traces of poisons in the reactant (such as water and air) and dependence of the catalyst activity on activation procedures and previous experimental use. Moreover, the activity of the catalyst may not be constant in time because of the induction period or of the catalyst decay.

The activity of the catalyst was monitored periodically by passing propylene at 4.403 atm and 7.88 g.cat-hr/g.mol, determining the percentage conversion and comparing with a reference activity.

Heterogeneous disproportionation catalysts can function over a wide range of temperature, the optimum temperature depending on both the nature of the support and on the

oxide employed (48, 52). Tungsten and molybdenum oxides supported on silica or alumina are some of the catalysts reported in the literature (39, 45, 51).

Preliminary studies showed unsupported tungsten oxide or molybdenum oxide to have no activity for propylene disproportionation up to 550°C. Similarly, all supports used in this investigation (silica, silica-alumina, γ-alumina, α-alumina, kesielguhar and zirconium oxide) did not show any activity towards this reaction up to 600°C.

The disproportionation of propylene over catalyst containing 10 wt% MoO_3 supported on silica and -alumina showed a remarkable activity and selectivity as a function of temperature between 150-490°C at 4.403 atm and 7.88 g. cat-hr/g.mol. However, MoO_3/γ-Al_2O_3 was more active than MoO_3/SiO_2. Both catalyst exhibited a fast decline in activity.

Tungsten oxide supported on silica gel have been reported in the literature (82) to give a very high conversion

and selectivity for propylene disproportionation. In this study the disproportionation of propylene over a 10 wt% WO_3/SiO_2 showed a comparable activity with the literature.

Effect of Support Material

The effect of temperature on conversion of propylene was studied over catalysts containing 10 wt% WO_3, supported on different supports at a W/F ratio of 7.88 g.cat-hr/g.mol and 4.403 atm. Preliminary experiments showed that tungsten oxide supported on zirconium oxide, kesielguhar or -alumina was quite inactive for propylene disproportionation under experimental conditions. On the other hand, WO_3 supported on silica, silica-alumina and γ-alumina showed activity for this reaction. Experimental data obtained for these is given in Appendix (C). Figures 4-1 and 4-2 show the temperature effect on conversion and yield for catalytic disproportionation of propylene in the range from 150-494°C and over 10 wt% WO_3 supported on silica, silica-alumina and -alumina.

(i) WO_3/γ-alumina. From Figure 4 - 2 and the results shown in Appendix (C) it is clear that -alumina supported WO_3 was quite active at low tempeature i.e. 150°C. The activity of the catalyst increased with increasing temperature

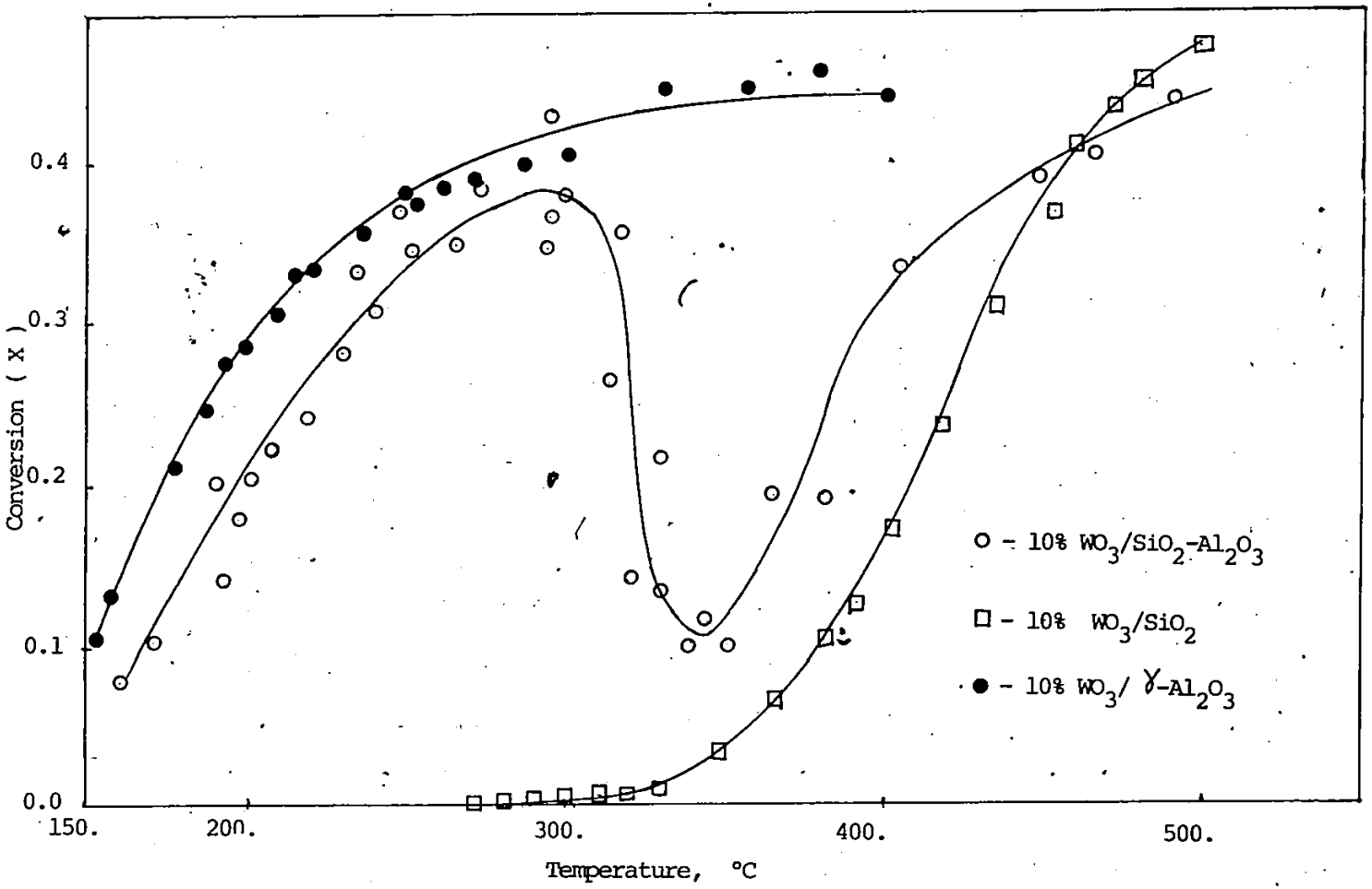

Figure 4-1 Effect of Temperature on Conversion of Propylene Over Supported Tungsten Oxide Catalysts at 4.403 atm, and 7.88 g.cat-hr/g.mol.

while its selectivity decreased. The yield followed the activity trend and reached a constant value of 36.5% at 275°C.

(ii) WO_3/SiO_2. The catalyst was active at higher temperatures i.e. 380°C. The conversion and yield increased as a function of temperature. Equilibrium conversion was obtained at 494°C while the yield was 42.5%

(iii) WO_3/Silica-alumina. This catalyst was active about 160°C and behaved in a manner similar to $WO_3/\gamma\text{-}Al_2O_3$ at lower temperature and WO_3/silica at higher temperatures. The activity increased with increasing temperature to a maximum yield of 35.6% at 275°C. As the temperature was further increased, the conversion and yield decreased to a minimum of 7.5% yield at 350°C. The catalyst then regained its activity to a maximum yield of 27.5 at 488°C. It was concluded that in silica-alumina supported tungsten oxide, there could be two types of active sites for disproportionation, site (I) and site (II). Site (I) is active at lower temperatures (160-290°C) and site (II) at higher temperature range (350-488°C). Site (I), which are active at low temperatures could be poisoned at higher temperatures because of the products formed from side reactions such as polymerization. $WO_3/SiO_2\text{-}Al_2O_3$ catalyst was found to deactivate faster than WO_3/γ- alumina. The catalyst could not regain its original activity after regeneration procedures. All three catalysts

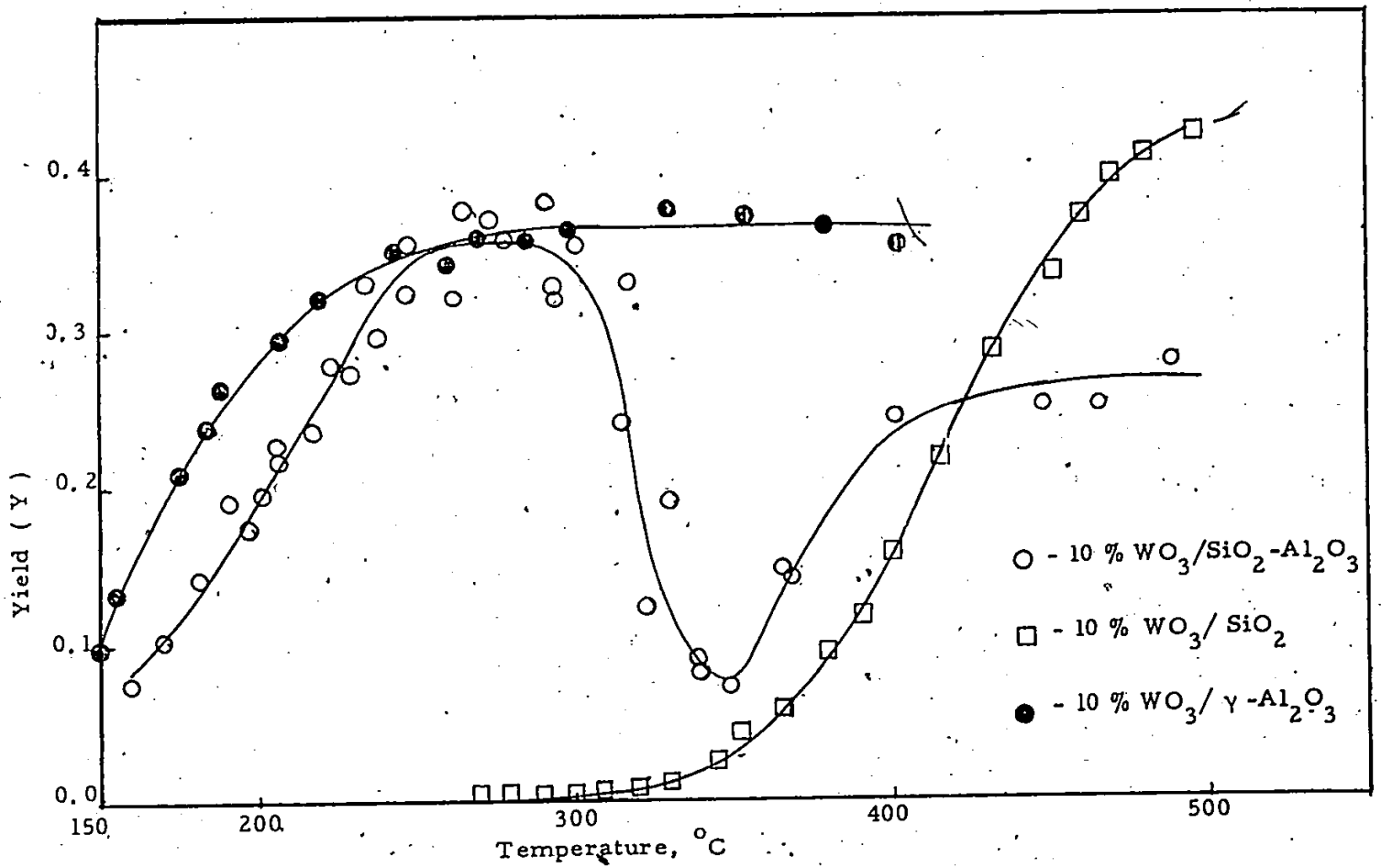

Figure 4-2 Effect of Temperature on Yield for Disproportionation of Propylene Over Supported Tungsten Oxide Catalysts at 4.4 atm and 7.88 g. cat.-hr/g. mol.

showed a decrease in selectivity with increasing temperature in the following order:

Silica-alumina > γ-alumina > silica.

A tunsten oxide catalyst supported on γ-alumina was chosen for the disproportionation of propylene, because it showed a remarkable activity and selectivity and could be used at relatively lower temperatures with comparable yields of ethylene and 2-butene. (Figure 1 and 2 and Appendix (C)).

Preliminary observation on a 10 wt% WO_3/γ-alumina showed that the catalyst activity increased as a function of the activation temperature in the range 450-650°C. A catalyst activated in a stream of dry nitrogen gave a maximum activity at 600°C. Similar activity was observed when the catalyst was activated in dry air. However, the air has to be purged completely from the reactor before introducing propylene. The initial period of activation (in air or nitrogen) was accompanied by the liberation of water vapor from the catalyst.

Effect of WO_3 Concentration

Figure 4-3 shows the conversion, yield and selectivity for disproportionation of propylene at 4.403 atm, 7.88 g.cat-hr/g.mole and 290°C for a series of WO_3/γ-alumina having concentrations ranging from 5 to 15 wt% WO_3. The results are given in Appendix (C). While the conversion increased with

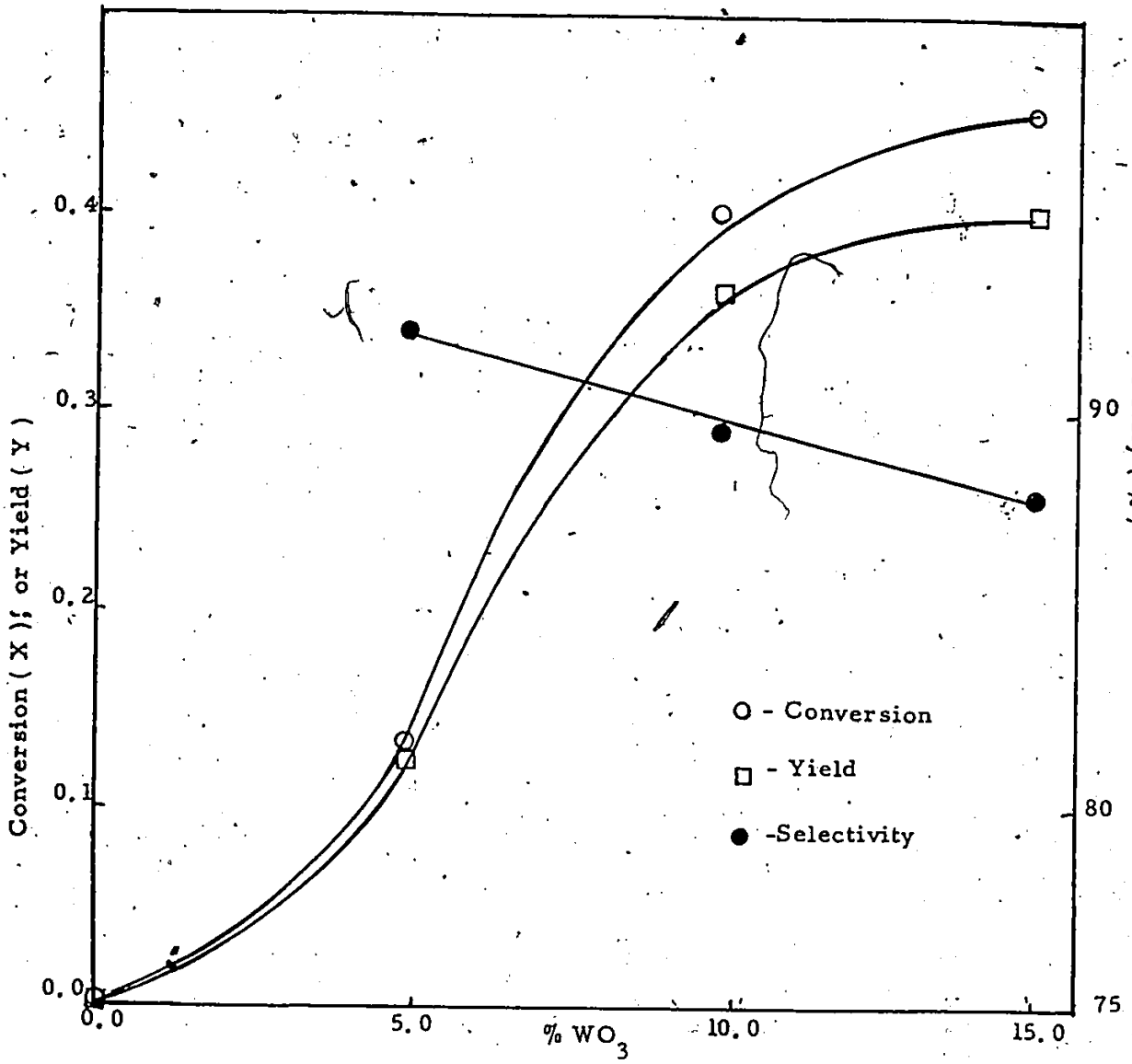

Figure 4-3 Effect of Tungsten Oxide Concentration Supported on -Alumina on Conversion, Yield and Selectivity for Disproportionation of Propylene at 4.403 atm, 290 °C and 7.88 g.cat-hr/g.mol.

the increase with the concentration of WO_3 on γ-alumina, selectivity decreased. It was observed that isomerization of 2-butene to 1-butene was less at lower concentration of WO_3. A catalyst containing 10 wt% WO_3/Al_2O_3 was chosen because of its activity and selectivity.

The catalystic disproportionation of propylene was studied over a 10 wt% $WO_3/\gamma-Al_2O_3$ at a W/F ratio of 7.88 g.cat-hr/g.mol, 4.403 atm and in the temperature range of 150-380°C. Results on this catalyst are given in Appendix (C). Figure 4-4 shows the effect of temperature on conversion, yield and selectivity.

The conversion increased from 9.5% at 150°C to 47.5% at 380°C. The selectivity, however decreased from 99.2 at 150°C to 79% at 380°C. The decrease in the selectivity was mainly as a result of isomerization of cis and trans-2-butene to 1-butene as shown in Table C-5 on page 197. Temperatures higher than 300°C, the production of liquid products (pentenes and hexenes) starts to become significant. Therefore the temperature range from 180-300°C was considered suitable for kinetic studies.

The effect of temperatures on the product distribution from the disproportionation of propylene over a 10 wt% WO_3/γ-alumina at 7.88 g.cat-hr/g.mol, 4.403 atm and temperatures

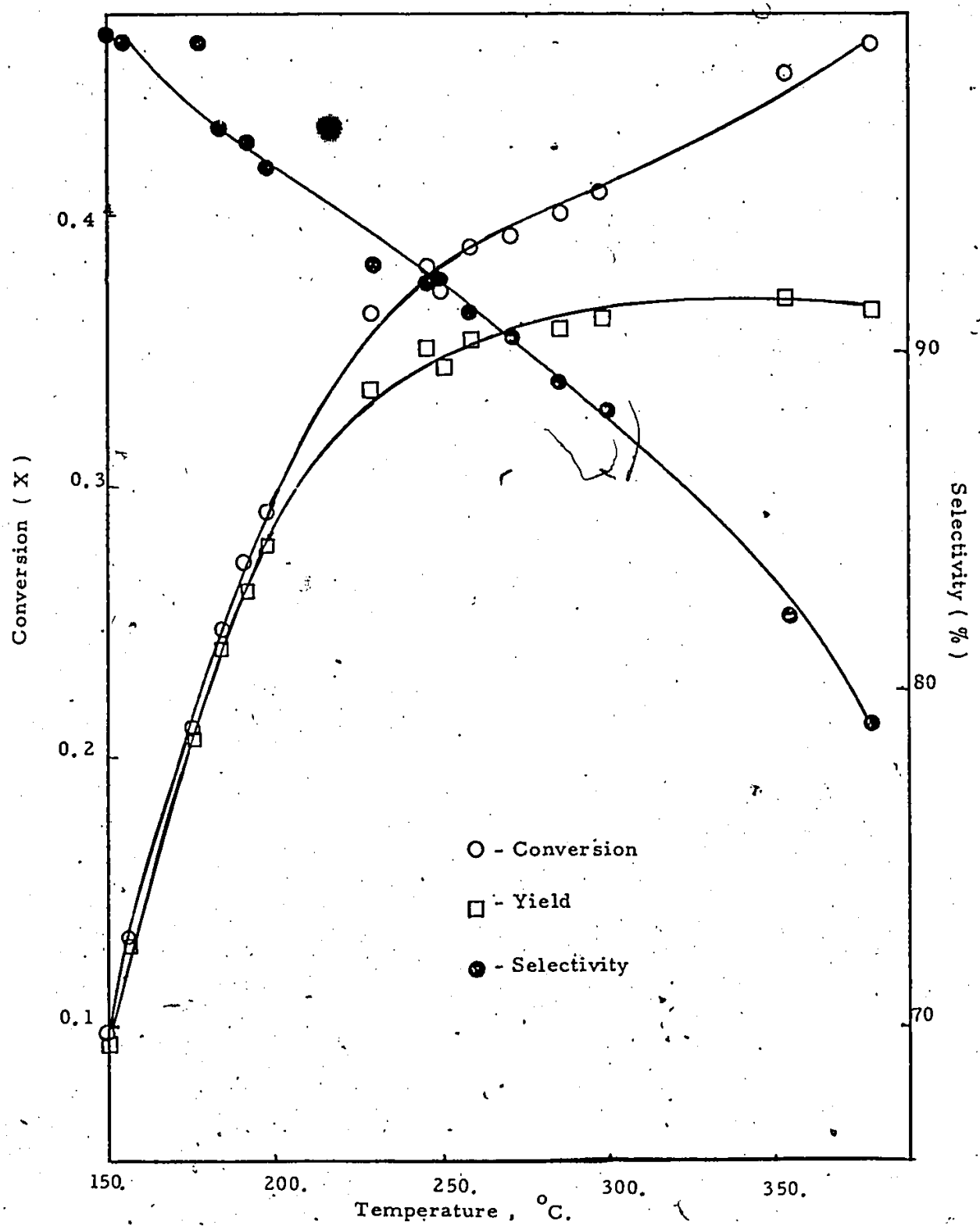

Figure 4-4 Effect of Temperature on Conversion , Yield and Selectivity for Disproportionation of Propylene Over 10 % WO_3/ γ-Al_2O_3

between 150-380°C is shown in Figure 4-5 and the results are given in Appendix (C). The distribution of products was not appreciably affected by the temperature. At lower temperatures (<218°C) the main products were ethylene and 2-butene. At higher temperatures (>218°C) the formation of products other than propane were due to isomerization, disproportionation and polymerization. Propane was formed by self hydrogenation accompanied by dehydrogenation of butene to give 1,3 butadiene. The molar ratio of ethylene to butene was about one at temperatures less than 310°C. The ratio decreased at higher temperatures due to the formation of higher molecular weight alkenes such as pentene and hexenes. The ratio of trans-2-butene to cis-2-butene was near equilibrium calculated at 0 psig. The rate of 1-butene formation as a function of temperature was faster than any other product. The isomerization of 2-butene to 1-butene favors the cis-2-butene as shown in Figure 4-5.

Figure 4-6 shows the effect of temperature on the percentage of double bond isomerization to 1-butene. The percentage of isomerization was defined as:

$$\% \text{ isomerization} = \frac{\text{mole fraction of 1-butene}}{\text{mole fraction of butenes}} \times 100 \quad (4\text{-}1)$$

The production of 1-butene increased linearly with increasing temperature. This indicates that the activation energy

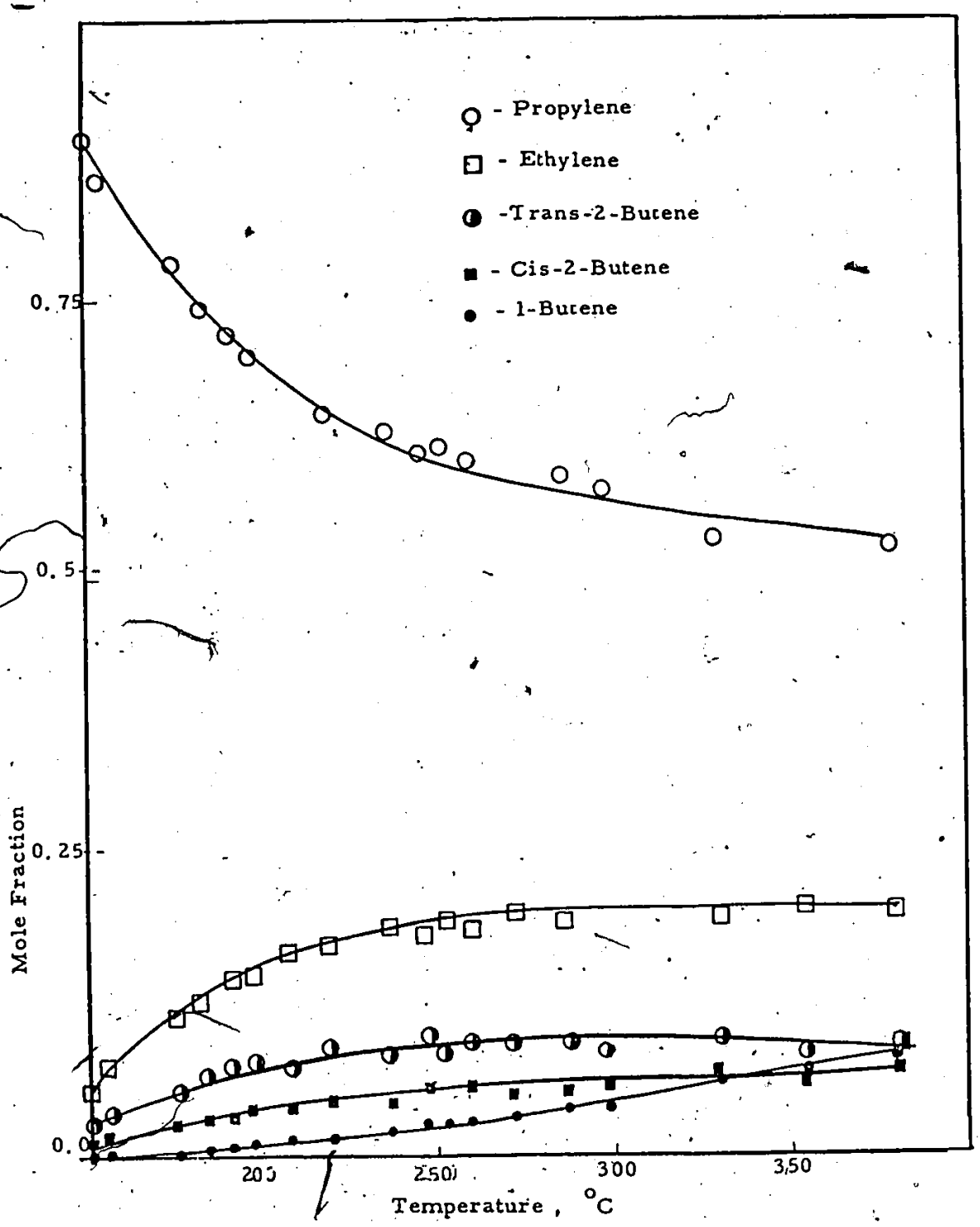

Figure 4-5 Effect of Temperature on Product Distribution for Disproportionation of Propylene at 4.4 atm and 7.88 g. cat-hr/g. mol.

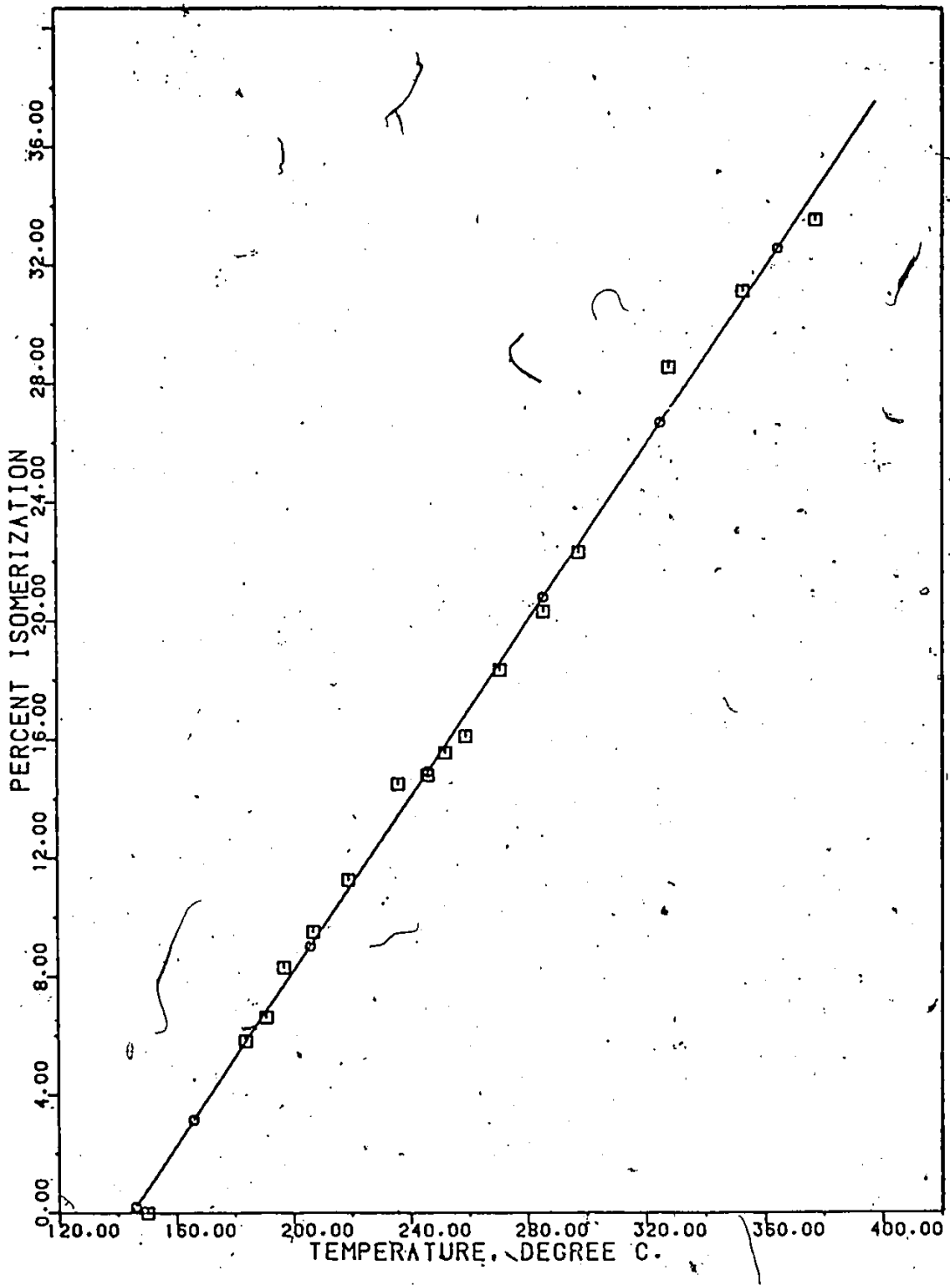

Figure 4-6 Effect of Temperature on the Isomerization of 2- Butene to 1-Butene.

for isomerization is higher than that of disporportionation.

Effect of Space Time

The effect of space time (W/F) on conversion, yield and selectivity for propylene disproportion over 10 wt% WO_3/ γ-alumina has been studied at 250°C, 5.763 atm in the space time range from 1.8 to 12.5 g.cat-hr/g.mol (Figure 4-7). The data are tabulated in Appendix (C). The conversion and yield increased slightly from 90% at 1.8 g.cat-hr/g.mol to 87.4% at 12.5 g.cat-hr/g.mole. The fraction of 1-butene in the product decreased with the decrease in space time. The ratio of trans to cis-2-butene at shorter contact time was lower than the equilibrium value. However, the ratio increased as the space time increased. Appendix (C-1 to C-4).

Effect of Total Pressure

The effect of initial pressure of propylene on conversion, yield and selectivity for propylene disproportionation over a 10 wt% WO_3/ γ-Al_2O_3 is given in Figure 4-8. Data are tabulated in Appendix (C). At 250°C and a W/F ratio of 10 g.cat-hr/g.mol, the initial pressure of propylene was varied from 3.041 to 7.124 atmospheres. Both conversion and selectivity increased as the pressure increased.

A 10 wt% WO_3/ γ-alumina was chosen to study the kinetics of catalytic disproportionation of propylene in a integral reactor. The kinetic data was collected in the temperature range 180-300°C, at pressures between 3.041 to 7.124 atm and space time of 1.06 to 17.88 g.cat-hr/g.mol.

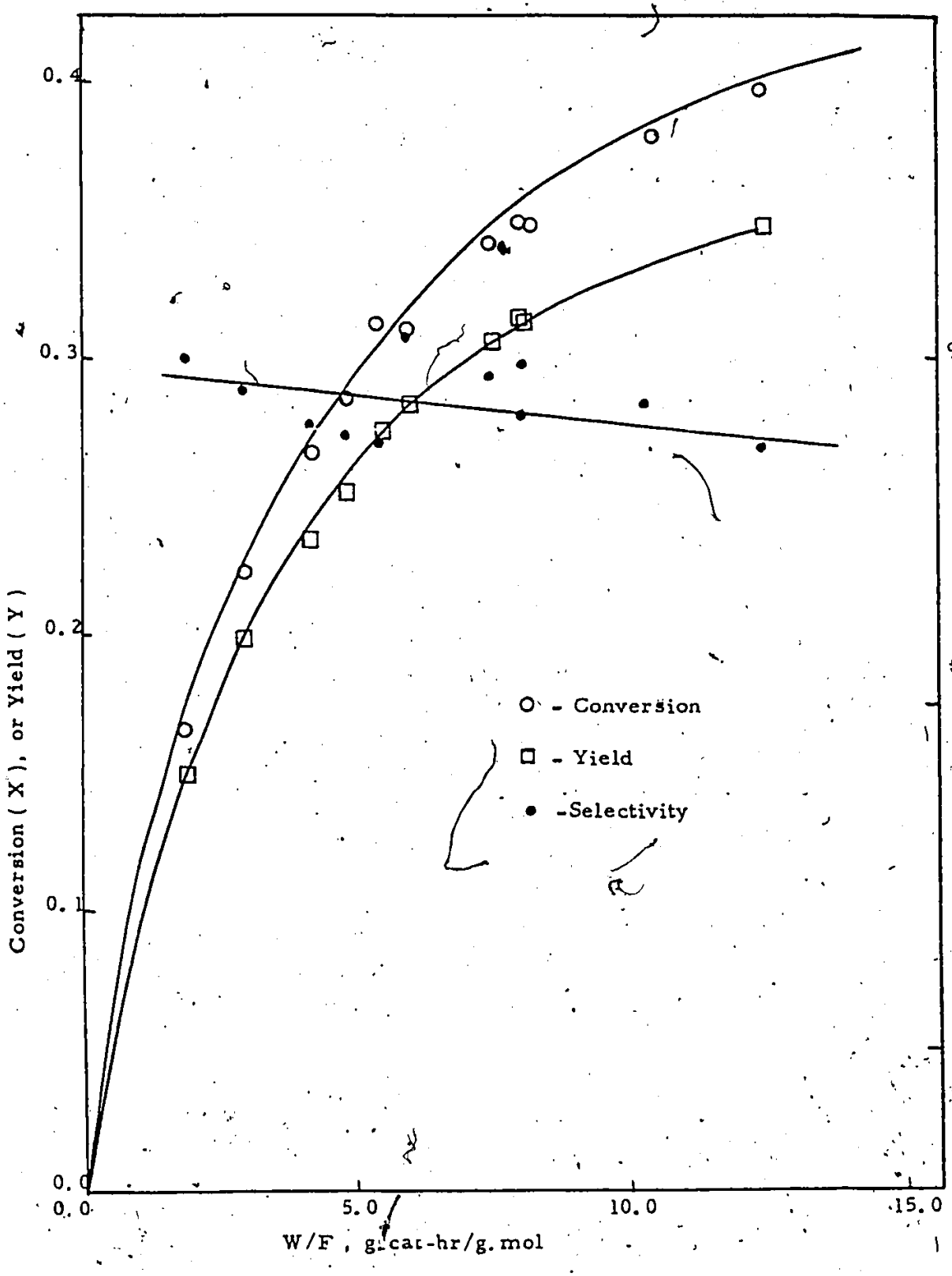

Figure 4-7 Effect of Space Time on Conversion, Yield and Selectivity for Disproportionation of Propylene at 250 °C and 5.76 atm.

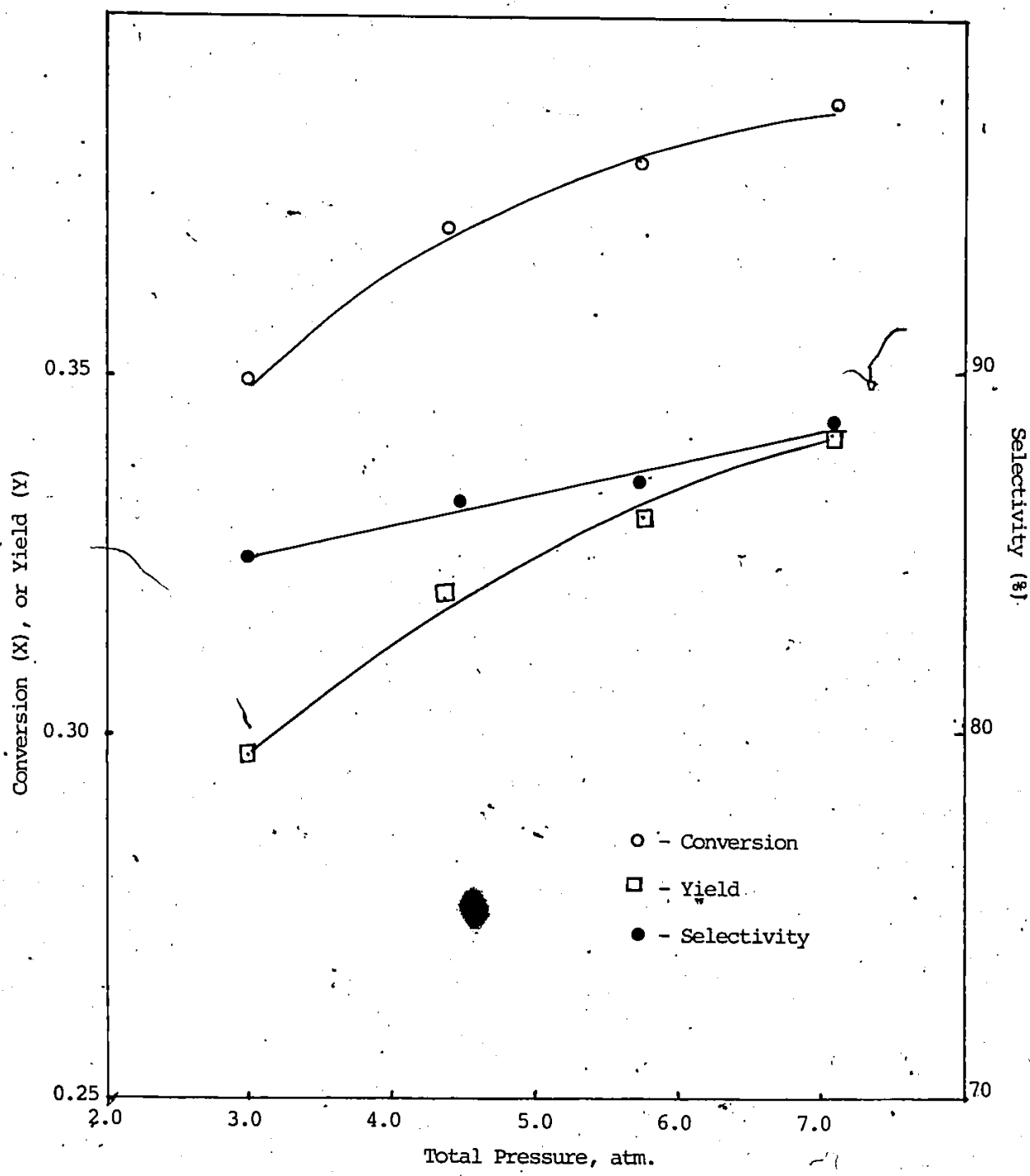

Figure 4-8 Effect of Total Pressure of Propylene on Conversion, Yield and Selectivity for Disproportionation of Propylene at 250 °C and 4.403 atm.

Characterization of the catalyst (10 wt% WO_3/γ-Al_2O_3)

The catalyst used in the kinetic disproportionation of propylene was 10 wt% WO_3 supported on γ-alumina.

The particle diameter (D_p) was determined using a micrometer. A random sample of 50 granules (28-42 mesh) was taken and the diameter of each granule was measured with a micrometer. The arithmetic average of these measurements gave the value of particle diameter as 0.486 mm. However, the average size from the screen sizes (28 and 42 Canadian Standard Sieve) was 0.478 mm.

The particle density (p) was determined by weighting 150 grandules and dividing it by the volume of 150 grandules calculated on the basis of average diameter of 0.486 mm and assuming the sphericity of the particle to be 0.9. The particle density thus determined was 1.664 g/cm^3.

A sample of the catalyst was analyzed by Bondar-Clegg and Company Ltd. The catalyst was found to contain 9.77 wt% WO_3 and 90.23 wt% γ-alumina. A semiquantitative analysis done by X-ray Fluorescence has shown the catalyst to contain the following impurities:

Na_2O, TiO_2	0.01-0.03%
Fe(Fe_2O_3)	0.1-0.3%
CaO, MgO	0.3-1.0%
Mn, Sr, Zr	Traces

The surface area and the pore volume distribution were determined by using a B.E.T. apparatus and microbalance by Technical Marketing Associates. The surface are (S_g) was found to be 146 m^2/g while the pore volume (V_g) was determined as 0.36 cm^3/g. The average pore radius (r) was calculated as follows:

$$r = \frac{2Vg}{sg} = \frac{2 \times 0.364\ cm^3/g}{1460000\ cm^2/g} = 50.0 \times 10^{-8}\ cm. \qquad (4\text{-}2)$$

$$r = 50.0\ \mu$$

The color of the WO_3/γ-alumina was similar to that of γ-alumina, bluish grey. The catalyst showed no yellowish color, characterisitcs of tungsten oxide. The catalyst turned to brownish grey after use.

The X-ray diffraction patterns of the catalyst were studied in the department of Geology, University of Ottawa. Table 1 shows the peak intensities and their 2-values for several catalysts. Four samples of the catalyst under different conditions were analyzed. The purpose was to detect for any active site responsible for the activity of the catalyst for the disproportionation of propylene. It was observed that all catalysts showed the peaks for -alumina. However none of them showed any WO_3 crystallite, which should appear at $2\theta = 23.5$.

The activity of the catalysts for disproportionation was found to be related to $Al_2(WO_4)_3$ complex, which appears in three peaks, 2θ = 38.3, 44.5 and 64.35. The activity of the catalyst increased with the increase in the intensities of those peaks. It was concluded that $Al_2(WO_4)_3$ formed at 600°C in a stream of dry nitrogen from the interaction of γ-alumina and WO_3 (Table 1).

TABLE 1

X Ray Diffraction Patterns of the Catalysts (9.77 wt% WO_3/γ- Al_2O_3)

Peak → 2θ	I 18.7	II 25.4	III 28.7	IV 38.3	V 44.5	VI 46.0	VII 64.35	VIII 65.5
1) Unactivated	2.04	0.83	3.91	1.69	2.73	10.8	0.	9.6
2) Activated	1.38	0.68	2.30	6.44	17.55	6.2	4.34	8.2
3) Activated Catalyst after use	1.43	1.1	3.0	6.93	14.28	9.61	2.4	9.9
4) Used deactivated catalyst	1.04	0.63	3.16	0.	0.	12.78	0.	10.8

Peaks IV, V, VII corresponds to $Al_2(WO_4)_3$

Peaks I, II, III, VI, VIII corresponds to γ- Al_2O_3

V. DISCUSSION

A. Kinetic Analysis of Experimental Data

The fundamental problem in the deisgn of catalytic processes is the relationship between the reaction rate and the operating variables. A kinetic model is a convenient and resonable representation of a reaction which is consistent with the experimental data and permits both interpolation and some extrapolation. A kinetic model is usually derived in terms of partial pressures of reactants and products based on the well-known Langmuir-Hindshelwood theory (65). When a reaction is catalyzed by a solid it is presumed that the actual combination of reactants occurs on the most active sites of the solid surface (66).

1. Steps in a Catalytic Reaction

When a chemical reaction takes place without the aid of a catalyst only chemical steps are involved. The case in quite different in a heterogeneous catalytic reaction. A complete study of the kinetics of catalytic rection involves the physical laws of diffusion and heat transfer as well as the behaviour of chemical reaction. The reaction of a porous solid catalyst may be involving the following steps:

1- Diffusion of the reactant from the main gas stream to the external surface of the catalyst.

2- Diffusion of the reactant through the catalyst pores into the interior of the porous catalyst.

3 - Adsorption of one or more of the reactants on the catalyst.

4 - A surface reaction between adsorbed reactants or one of the gaseous reactants and an adsorbed reactant on the catalyst surface.

5 - Desorption of the product molecules from the catalyst.

6 - Diffusion of the products from the interior of the catalyst to its surface.

7 - Diffusion of the products from the external surface of the catalyst to the main stream.

Steps 1,2,6 and 7 are definetely physical steps and the rates of these steps are determined by the laws of diffusion. Steps 3,4 and 5 are chemical steps, which give an insight into the nature of catalytic reaction. Since the seven steps listed above may take place in consequence, it is possible for any of them to control the overall rate of reaction. If the rate of one step is appreciably slower than the others, the overall rate will adjust itself to that of the slow step. This step is known as the rate controlling step or rate determining step, while the others are considered to be at equilibrium. Obviously in making a kinetic study of such a system it is necessary to take precautions to insure that physical steps such as external mass transfer and pore diffusion are not the controlling steps. Some methods have been proposed by various investigators (67,68) to insure the

minimization of the effect of physical steps on the reaction rate.

2. Factors Affecting the Rate Mechanism

Hougen (69) in an evaluation of kinetic models and kinetic rate data in a flow system for heterogeneous reactions stated five serious sources of error that might arise. These are summarized as follows and are arranged in order of decreasing importance:

1 - Variation in catalyst activity

2 - Neglect of pore diffusion

3 - Neglect of external resistance to mass and heat transfer

4 - Departure from plug flow

5 - Neglect of pressure drop due to flow

In order to derive a true rate equation, the above mentioned factors in addition to heterogeneous reactions catalyzed by the reactor should be either eliminated or minimized with appropriate corrective measures. These are discussed in the following section.

i. Variation in Catalytic Activity

There is no literature on tungsten oxide supported on γ-alumina catalysts, therefore it was necessary to determine the extent of deactivation of this catalyst with time. In order to achieve this, a few tests were made to

study the rate of deactivation as a function of time on stream at each of the temperatures used in this investigation. Figure 5-1 is a plot of percent conversion versus time on stream at 180, 210, 250 and 300°C. All runs were carried out at a pressure of 4.403 atm and space time of 7.88 g.cat-hr/g.mol. The results are given in Appendix (C).

Tungsten oxide catalyst are very sensitive to poison such as water and air (16). These catalysts show an induction period when supported on silica gel (29,38,43). However, this phenomena was not observed on WO_3/γ-alumina. The activity of the catalyst used in this study was fairly constant at 180 to 250°C. However, at 300°C the catalyst lost its activity especially when operated at higher values of space time. This decline in activity was suspected because of polymerization products which deactivate active sites on the surface of the catalyst. Carbon deposition was observed only when there was a malfunction in the apparatus. In that case the catalyst was reactivated in a stream of dry air at 600°C, before being used again. The catalyst had a stable activity for all temperatures over a period of five hours with gradual loss of activity thereafter. The activity of the catalyst was monitored by checking whether the activity remained the same as of initial runs at different times in the experimental program.

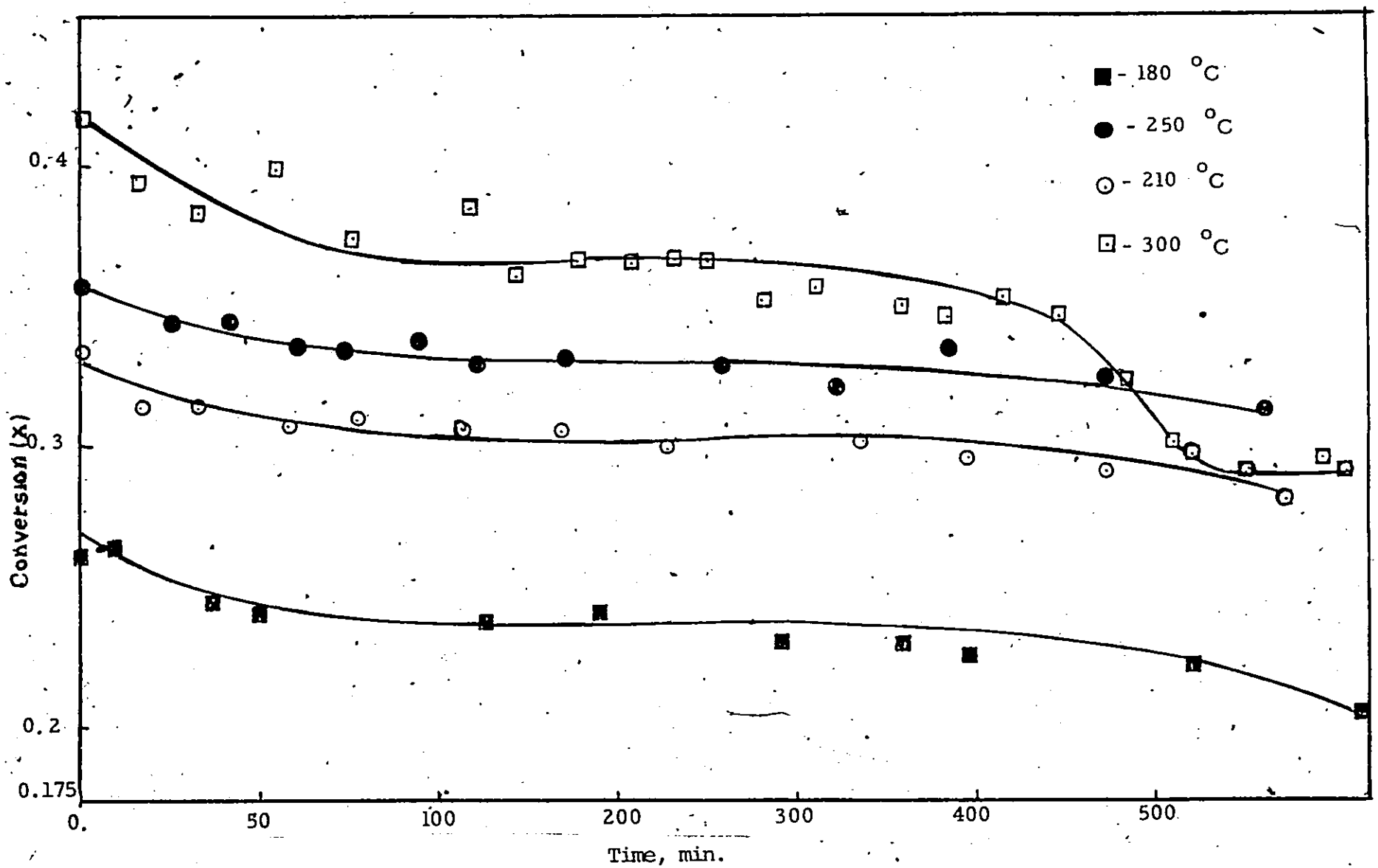

Figure 5-1 Activity as a Function of Time for Propylene Disproportionation Over 10 wt%/ -Alumina at 4.403 atm and 7.88 g.cat-hr/g.mol.

Effect of Internal Diffusion

In a heterogeneous catalyzed reaction, most of the reaction occurs on the inner surface of the porous structure of a catalyst. The diffusion of reactants into and that of the products out of the pores could become an important factor in controlling the reaction rate. Depending on whether the mean free path between intermolecular collisions is small or large compared with the pore radius, two kinds of diffusion in pores are possible. These are known as (i) molecular diffusion, and (ii) Knudsen diffusion.

Molecular Diffusion

It predominates with all catalysts at very high pressures ($\sim$ 100 atm) or atmospheric pressure with very large pores ($\sim$ 5000 ^{o}A radius). The effect of molecular diffusion in the present study was minimized by using high velocity of gas stream passing through the catalyst bed. The effect of molecular diffusion has been studied by varying the feed rate while the reciprocal of space velocity was kept constant. Figure (5-2) shows that the conversion did not vary with the flow rate, and it was assumed that molecular diffusion had negligible influence on the reaction rate when the flow rates greater than 0.4 g.mol/hr. was chosen. The results are given in Appendix (C).

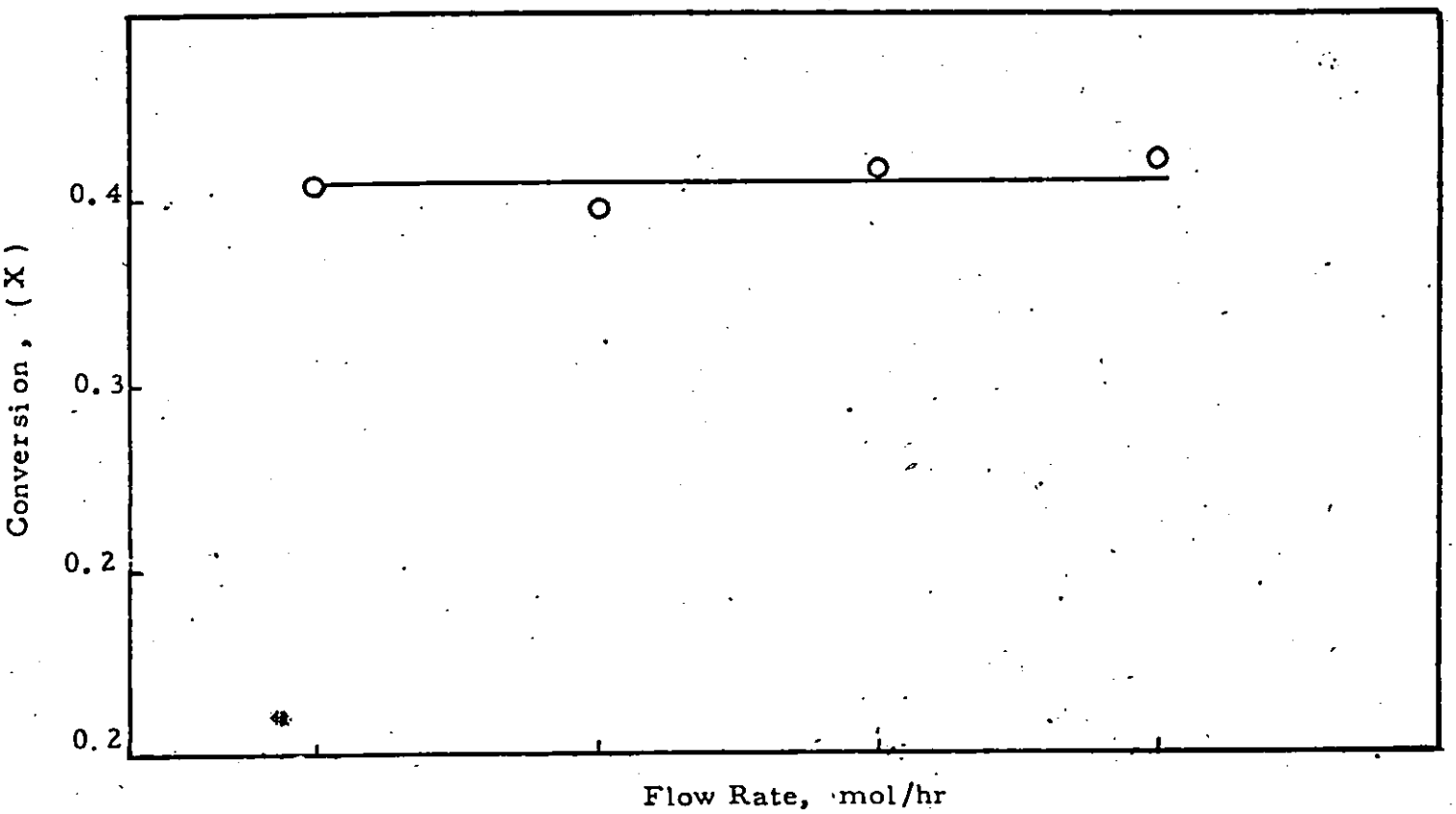

Figure 5-2 Effect of Flow Rate on Conversion of Propylene at W/F, 10 g. cat-hr/g. mol 300 °C, and 4.4 atm.

(ii) Knudsen Diffusion

The Knudsen diffusivity depends on the molecular velocity and the pore radius, and is independent of pressure. If the mean free path for gases is of the order of 1000 ^{o}A at atmospheric pressure, diffusion in micropores of the catalyst will be predominantly by Knudsen mechanism. The effective Knudsen diffusivity is given as:

$$D_{k,eff} = 19400 \frac{\beta^2}{\tau S_g \rho_p} \sqrt{\frac{T}{M}} \qquad (5\text{-}1)$$

where β = porosity of catalyst

τ = tortuosity of catalyst

S_g = specific surface area of catalyst

ρ_p = catalyst particle density

T = absolute temperature

M = molecular weight of the gas mixture

The effect of Knudsen diffusion can be evaluated from the knowledge of effectiveness factor of the catalyst. This factor is defined as the ratio of the actual reaction rate per unit mass of the catalyst to the rate which would result when the concentration at all interior surfaces was the same as the exterior surface of the catalyst.

An estimate of the effectiveness factor for the catalyst used in this study was calculated by using a modified-Thiele method (67), and a value of nearly unity was obtained. The detailed calculations are given in Appendix (E). The importance of Knudsen diffusion was determined by studying the effect of particle size on the reaction rate. If pore diffusion effects are significant, a decreased particle size results in increased reaction rate due to shorter average pore length in smaller particles. Figure 5-3 shows a plot of percent propylene conversion versus particle size at 300°C, 4.403 atm and a W/F ratio of 10 g. cat-hr/g.mol. This plot shows particle diameter to have little or no effect on conversion and therefore Knudsen diffusion effect was not rate controlling step and hence could be neglected between 375 and 1000u. Catalysts of -28+42 mesh size (478 μ) were used for Kinetic studies. Results of Figure 5-3 are given in Appendix (C).

iii. External Diffusion

The partial pressure and temperature at the gas-solid interface which assumed to be that of the bulk, may differ because of the resistance due to heat and mass transfer effects. It is therefore necessary to evaluate and eliminate these resistances. The rate of mass and heat transfer per unit mass are defined by:

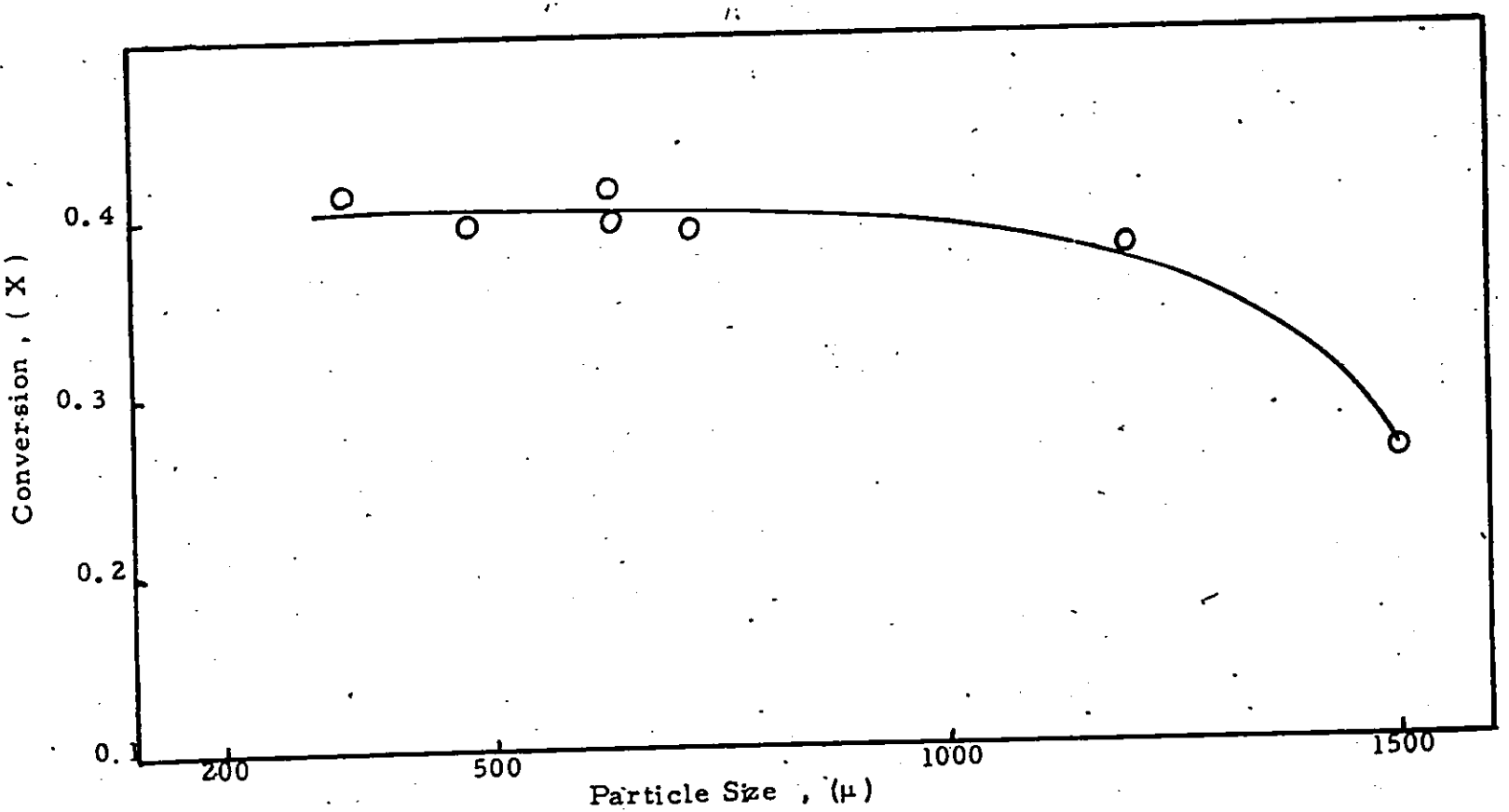

Figure 5-3 Effect of Particle Size on Conversion of Propylene at 300 °C, 4.4 atm and 10 g.cat-hr/g.mol.

$$r_{m_A} = k_{G_A} a_m \phi (P_A - P_{Ai}) \qquad (5\text{-}2)$$

and

$$g_{m_A} = r_{m_A} \Delta H_A = h_G a_m \phi (T - T_i) \qquad (5\text{-}3)$$

where

r_{m_A} = rate of reaction or mass transfer of A per unit mass of catalyst

g_{m_A} = heat transfer due to heat of reaction per unit mass of catalyst

k_{G_A} = mass transfer coefficient for component

h_G = heat transfer coefficient per unit - exterior surface of catalyst particle

a_m = external surface area of the catalyst per unit mass

ϕ = shape factor, equal to 1.0 for spheres and 0.9 for irregular grains

P_A = partial pressure of component A in the ambient stream

P_{Ai} = partial pressure of component A at the catalyst surface

T = temperature of the ambient stream

T_i = temperature of the catalyst

The transfer coefficients h_G and k_G can be calculated from the dimensionless Chilton-Colburn (70) j-factor.

$$j_D = \frac{k_G P_{fA}}{G_m} \left(\frac{\mu}{\rho D_{AM}}\right)^{2/3}_f \qquad (5\text{-}4)$$

$$j_H = \left(\frac{h_G}{C_p G_m}\right) \left(\frac{C_p \mu}{K}\right)^{2/3}_f \qquad (5\text{-}5)$$

where

P_{fA} = film pressure factor, defined by equation (5-11)

μ = viscosity of the gas

ρ = density of the gas

C_p = specific heat of the gas

D_{AM} = average diffusion coefficient of component A

K = thermal conductivity of the gas

G_m = the molal mass velocity of gas based on the total cross-sectional area of the catalyst bed

$\frac{C_p \mu}{K}$ = the dimensionless Prandtl number

$\frac{\mu}{\rho D_{AM}}$ = Schmidt number

and subscript f indicates properties at the average conditions of the gas film for $D_p G_m/\mu$ >350

j_H and j_D can be obtained from Gramson, Thodos and Hougen (71) equation: $J_H = 1.06 \left(\frac{D_p G_m}{\mu}\right)^{-0.41}$ (5-6)

$$j_D = 0.99 \left(\frac{D_p G_m}{\mu}\right)^{-0.41} \qquad (5\text{-}7)$$

for $D_p G_m/\mu < 350$

j_H and j_D can be obtained from Wilke and Hougen (72) equations:

$$j_H = 1.95 \left(\frac{D_p G_m}{\mu}\right)^{-0.51} \qquad (5\text{-}8)$$

$$j_D = 1.82 \left(\frac{D_p G_m}{\mu}\right)^{-0.51} \qquad (5\text{-}9)$$

where $(D_p G_m/\mu)$ modified Reynolds

D_p = effective particle diameter $\sqrt{\frac{a_p}{\pi}}$

a_p = average surface area per particle

The term P_{fA}, the film pressure factor for component A which account for the flow of the fluid in equation (5-4) for the reaction

$$aA = rR + sS \qquad (5\text{-}10),$$

is defined by:

$$P_{fA} = \frac{(\pi + \partial_A P_A) - (\pi + \partial_A P_{Ai})}{\ln \frac{(\pi + \partial_A P_A)}{(\pi \quad \partial_A P_{Ai})}} \qquad (5\text{-}11)$$

where $\partial = \frac{r + s - a}{a}$ (5-12)

If the ratio of $(\pi + \partial_A P_A) / (\pi + \partial_A P_{Ai})$ is less than 1.2, the arithmatic mean is sufficiently accurate for practical purposes.

Yoshida et al. (73) have developed a simple and systematic method for evaluating the drop in pressure and temperature between the bulk-gas stream and the external catalyst particle. They used modified Reynolds number and dimensionless Prandtland Schmidt numbers to calculate the pressure and temperature gradients as follows:

$$\Delta T = Q(j_H)^{-1} (P_r)_f^{2/3} \qquad (5\text{-}13)$$

$$\Delta Y = \frac{\Delta P_A}{P_A} = R(j_D)^{-1} Y_{fA} (Sc)^{2/3} \qquad (5\text{-}14)$$

where ΔT = temperature drop across the film

ΔP_A = drop in pressure of component A across the gas film

$$Q = \frac{r_{m_A} \Delta H_A}{a_m \phi C_p G_m} \qquad (5\text{-}15)$$

P_r = Prandtl number = $\frac{C_p \mu}{K}$

$$R = \frac{r_{m_A}}{a_m \phi G_m} \qquad (5\text{-}16)$$

$$Y_{fa} = \frac{P_{fA}}{\pi}$$

Sc = Schmidt number = $\frac{\mu}{\rho D_{AM}}$

The j-factors are related to the modified Reynolds number ($G_m / a_v \phi \mu$) as follows:

For $0.01 < Re < 50$

$$j_D = 0.84\ Re^{-0.51} \qquad (5\text{-}17)$$

For $50 < Re < 1000$

$$j_D = 0.57\ Re^{-0.41} \qquad (5\text{-}18)$$

and $$j_H = 1.076\ j_D \qquad (5\text{-}19)$$

The terms ΔT and Q have the dimensions of temperature while all other terms are dimensionless.

Yoshida et al. (73) used the data of many investigators to find the radiant fall in a narrow band on ΔY_A vs R and ΔT vs Q plot indicating that R and Q are the most significant factors in controlling the pressure and temperature gradients respectively.

Both the temperature and pressure drop across the gas film are proportional to $r_A D_p^{\ n} \quad G_m^{\ n-1}$; since n is either 0.41 or 0.51, it would be possible to eliminate heat and mass transfer resistances effectively by decreasing the particle size and increasing the gas flow rates.

A sample calculation based on the method of Yoshida et al. (73) for estimating the temperature and pressure drops from the bulk gas stream to the surface of the catalyst is

given in Appendix (F). The highest partial pressure gradient thus calculated was found to be of the order of 0.0001 atm and the temperature at the catalyst surface was calculated to be 0.1 ^{o}C higher than that of the main gas stream. Hence, these effects could be considered negligible.

iv. Appreciable Departure from Plug Flow

For a continuous plug flow reactor operating at steady state, the relationship between the reciprocal of space velocity (W/F) and conversion (X) is obtained by considering mass balance in an elementary section of the reactor containing an increment mass of catalyst dW in which a conversion dX is produced.

Thus: $FdX = rdW$ (5-20)

where r = reaction rate, moles / mass of catalyst-time

W = mass of catalyst in the reactor

F = feed rate, moles/time

X = conversion, moles/moles of feed

Integration yields

$$W/F = \int_{o}^{x} \frac{dX}{r} \qquad (5\text{-}21)$$

When deriving equation (5-21) it was assumed that the gases were passing through the catalyst bed under the condition of plug flow, i.e. that the velocity profile across the width

of the reactor is flat. The flow patterns in packed beds are affected by the packing shape, packing depth, the position of flow, packing size, and the tube size. It is reported that the deviation from a uniform velocity profile is not very significatn if the ratio of the tube to pellet diameter is greater than 30 (74). The ratio of reactor to particle diameter is the present study was about 26. In addition, a porous stainless steel plate was inserted at the enterence of the reactor to break the velocity patterns of the incoming gases. Therefore, it can be assumed that no appreciable error would be caused by assuming a plug flow.

V. Neglect of Pressure Drop Due to Flow

By increasing the gas flow rate, several sources of errors could be eliminated or minimized. however, this could cause an increase in pressure drop through the catalyst bed. The difference between inlet and outlet pressure of the catalytic bed would therefore become very large. the basis of arithmetic or logarithmic mean of inlet and outlet pressures might not be corrected in determining the total pressure of reaction.

pressures might not be correct in determining the total pressure of reaction.

The pressure drop through a packed bed is given by Ergun equation (75) for either laminar or turbulent flow. In this investigation, the pressure drop through the catalyst bed was measured experimentally. The maximum pressure drop was less than 0.2 atm for the highest flow rate used. Further calculations using Ergun equation and the most severe conditions showed the pressure drop to be 0.001 atm. The reaction pressure used in this study was the outlet pressure of the reactor.

vi. Homogeneous Reaction

Propylene disproportionation reactions require very high temperature to occur. Schneider et al. (9) reported the non-catalytic pyrolysis of propylene at 725°C and 0.2 atm. In this study, blank runs of propylene at 500°C in an empty reactor did not produce any detectable products beside propylene.

3. Correlation of Rate Equations

Among the various steps in heterogeneous catalytic reactions as described earlier, the diffusion steps (1,2,6 and 7) which are physical steps were either eliminated or

minimized by appropriate selection of physical conditions (flow rate, particle size, etc.). The remaining steps (3, 4 and 5) which are chemical steps were examined in detail in order to determine which one offered the greatest resistance to the overall reaction. For each of the three steps, namely, adsorption of reactants, surface reactions and desorption of products, several mechanisms can be postulated depending on whether one or both of the reactants are adsorbed on the catalyst surface, and whether these molecules are dissociated or not.

i. Adsorption Isotherm

Chemical adsorption has two major applications in the study of heterogeneous catalytic reactions. It has been found useful in measuring the fraction of the catalyst surface which consists of a catalytically active component as compared to the portion which acts as a support or as a promoter.

In order to develop the kinetics of gas-solid catalytic reactions, it is necessary to have available an expression relating the rate and the amount of adsorption to the partial pressure of the gas in contact with the adsorbed layer on the surface.

At equilibrium and at constant temperature the relationship between pressure and quantity adsorbed is known as an adsorption isotherm. Three theoretical isotherms, those of Langmuir, Freundlich and Temkin, are well known. Each is characterized by certain assumptions and each is applicable to certain experimental system. Among these the Langmuir isotherm has been widely used for its simplicity. Some of the key assumptions are: 1. adsorption occurs on a finite number of equivalent sites on a uniform surface, 2. the adsorption energy of all sites is the same and is unaffected by adsorption on neighboring sites, 3. each site can adsorb one and only one gas molecule, and 4. all adsorption occur by the same mechanism.

At constant temperature assuming that dissociation does not occur upon adsorption the rates of adsorption (r_{A_a}) and desorption (r_{A_d}) of component A are given by: (65)

$$r_{A_a} = K_{A_a} P_A (1-\theta_A) \qquad (5\text{-}22)$$

and $$r_{A_d} = K_{A_d} \theta_A \qquad (5\text{-}23)$$

and therefore at equilibrium $$\theta_A = \frac{K_A P_A}{1 + K_A P_A} \qquad (5\text{-}24)$$

where $K_A = K_{A_a} / K_{A_d}$.

For a system with many components

$$\theta_A = \frac{K_A P_A}{1 + \Sigma K_I P_I} \qquad (5\text{-}25)$$

where θ_A = the fraction of the catalyst surface covered by A

K_A = the equilibrium adsorption constant of component A

P_A = the partial pressure of component A in the gas phase

K_I = the equilibrium adsorption constant of component I (including A)

P_I = the partial pressure of component I (including A) in the gas phase.

ii. Langmuir-Hinshelwood Mechanism

The derivation of Hougen-Watson type rate equations is based on the Langmuir mechanism for adsorption (99) and on the assumption that only one of the reaction steps is the rate controlling step, all the other steps are assumed to be at equilibrium.

The Langmuir-Hinshelwood mechanism (67) for a reaction between adsorbed A and adsorbed B occurs as follows:

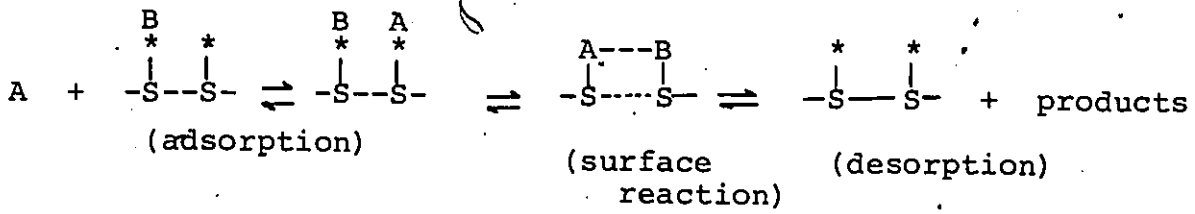

Another type of mechanism for surface reaction is known as Langmuir-Rideal mechanism, which occurs between adsorbed B and A in the gas phase. This mechanism may occur as follows:

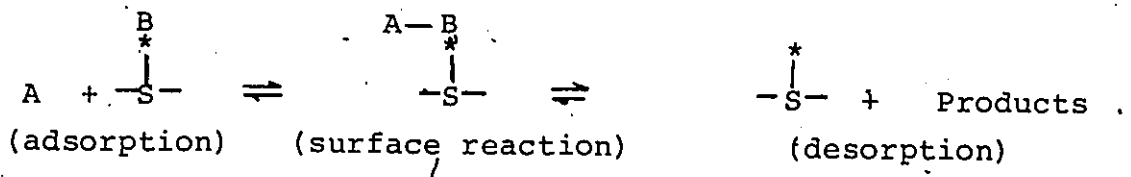

As an example, a rate equation for a bimolecular reaction considered in this study $2A \rightarrow R + S$ is developed (76,88). The rate determining step of this reaction is assumed to be a surface reaction between two adsorbed A molecules to give R and S. The forward reaction is proportional to the concentration of adjacent adsorbed A-A pairs, C_{AA}.

$$r_f = k C_{AA} \qquad (5\text{-}26)$$

where r_f = forward reaction rate, moles of product formed per unit time per unit mass of catalyst

k = reaction velocity constant for surface reaction

C_{AA} = molal concentration of adjacently A-A molecules per unit mass of catalyst.

Since the surface concentration of A is C_A and each adsorbed A is surrounded by S sites including vacant and occupied, the coverage sites by another A molecule is θ_A, the surface concentration of A-A pairs would be

$$C_{AA} = C_A \cdot \theta_A \cdot S = C_A \cdot S \cdot C_A/L = \frac{S}{L} \cdot C_A^2 \quad (5\text{-}27)$$

where L = total molal active sites per unit mass of catalyst

and $\theta_A = C_A L$.

Substituting equation (5-27) in equation (5-26) gives:

$$r_f = \frac{k.S}{L} \cdot C_A^2 = kSL \cdot \theta_A^2 \quad (5\text{-}28)$$

θ_A can be obtained by substituting equation (5-25)

$$r_f = \frac{kSL \; K_A^2 \; P_A^2}{(1 + K_A P_A + K_R P_R + K_S P_S)} \quad (5\text{-}29)$$

If the reverse reaction is included, the net forward reaction rate becomes:

$$r = \frac{kSL \; K_A^2 \; (P_A^2 - P_R P_S/K)}{(1 + K_A P_A + K_R P_R + K_S P_S)^2} \quad (5\text{-}30)$$

where K = thermodynamic equilibrium constant for the overall reaction.

The initial rate, defined as the rate when the partial pressure of products is zero, for this reaction:

$$r_o = \frac{kSL\ K_A^2\ P_A^2}{(1 + K_A P_A)^2} \qquad (5\text{-}31)$$

Yang and Hougen (77) and Hougen and Watson (76) presented a convenient method for developing the simplified expressions similar to equation (5-30). Their procedure shows that, in general, rate expressions may be developed by a combination of three terms, a kinetic term, a potential term and an adsorption term arranged in the following manner:

$$r = \frac{\text{(kinetic term) (potential term)}}{\text{(absorption term)}^n} \qquad (5\text{-}32)$$

The kinetic term includes all factors appearing in the numerator of the rate equation other than the driving potential. The driving potential in any rate equation fulfills the conditions of becoming zero under equilibrium conditions. The adsorption term includes any adsorption reactant or products. It is raised to the power n, where n is the number of active sites involved in the reaction.

Following the method of Hougen and Watson (76), the rate equations for the possible reaction mechanisms for the catalytic disproportionation of propylene to ethylene and

butene have been derived (16 models). These models are presented in Table 2.

iii. Assumptions in Deriving the Rate Equations

In the development of the rate equations proposed, we have made the following assumptions:

1. The resistance to the physical steps is small and only chemical steps control the reaction.
2. The resistance to diffusion is negligible that the partial pressure at the interface if practically the same as that of the bulk stream.
3. Only one of the steps of the reaction is rate controlling and there is no shift of the rate determining step during the reaction.
4. The specific rate constant and the equilibrium adsorption constants are independent of total pressure.

iv. Model Discrimination of Rate Equation

Modelling of reaction is vital for the optimum design and operation of process reactors as well as for analysis of mechanisms of heterogeneous catalytic reactions. Recently a number of modellng studies have been published and many useful techniques have been developed. These modelling techniques consist of two principal steps: (a) identification of adequate models, and (b) estimation of the parameters in the best model obtained in the first step.

TABLE - 2

Rate Equation Derived Using Hougen-Watson Method

No	Rate Controlling Step	Mechanism	Rate Equation	Linearized Initial Rate
1	Adsorption of Propylene	Surface reaction between molecularly adsorbed propylene and propylene in gas phase	$r = \frac{k(P_p - P_E P_B / K P_p)}{(1 + K_E P_E + K_B P_B + \frac{K_p P_E P_B}{K P_p})}$	$ro = /K P_p$
2	Adsorption of Propylene	Surface reaction between two molecularly adsorbed propylene molecules	$r = \frac{K(P_p - P_E P_B / K P_p}{(1 + K_p P_p + K_E P_E + K_B P_B \frac{+K_p P_E P_B}{K P_p})}$	$\frac{P_p}{ro} = \frac{1}{K} + \frac{K_p P_p}{K}$
3	Adsorption of Propylene	Surface reaction between atomically adsorbed propylene and molecularly adsorbed propylyene molecules	$r = \frac{K(P_p - P_b P_E / K P_p)}{(1 + K_E P_E + K_B P_B + K_p P_p + \sqrt{\frac{K_p P_E P_B}{K P_p}})^2}$	$\frac{P_p}{ro} = \frac{1}{K} + \frac{K_p P_p}{K}$
4	Adsorption of Propylene	Surface reaction between atomatically adsorbed propylene and propylene in gas phase	$r = \frac{k(P_p - P_B P_E / K P_p)}{(1 + K_E P_E + K_B P_B + \sqrt{\frac{K_p P_E P_B}{K P_p}})^2}$	$ro = K P_p$
5	Adsorption of Propylene	Surface reaction between atomically adsorbed propylene and molecularly adsorbed propylene	$r = \frac{k(P_p - P_E P_B / K P_p)}{(1 + \sqrt{K_p P_p} + K_E P_E + K_B P_B + \frac{K_p P_E P_B}{K P_p})}$	$\frac{P_p}{ro} = 1 + \frac{\sqrt{K_p}}{k} P_p$

No	Rate Controlling Step	Mechanism	Rate Equation	Linearized Initial Rate
6	Desorption of Ethylene	Surface reaction between two molecularly adsorbed molecules or one molecule adsorbed	$r=\frac{kK(P_p^2/P_B-P_E/K)}{(1+K_BP_B+K_pP_p+KP_EP_p^2/P_B)}$	ro= K
7	Desorption of Ethylene	Surface reaction between atomically adsorbed propylene and a molecularly adsorbed molecules	$r=\frac{kK(P_p^2/P_B-P_E/K)}{(1+K_BP_B+K_pP_p+\sqrt{K_pP_p+K\frac{K_EP_p}{P_B}}^2)}$	ro= K
8	Desorption of Ethylene	Surface reaction between atomically adsorbed propylene and propylene in gas phase	$r=\frac{kK(P_p^2/P_E-P_B/K)}{(1+\sqrt{K_pP_p}+K_BP_B+KK_EP_p^2/P_B)}$	ro= K
9	Desorption of Butene	Surface reaction between two molecularly adsorbed propylene or one molecule adsorbed	$r=\frac{kK(P_p^2/P_E-P_B/K)}{(1+K_pP_p+K_EP_E+KK_BP_p^2/P_E)}$	ro= K
10	Desorption of Butene	Surface reaction between molecularly adsorbed propylene and atomically adsorbed propylene	$r=\frac{kK(P_p^2/P_E-P_B/K)}{(1+K_EP_E+K_pP_p+\sqrt{K_pP_p}+KK_BP_p^2/P_E)}$	ro= K
11	Desorption of Butene	Surface reaction between atomically adsorbed propylene and propylene in the gas phase	$r=\frac{kK(P_p^2/P_E-P_B/K)}{(1+K_EP_E+\sqrt{K_pP_p}+KK_BP_p^2/P_E)}$	ro= K

No	Rate Controlling Step	Mechanism	Rate Equation	Linearized Initial Rate
12	Surface Reaction	Surface reaction between two molecularly adsorbed molecules	$r=kK_p(P_p^2-P_EP_B/K)/(1+K_pP_p+K_BP_B+K_EP_E)^2$	$\frac{P_p}{\sqrt{ro}}=\frac{1}{K}+\frac{K_p}{K}P_p$
13	Surface Reaction	Surface reaction between molecularly adsorbed propylene and propylene in gas phase	$r=kK_p(P_p^2-P_EP_B/K)/(1+K_pP_p+K_BP_B+K_EP_E)$	$\frac{P_p^2}{ro}=1+K_pP_p$
14	Surface Reaction	Surface reaction between atomically adsorbed propylene and propylene in gas phase	$r=kK_p^2(P_p^2-P_EP_B/K)/(1+K_EP_B+K_BP_B+\sqrt{K_pP_p})^2$	$\frac{P_p}{ro}=\frac{1}{K}+\frac{K_pP_p}{K}$
15	Surface Reaction	Surface reaction between atomically adsorbed propylene and molecularly adsorbed propylene	$r=kK_p^2(P_p^2-P_EP_B/K)/(1+K_EP_E+K_BP_B+K_pP_p+P_pP_p)^3$	$\frac{P_p^2}{ro}=3\frac{1}{K}+3\frac{1}{k}(\sqrt{K_pP_p}+K_pP$
16	Uncatalyzed reaction		$r=k(P_p^2-P_EP_B/K)$	$ro=KP_p^2$

Mechanism discrimination procedures have involved considerable sophistication since the linearized least squares techniques first presented by Hougen and Watson (89, 76). This procedure has been often criticized because the linearization procedure applied to the rate equations often necessitated the combination of independent variables (partial pressures) with experimental response (reaction rate). The first significant improvement over this procedure was presented by Yang and Hougen (77). Their major contribution, was a method of reducing the number of possible mechanisms before regression analysis. This was done by the use of the method of initial rates. These simplified models could then be easily analyzed by linear least-squares or more simply could be plotted to determine the effect of total pressures on initial rates. While many possible mechanisms may be eliminated by either of these simple procedures some good initial estimates of model parameters are generated for later use in more sophisticated discrimination and parameter evaluation techniques.

(a) Correlation of Initial Rate Data

The mechanism discrimination procedure used in this investigation relied on initial and integral rates. The first

step in mechanism discrimination was to derive all the possible rate equations as mentioned earlier. These mechanisms were based on all possible rate controlling steps based on whether one or two molecules adsorbed and whether dissociation occurs. For each of the hypothesized mechanisms, the initial rate expression was derived by letting P_E and P_B approach zero. The result for the dual site mechanism is:

$$r_o = kP_p^2 / (1 + K_pP_p)^2 \qquad (5\text{-}33)$$

This expression could be linearized as follows:

$$\frac{r_o}{P_p^2} = k / (1 + K_pP_p)^2 \qquad (5\text{-}34)$$

Inverting equation (5-34)

$$P_p^2 / r_o = (1 + K_pP_p)^2 / k \qquad (5\text{-}35)$$

Taking the square root of both sides:

$$P_p / \sqrt{r_o} = (1 + K_pP_p) / \sqrt{k} \qquad (5\text{-}36)$$

or

$$P_p / \sqrt{r_o} = b + mP_p \qquad (5\text{-}37)$$

Where $b = 1/\sqrt{k}$ and $m = K_p / \sqrt{k}$. Therefore, if the model is adequate a plot of $P_p/\sqrt{r_o}$ vs P_p should be linear. A list of all possible rate equations and their linearlized initial rate equations is given in Table 2.

Yang and Hougen (77), who considered several reactions, have shown that by considering the effect of total

pressure on the initial rate, it is possible to reduce the number of apparent controlling mechanims and finally to test some of them for their suitability in representing the experimental data.

Initial rates are easy to use since rate equations are in a simpler form and are obtained by neglecting the partial pressure of products. However, it is difficult to calculate the initial rate with certainty since it requires estimating the slope at low conversion by extrapolation.

The conversion versus space time (W/F) data were fitted by a polynomial up to third degree. A polynomial of the third degree was found to fit the data best at all pressures.

Initial rates were found by analytically differentiating the polynomial at the origin. The initial rates were plotted as a function of total pressure of reaction as shown in Figure (5-4), while the results are given in Appendix (G). The shape of the curves in Figure (5-4) were compared to those of Yang and Hougen (77).

A more exact method of model discrimination of the remaining models is the plotting of linearized initial rate equations. The equation which applies should result in a straight line and others should result in curved lines. By using

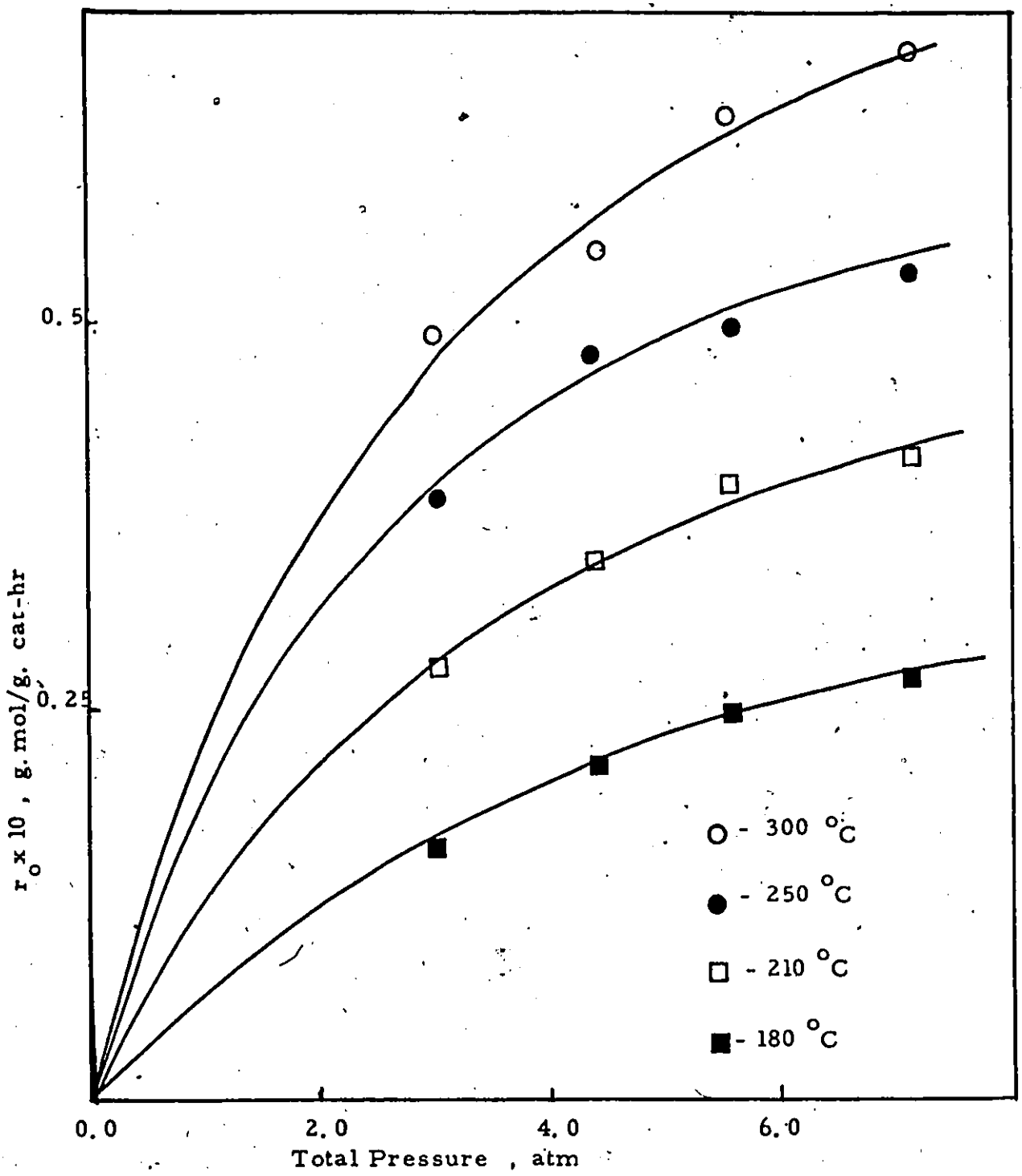

Figure 5-4 Effect of Total Pressure on Initial Rate for Disproportionation of Propylene.

this method, it was concluded that the data can be reported sented by a single-site mechanism (Rideal-Langmuir) or a dual-site mechanism (Langmuir-Hinshelwood). All the other models did not satisfy the initial rate data. Figure (5-5) and (5-6) appear nearly linear, indicating that both proposed models fit the initial rate data well. This representation of the data of both figures by straight lines may be quantitatively justified by conducting an analysis of variance to determine the minimum degree of polynomial required to fit the data (78). The data were fitted by first and second order polynomial and the residual mean squares for each data set are shown in Table 3. From the results presented in Table 3, one can conclude that the single-site model can be best represented by a curve. Moreover, the equation $P_P^2/r_o = 1/k + \frac{K_p}{k} P_P$, plotted as P_P^2/r_o versus P_P was correlated by negative slope and intercept at all temperatures. The linear least squares analysis has shown that based on the initial rate data, the dual-site mechanism represented the experimental data best.

(b) Correlation of Conversion Data

In a steady state flow reactor, the relationship between conversion, flow rate and reaction rate is given by the equation:

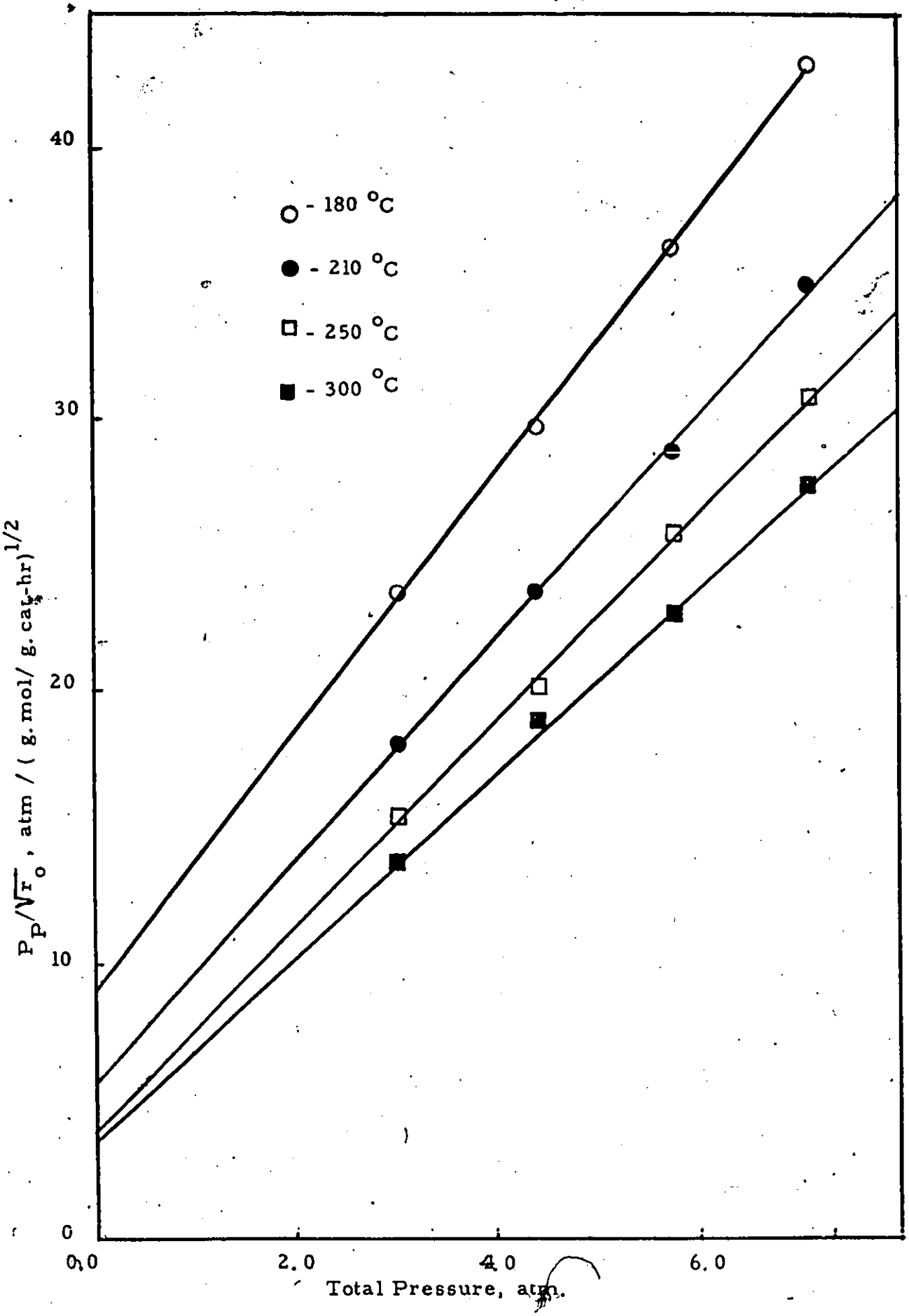

Figure 5-5 Initial Rate Correlation Using Dual-Site Langmuir-Hinshelwood Model

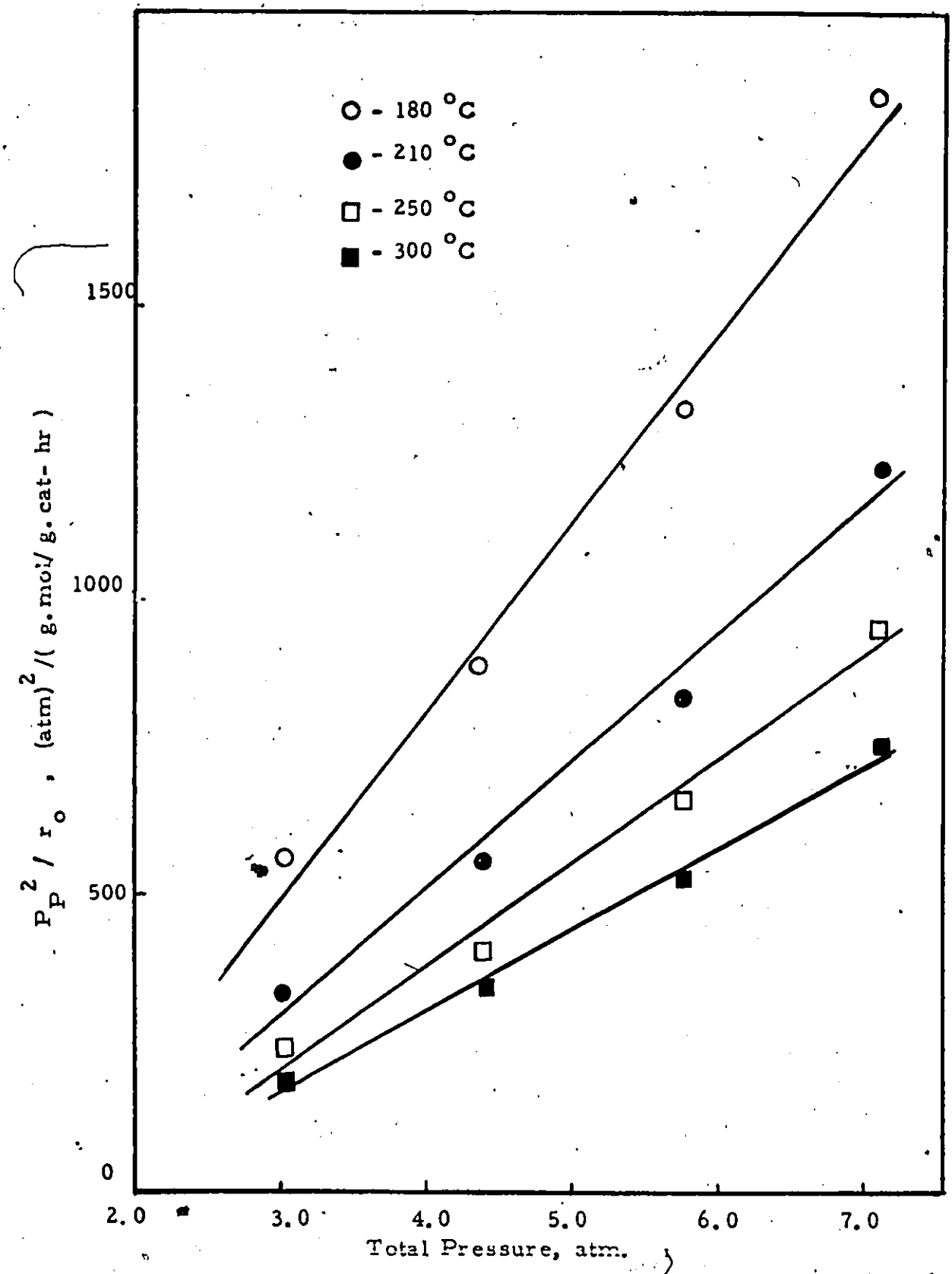

Figure 5-6 Initial Rate Correlation Using a Single - Site Mechanism

TABLE 3

RESIDUAL MEAN SQUARES FOR RIVAL MODELS

Model	Mean Square for Linear Relationship	Mean Square for Quadratic Relationship	Ratio of Linear to Quadratic	k	Kp
Single Site Model					
180°C	0.495×10^{4}	0.372×10^{3}	13.315	-0.002	-1.426
210°C	0.292×10^{4}	0.260×10^{3}	11.252	-0.002	-0.597
250°C	0.188×10^{4}	0.172×10^{3}	10.929	-0.003	-0.533
300°C	0.588×10^{3}	0.695×10^{2}	8.401	-0.004	-0.565
Dual Site Model					
180°C	0.317×10^{-1}	0.132×10	0.024	0.012	0.520
210°C	0.555×10^{-1}	0.608	0.091	0.030	0.714
250°C	0.964×10^{-1}	0.346	0.278	0.073	1.033
300°C	0.717×10^{-1}	0.979×10^{-1}	0.717	0.069	0.876

$$FdX = rdW \qquad (5\text{-}38)$$

which on integration yields:

$$\int_0^W \frac{dW}{F} = \int_0^X \frac{dX}{r} \qquad (5\text{-}39)$$

$$W/F = \int_0^W \frac{dX}{r} \qquad (5\text{-}40)$$

All the rate equations based on the dissociation of propylene were ruled out because of initial rate dependency and experimental evidence that propylene does not dissociate upon adsorption.

The remaining rate equations 1,2,6,9,12 and 13 were substituted in equation (5-40) and the partial pressures were substituted as a function of conversion as follows:

$$P = \pi(1-X) \qquad (5\text{-}41)$$

$$P = P = \frac{\pi}{2}(X) \qquad (5\text{-}42)$$

and the equations were integrated. The integrated rate equations of the possible mechanisms are given in Table 4.

In this investigation only pure propylene feed was used, therefore, the partial pressure of ethylene and butene were the same. Hence, the effect of conversion on K and K could not be separated, which means that only the sum of k and K could be evaluated. The linear least squares analysis of initial rate data of model 12 provided initial parameter estimates of the combined rate constant, k, and for the equilibrium adsorption constant K_p. Also based on the data

TABLE 4

INTEGRATED RATE EQUATIONS

Mechanism #	
1	$W/F = \frac{1}{k}\left(\left(\frac{1}{\tau}\right) \int_0^x \frac{dx}{\chi} + \left((K_E+K_B)/2 - \frac{1}{\tau} \right) \int_0^x \frac{dx}{\chi} + \left(\frac{K_p}{4k} - \frac{(K_E+K_B)}{2}\right) \int_0^x \frac{dx}{\chi} \right)$
2	$W/F = \frac{1}{k}\left(\left(\frac{1}{\tau} + K_p\right) \int_0^x \frac{dx}{\chi} + \left(\frac{(K_E+K_B)}{2} - \frac{1}{\tau} - 2K_p\right) \int_0^x \frac{dx}{\chi} + \left(\frac{K_p}{4K} - \frac{(K_E+K_B)}{2} + K_p\right) \int_0^x \frac{2dx}{\chi} \right)$
6	$W/F = \frac{1}{2kK}\left(2KK_E \int_0^x \frac{dx}{\chi} + \left(\frac{1}{\tau} + K_p - 4KK_E\right) \int_0^x \frac{dx}{\chi} + \left(\frac{K_B}{2} - K_p - 2KK_E\right) \int_0^x \frac{dx}{\chi} \right)$
9	$W/F = \frac{1}{2kK}\left(2KK_B \int_0^x \frac{dx}{\chi} + \left(\frac{1}{\tau} + K_p - 4KK_B\right) \int_0^x \frac{dx}{\chi} + \left(\frac{K_E}{2} - K_p + 2KK_B\right) \int_0^x \frac{dx}{\chi} \right)$
12	$W/F = \frac{1}{kK_p^2}\left(\left(\frac{1}{\tau} + K_p\right)^2 \int_0^x \frac{dx}{\chi} + 2\left(\frac{(K_E+K_B)}{2} - K_p\right)\left(\frac{1}{\tau} + K_p\right) \int_0^x \frac{dx}{\chi} + \left((K_E+K_B) - K_p\right)^2 \int_0^x \frac{dx}{\chi} \right)$
13	$W/F = \frac{1}{\tau\, kK_p}\left(\left(\frac{1}{\tau} + K_p\right) \int_0^x \frac{dx}{\chi} + \left(\frac{(K_E+K_B)}{2} - K_p\right) \int_0^x \frac{dx}{\chi} \right)$

$$\chi = 1 - 2x + (1 - 1/4K)\, x^2$$

presented by Cvetonovic and Amenomiya (91), initial estimates for the combined adsorption coefficient of ethylene and butene $K_{E\beta}$ was taken equal to 2.5 K_p.

The equilibrium rate constant was calculated from the data by Rossini (96), assuming cis and trans-2-butene to be in equilibrium at each temperature. (Appendix A). Finally, a non-linear regression technique based on the Box-modified Gauss method was used to test the validity of the intigrated equations shown in Table 5. The above parameters were used as initial estimates (θo).

The Box-modified Gauss method uses intial estimates of parameters (θo),.. and . The new estimate of θi is determined according to the equation. $\theta_i = (\theta i) + \underline{B}$ (5-43)

where $\underline{\beta} = \frac{1}{1+\lambda} (X_o T X_o)^{-1} X \; T \; Z$ (5-44)

This iterative procedure is continued until the solution converges, that is, until in a successive iteration j and (j + 1),

$$((\theta_i)\; j + 1 - (\theta_i)\; j)/\theta_{ij} \qquad i = 1,2,3,...$$

This procedure ruled out mechanism 1,2,6,9, and 13 since negative adsorption constants were obtained.

It was found that the dual-site mechanism (Langmuir Hindshelwood) fitted the experimental data best. The rate equation based on the mechanism can be expressed as:

$$r = \frac{k(P_p^2 - P_E P_B / K_{E\beta} P_{E\beta})}{(1 + K_p P_p + K_{E\beta} P_{E\beta})^2} \qquad (5\text{-}45)$$

where $K_{E\beta} = K_E + K_\beta$

The values of k, k_p and $K_{E\beta}$ between 180 to 300°C along with their 95% confidence region are listed in Table 5.

TABLE 5

TEMPERATURE DEPENDENCY OF RATE PARAMETERS DETERMINED

FROM NONLINEAR ANALYSIS OF INTEGRAL DATA.

Temperature ^{o}C	Combined Reaction Rate constant, k (g.moles/hr.g cat) Atm^{-2}	Propylene Adsorption Coefficient K_p Atm^{-1}	Combined Ethylene-Butene Adsorption Coefficient, K_{EB} Atm^{-1}
180	0.025 $\pm$ 0.0113	0.525 $\pm$ 0.1750	1.731 $\pm$ 0.8034
210	0.036 $\pm$ 0.0155	0.483 $\pm$ 0.1556	2.022 $\pm$ 0.9058
250	0.054 $\pm$ 0.0222	0.438 0.1359	2.420 $\pm$ 1.0402
300	0.083 $\pm$ 0.0325	0.396 $\pm$ 0.1178	2.923 $\pm$ 1.2035

v. Temperature Effect on Rate Constants

The temperature dependance of k, K_p and K_{EB} is shown in Figure 5-7. Assuming the temperature dependence of these parameteres could be described by the Arrhenius activation theory, the activation energy and the fequency factor of the rate constant and adsorption constants were calculated using non-linear regression analysis. The methematical expression decribing the temperature dependence of k, K_p and K_{EB} are given in the following equations:

$$k = 7.122 \exp(-5{,}059/RT) \quad (5\text{-}46)$$

$$K_p = 0.137 \exp(1{,}212/RT) \quad (5\text{-}47)$$

$$K_{EB} = 21.126 \exp(-2{,}252/RT) \quad (5\text{-}48)$$

These constants appear to follow Arrhenius behavior in the temperature range studied.

The values of the constants obtained from Table 5 were substituted in equation 12 of Table 4 to determine W/F vs X relation. Figures 5-8 to 5-23 show the comparison between experimental and prdicted values by substituting the appropriate values of K's in the relation the circles represent the experimental data. A sample calculation is given in Appendix (D).

The values of adsorption equilibrium constnats for each component were further tested to verify their compliance summary of rules with Boudart's rule (79) for entropies of adsorption.

The values of standard entropy of adsorption (ΔS_a^o) and standard enthalpy of adsorption (ΔH_a^o) for propylene and for ethylene and butene were obtained by rewriting equation (5-45) and (5-46) in

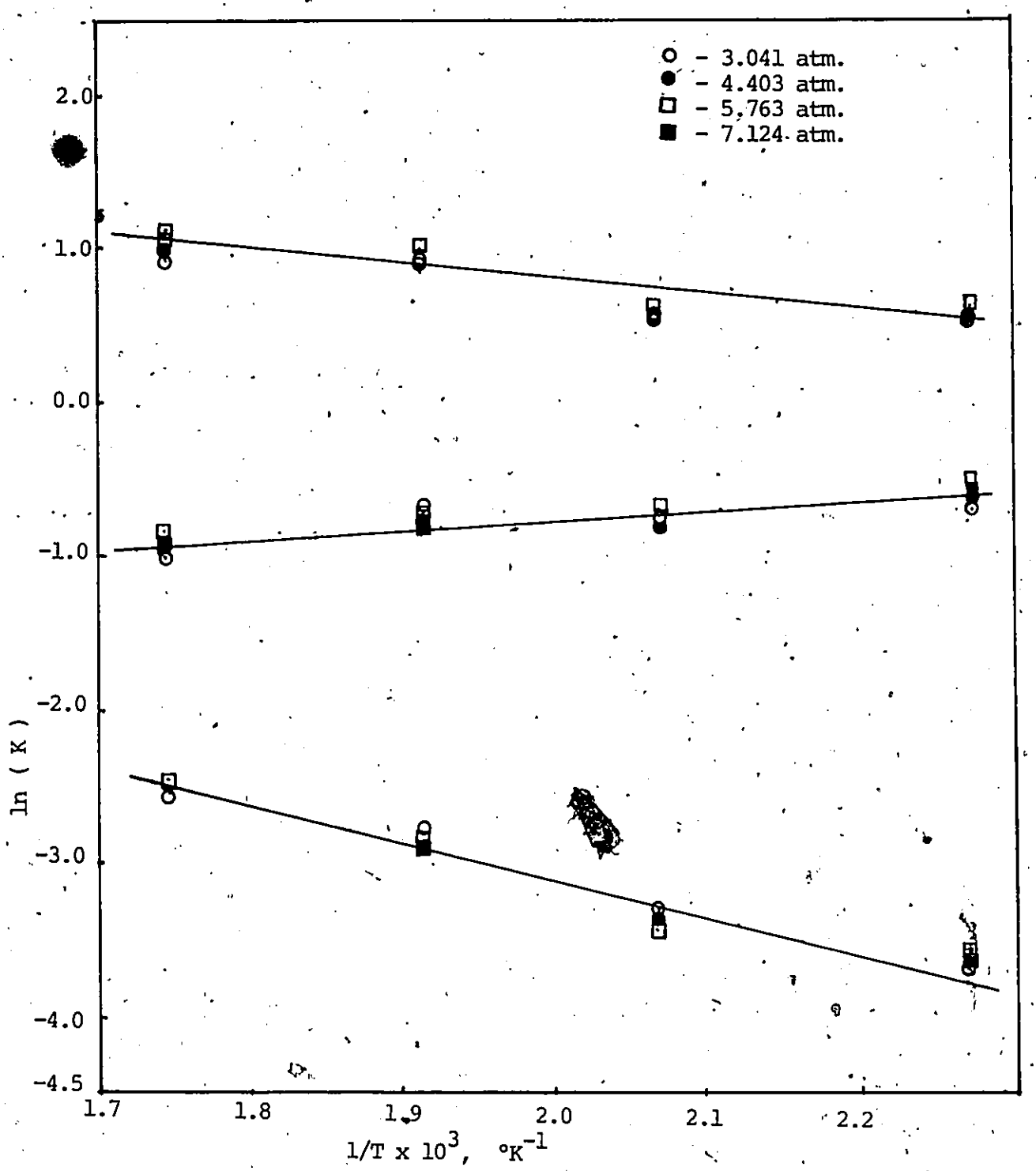

Figure 5-7 Temperature Dependency of k, K_p and K_{EB}

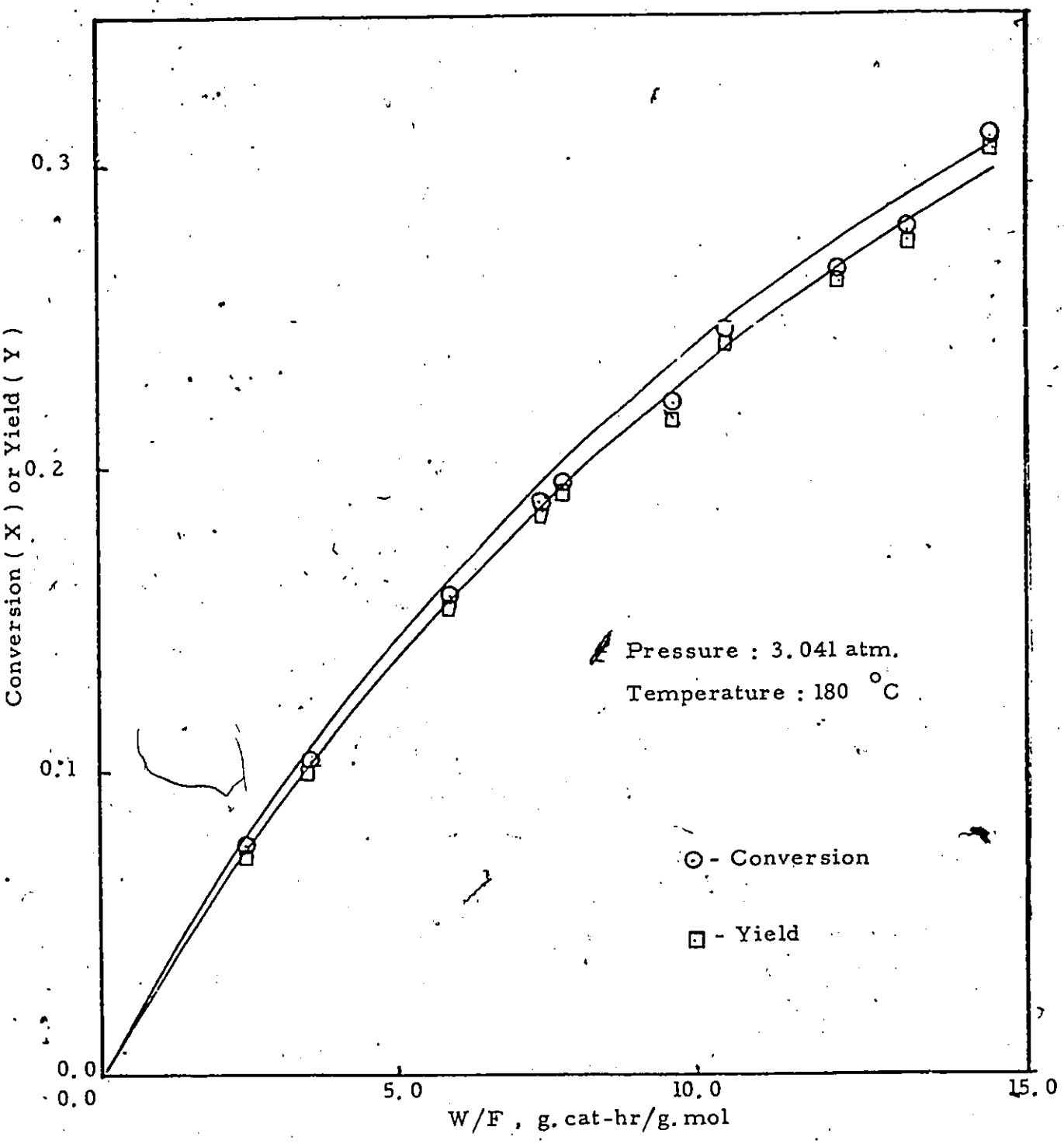

Figure 5-8 Effect of W/F on Conversion and Yield

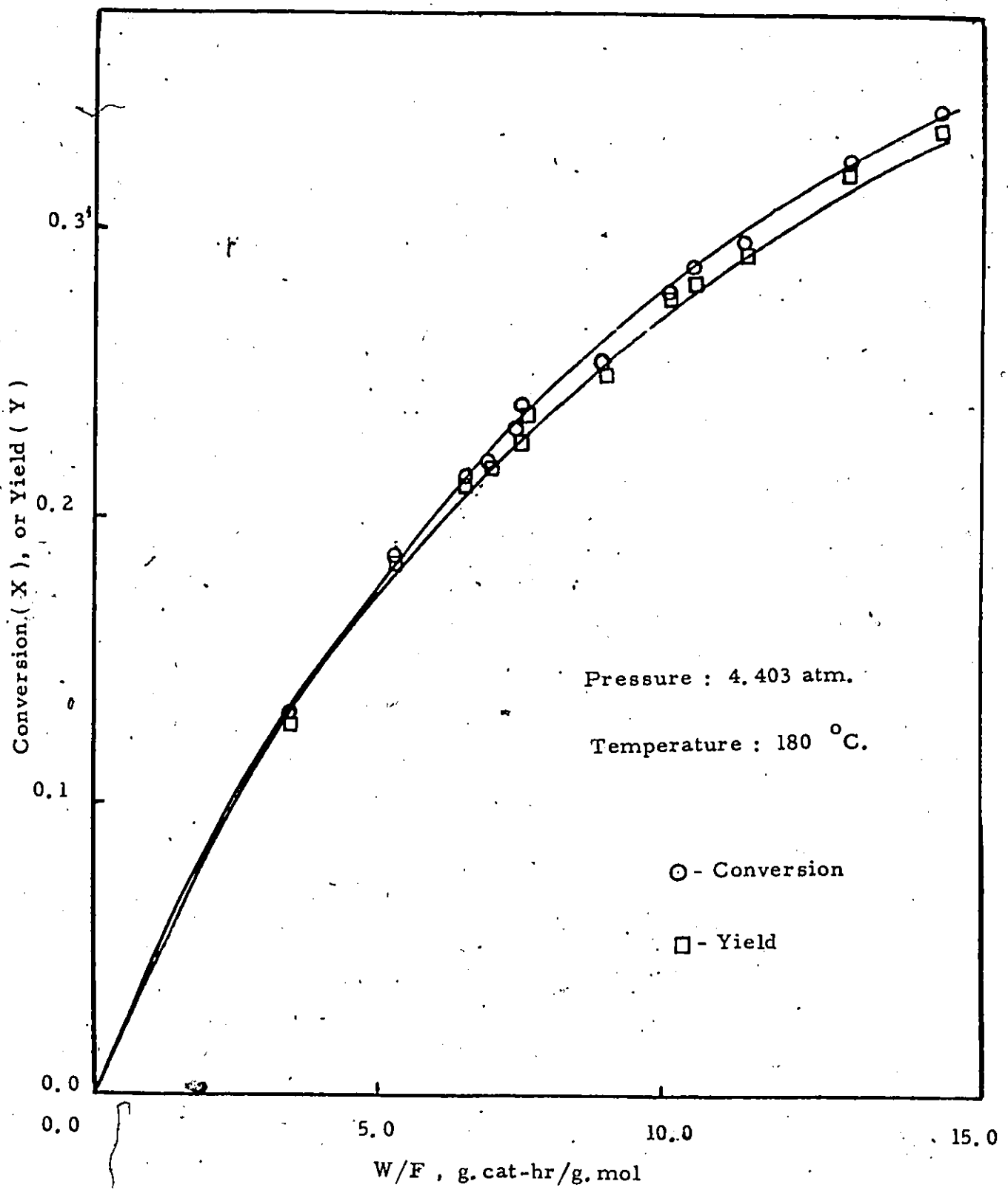

Figure 5-9 Effect of W/F on Conversion and Yield

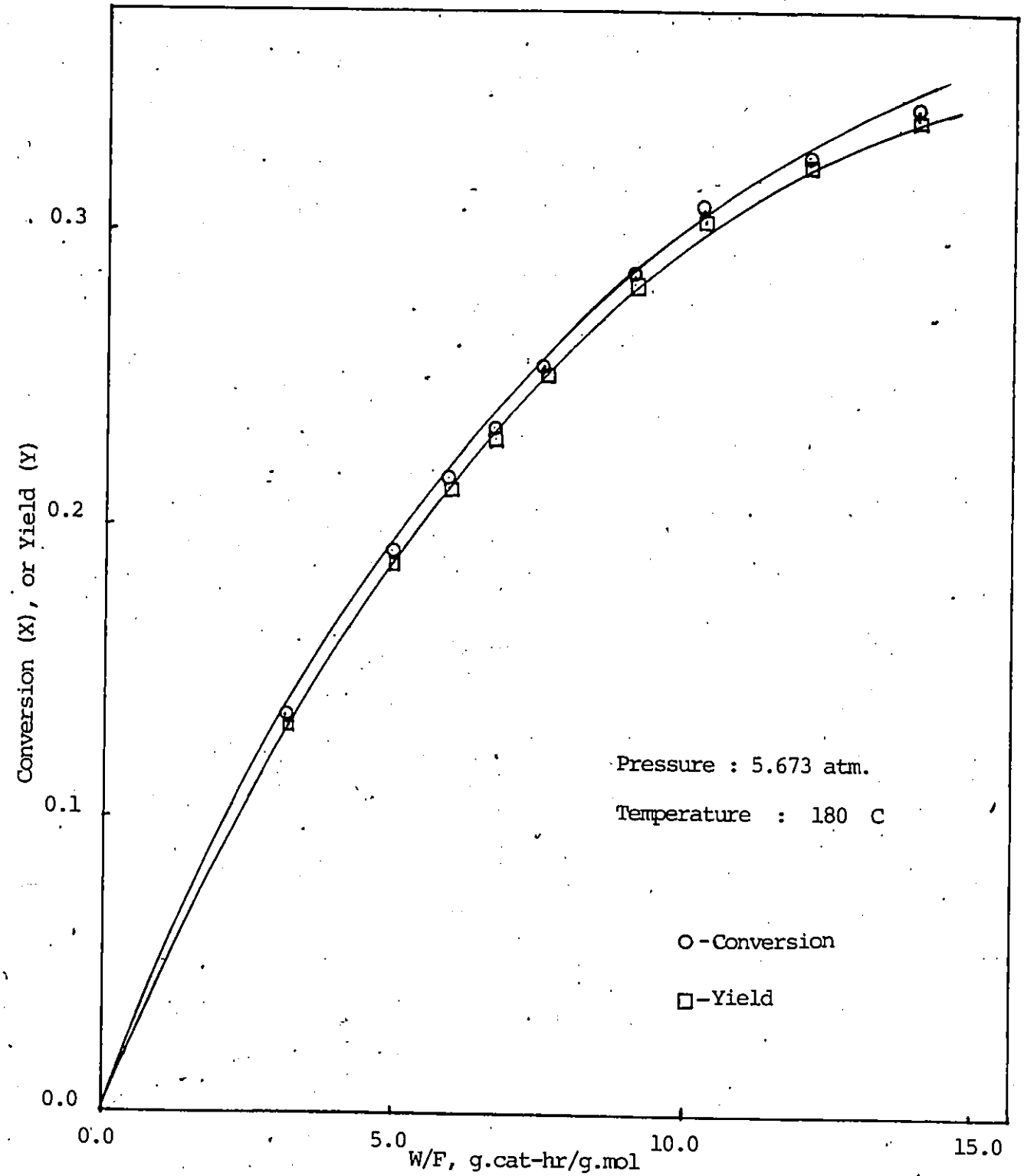

Figure 5-10 Effect of W/F on Conversion and Yield.

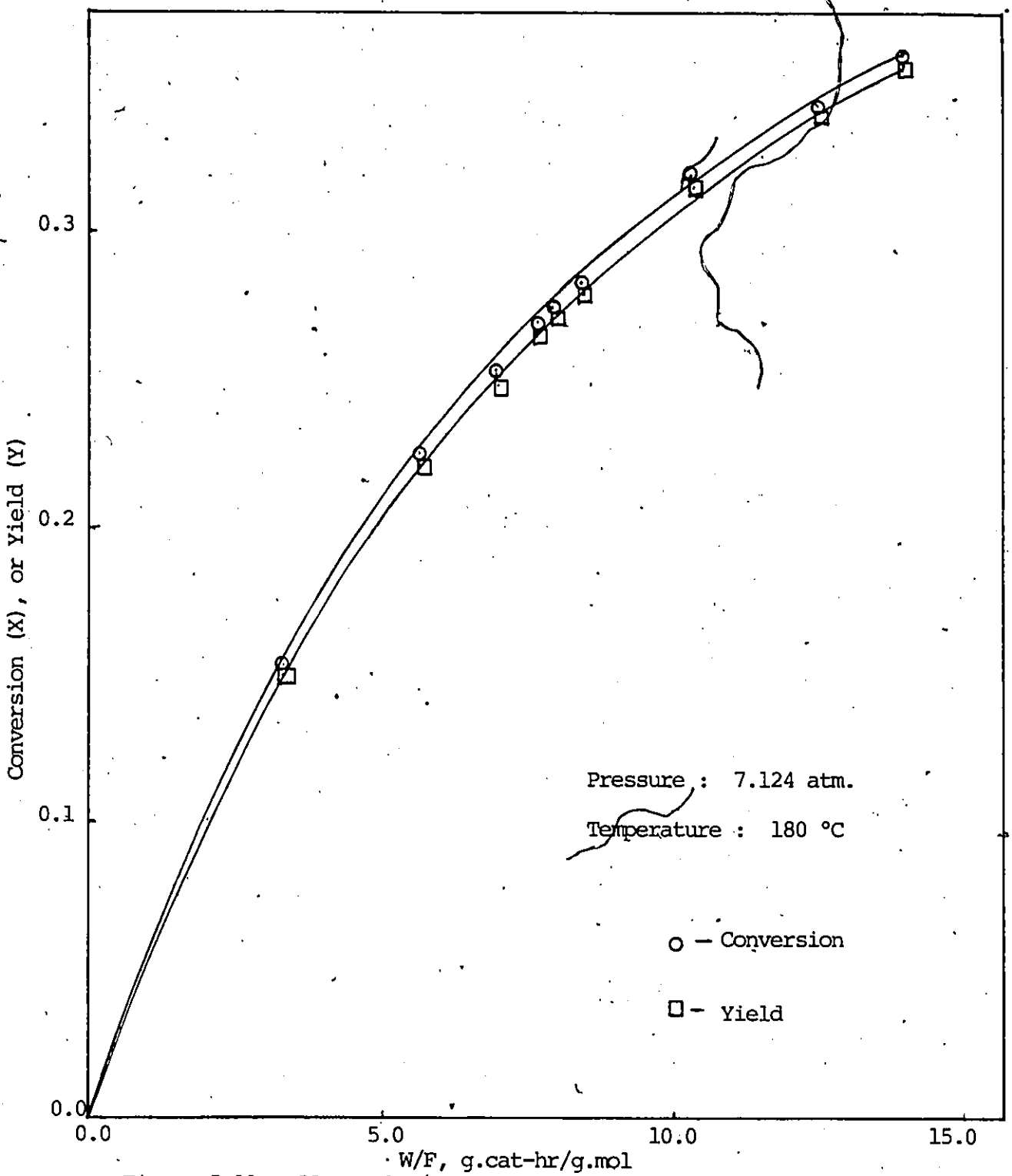

Figure 5-11 Effect of W/F on Conversion and Yield.

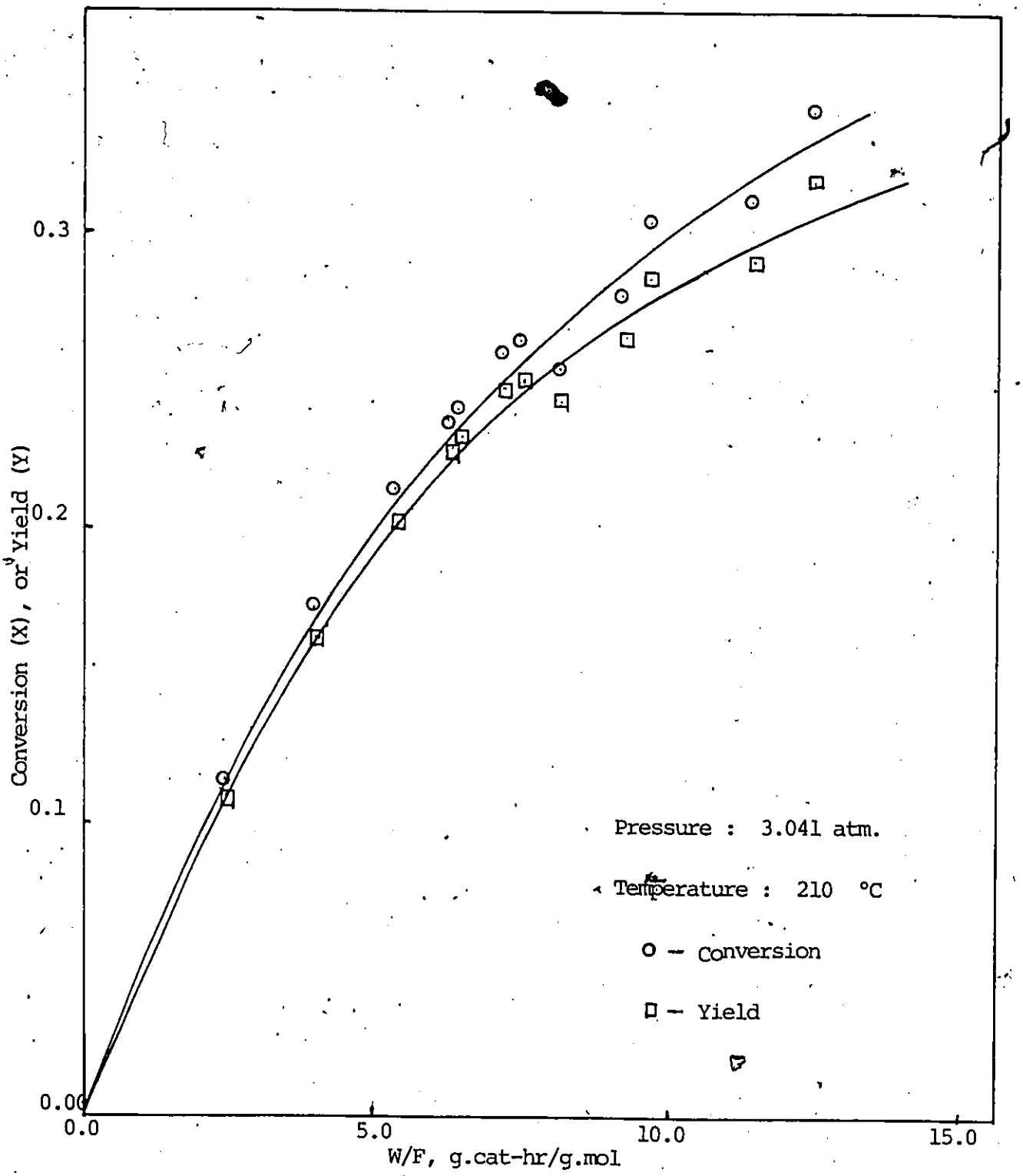

Figure 5-12 Effect of W/F on Conversion and Yield.

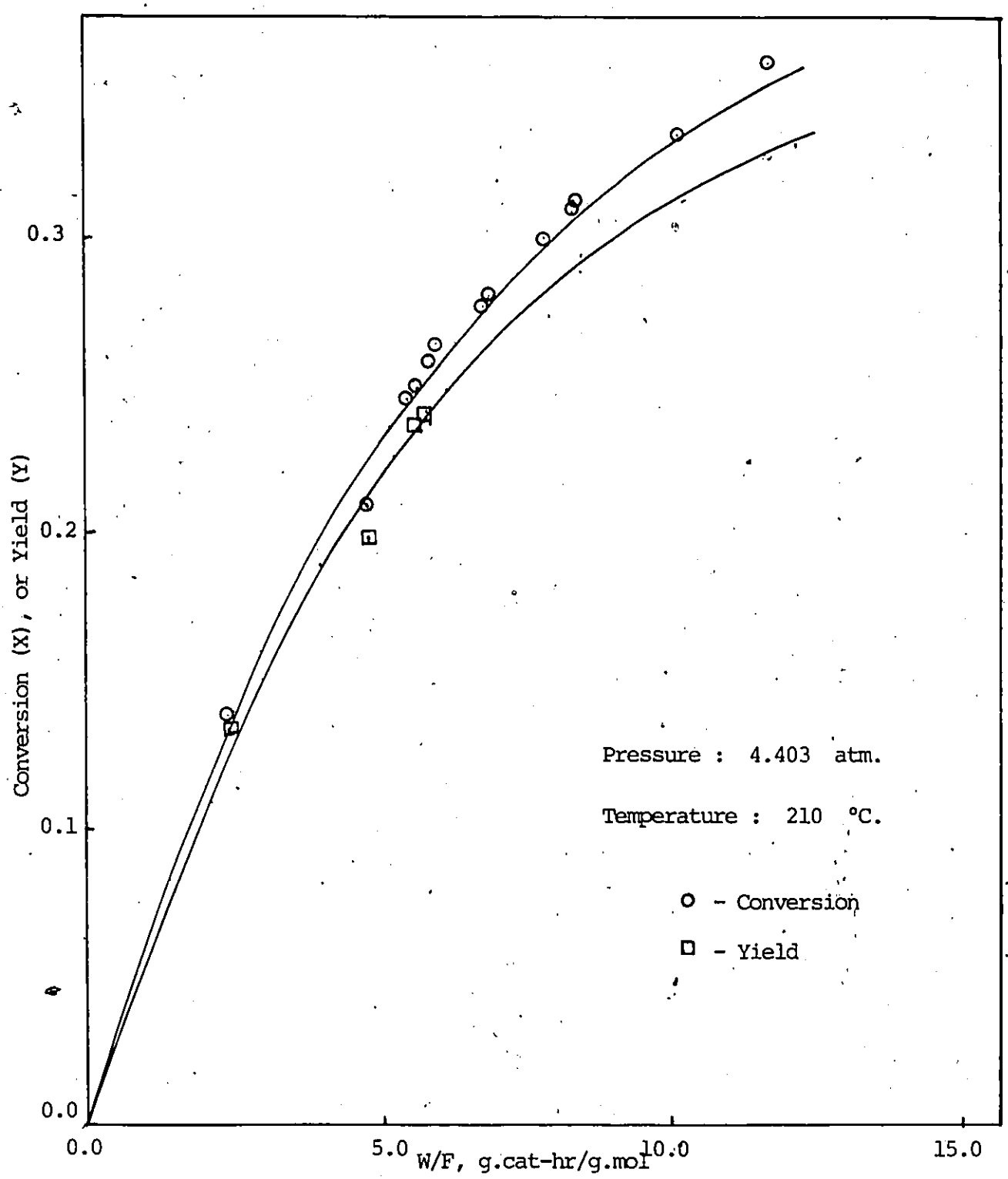

Figure 5-13 Effect of W/F on Conversion and Yield.

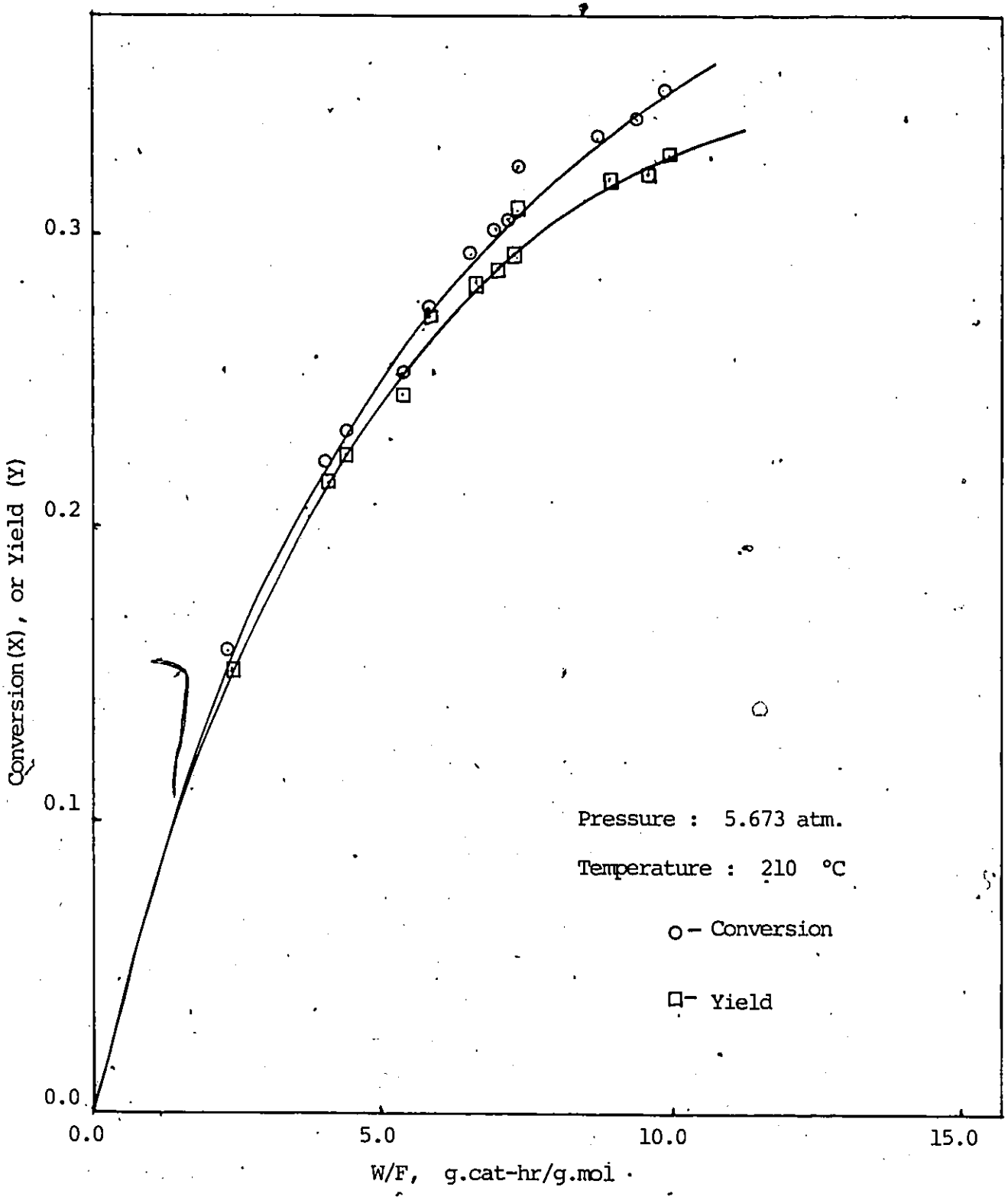

Figure 5-14 Effect of W/F on Conversion and Yield.

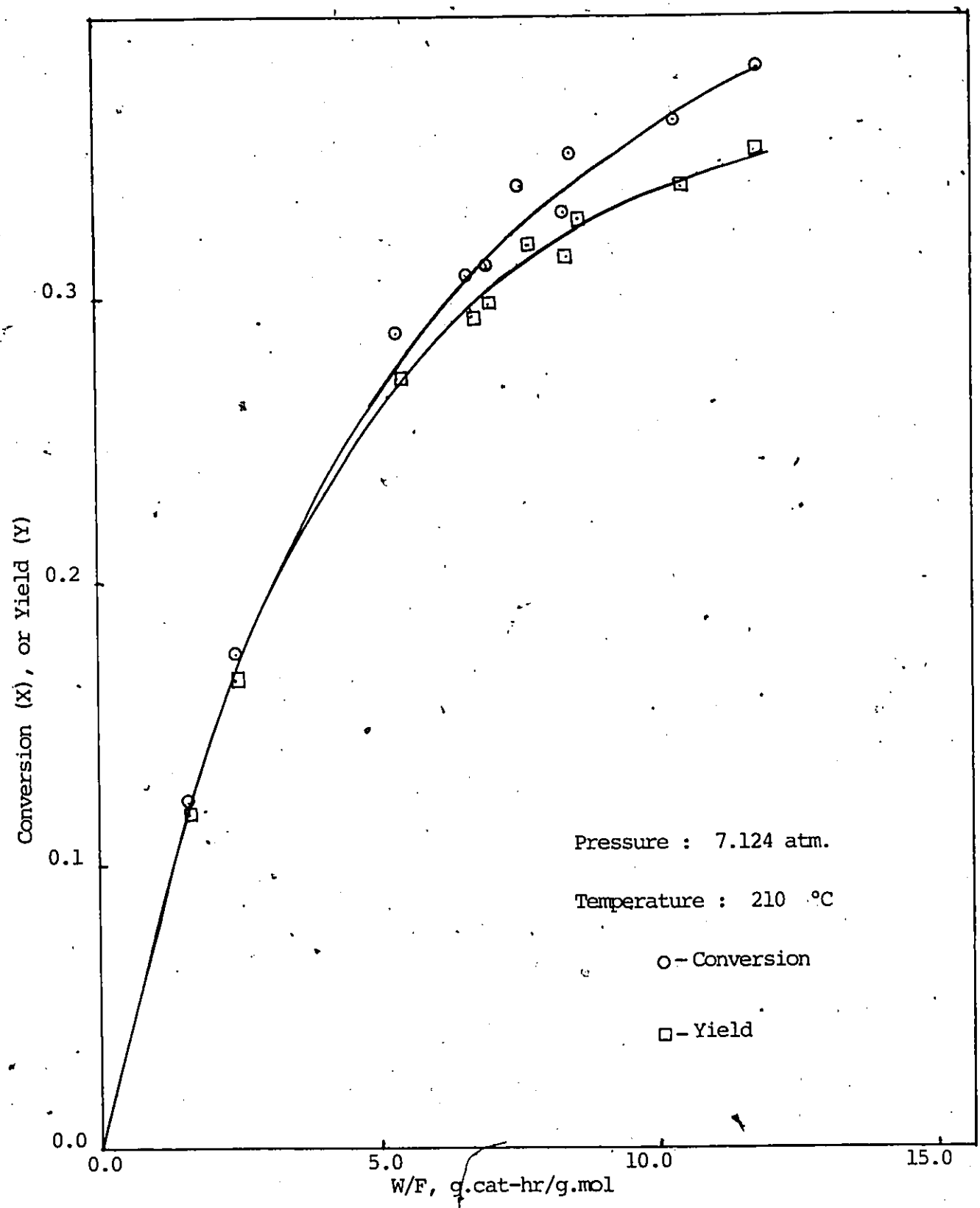

Figure 5-15 Effect of W/F on Conversion and Yield.

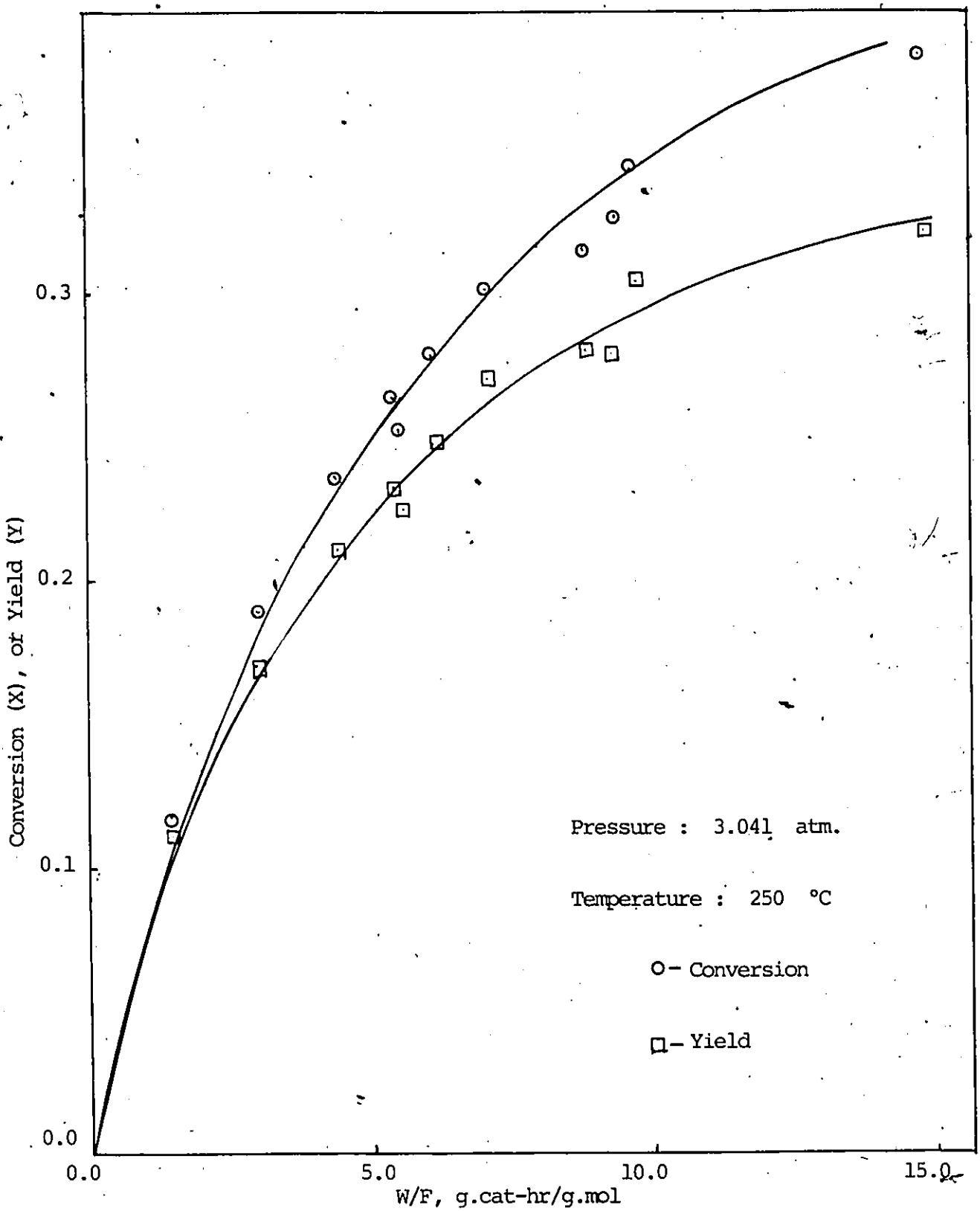

Figure 5-16 Effect of W/F on Conversion and Yield

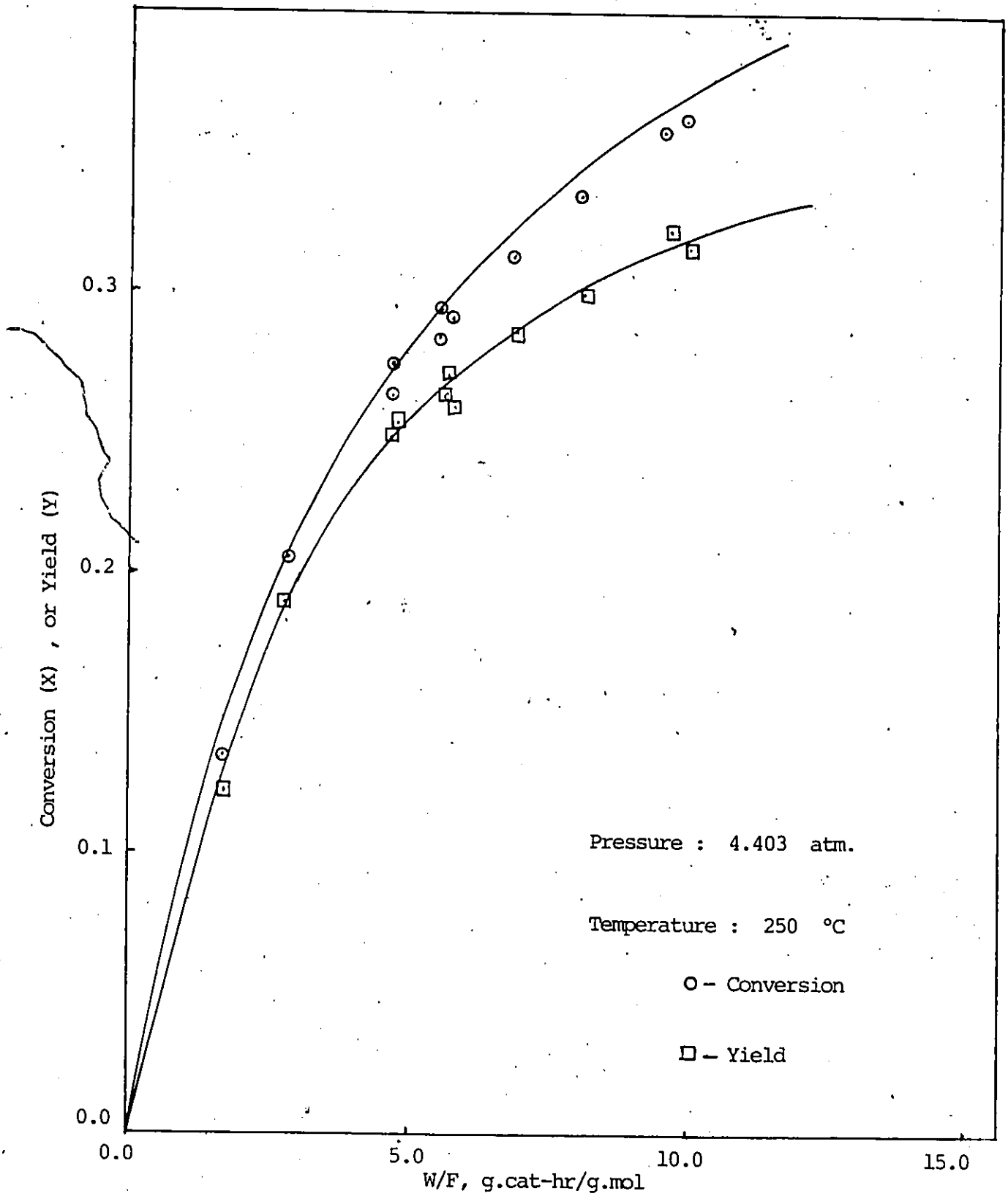

Figure 5-17 Effect of W/F on Conversion and Yield

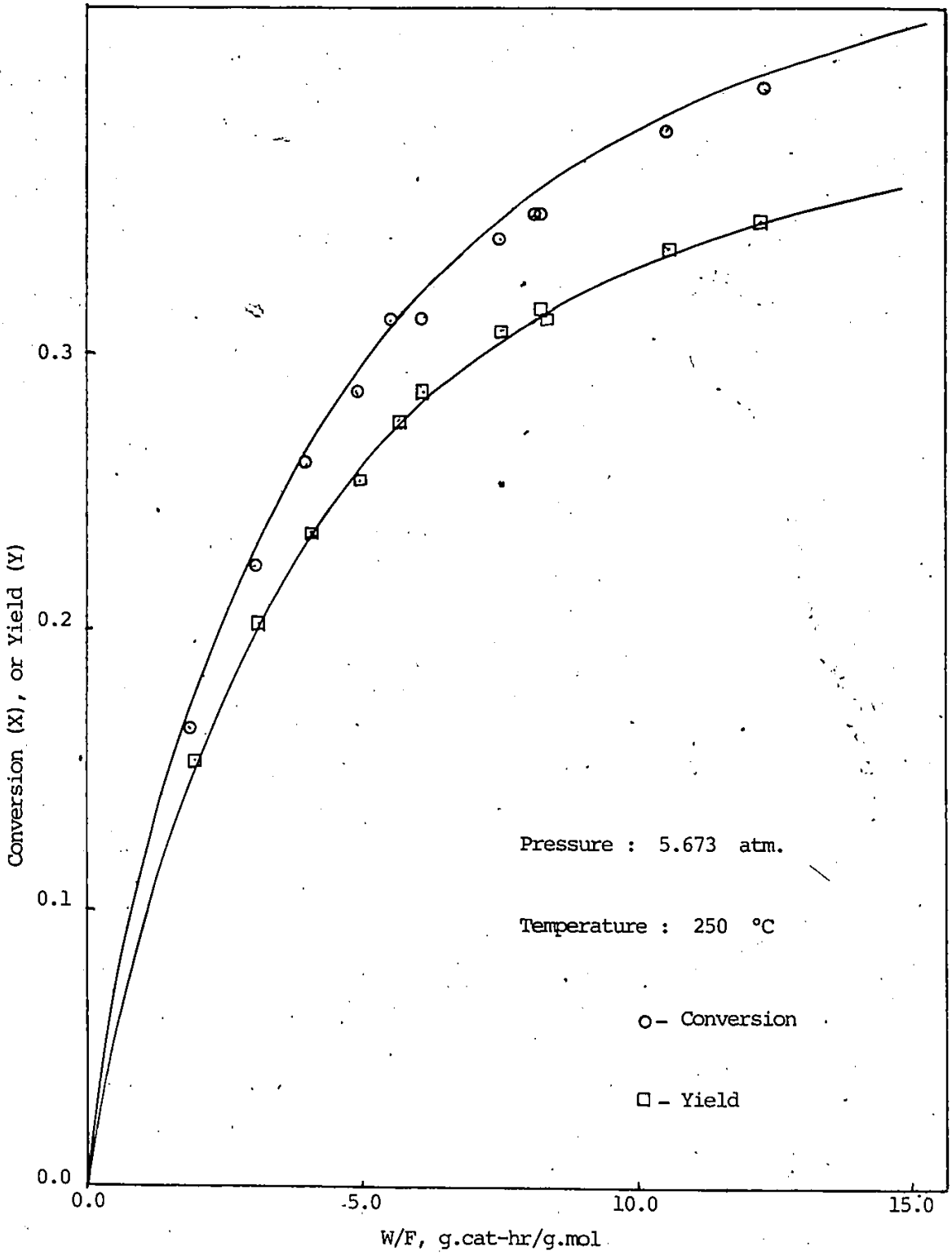

Figure 5-18 Effect of W/F on Conversion and Yield

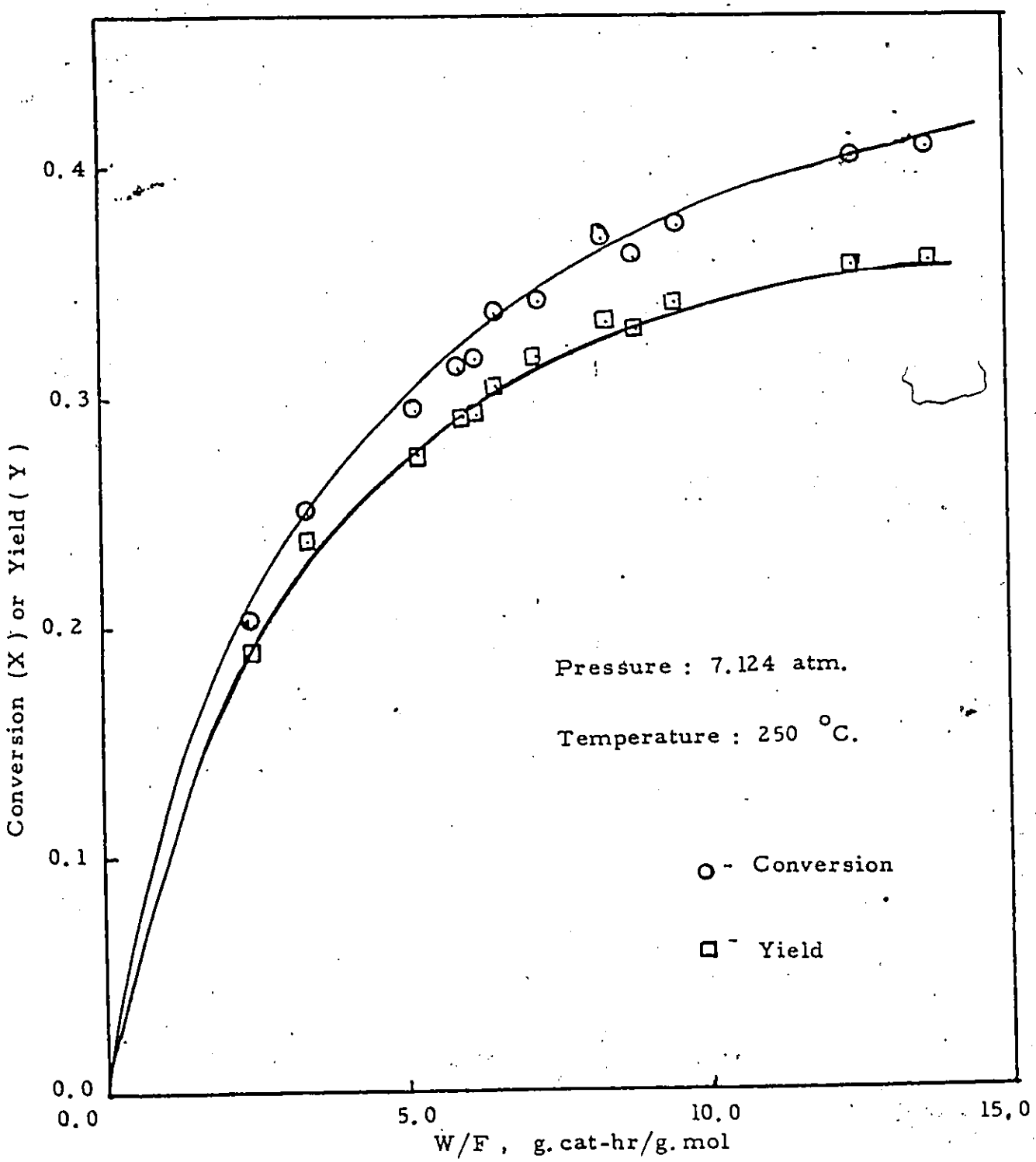

Figure 5-19 Effect of W/F on Conversion and Yield

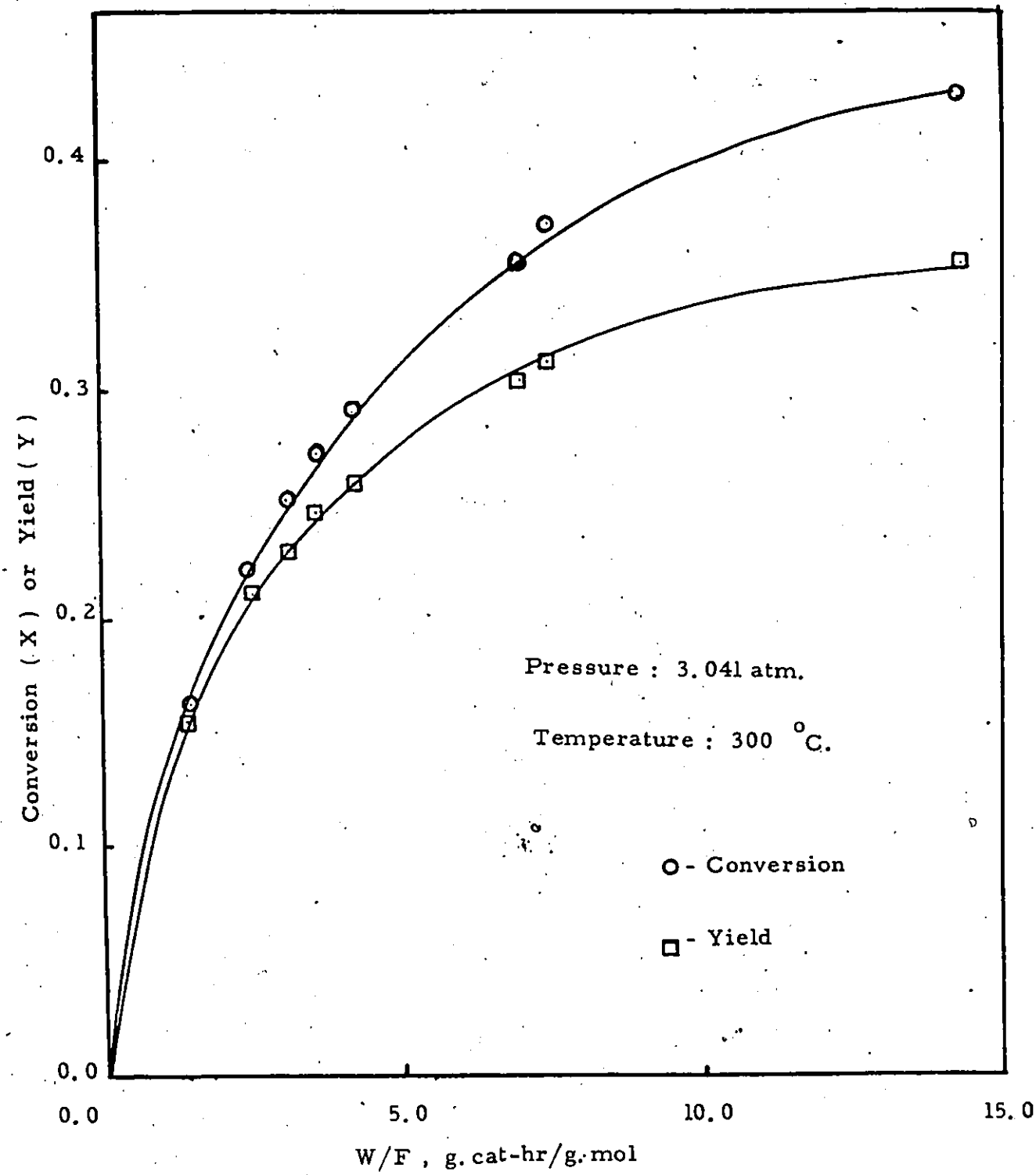

Figure 5-20 Effect of W/F on Conversion and Yield

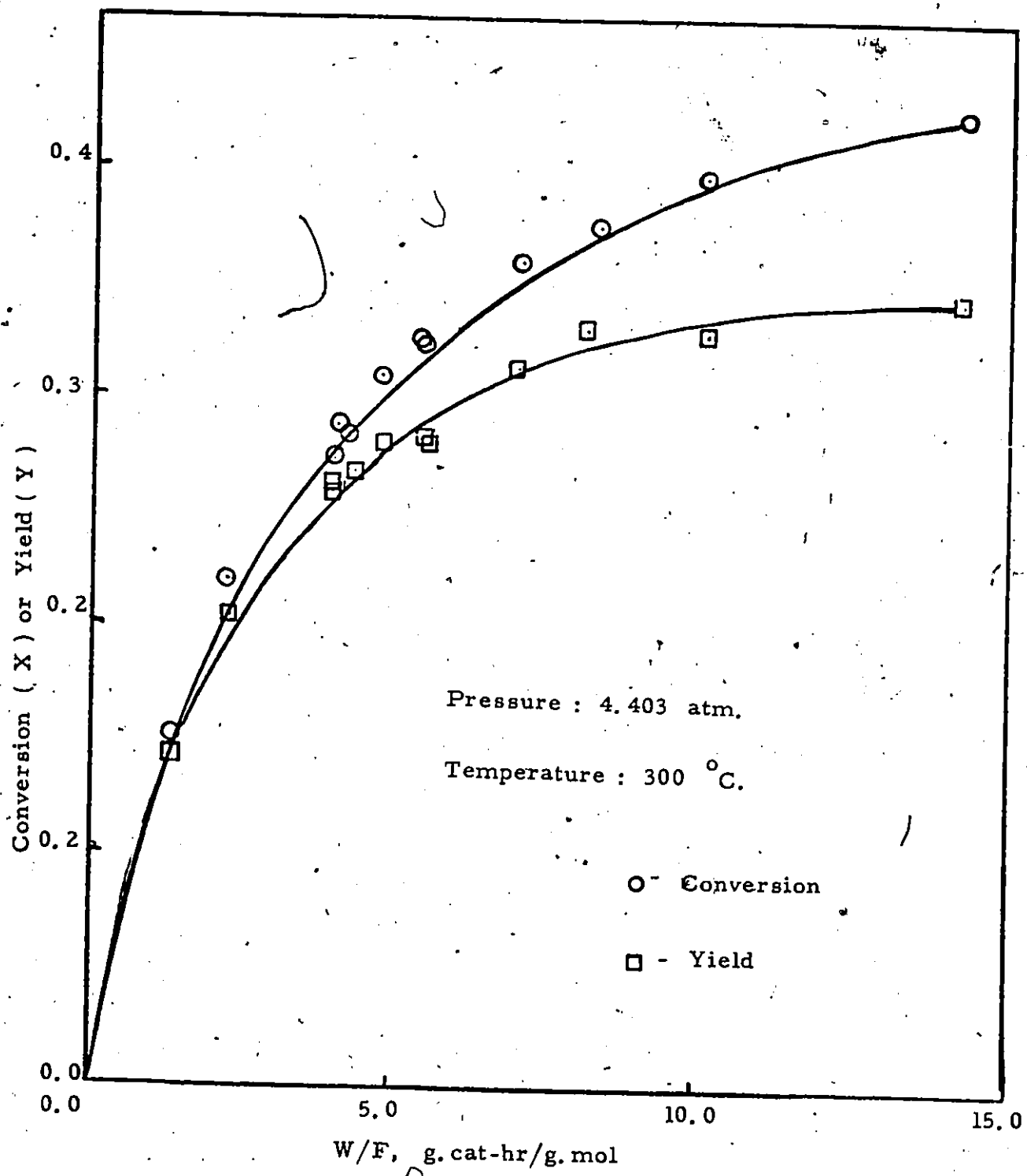

Figure 5-21 Effect of W/F on Conversion and Yield

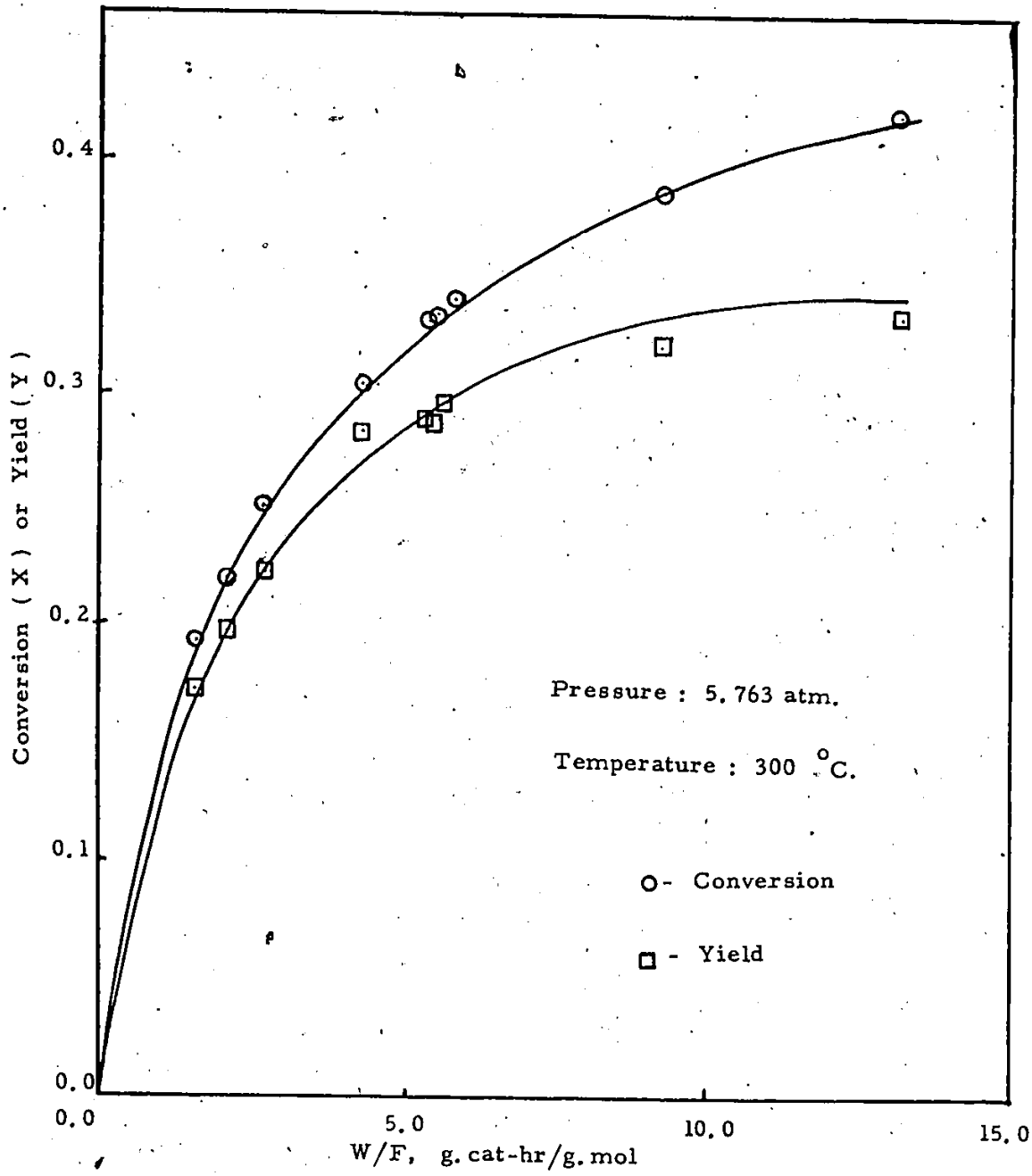

Figure 5-22 Effect of W/F on Conversion and Yield

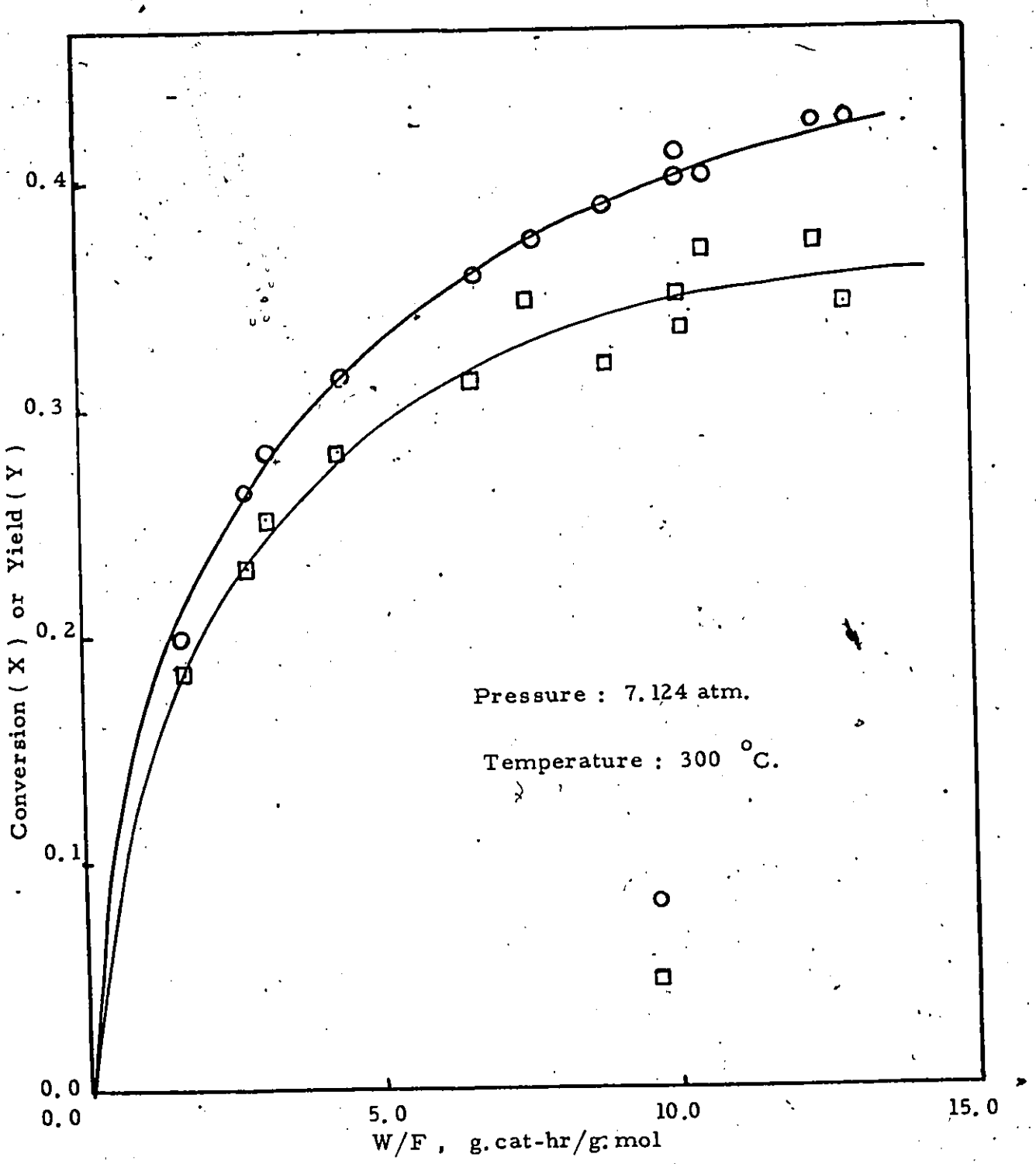

Figure 5-23 Effect of W/F on Conversion and Yield

the form :

$$K = e^{\Delta S_a^{\circ}/R} \cdot e^{-\Delta H_a^{\circ}/RT} \qquad (5\text{-}49)$$

while the values of standard entropy S_g° were obtained from the literature (80). Table 6 is a summary of these results:

TABLE 6

Rule		Propylene	Ethylene and Butene
I	$\Delta S_a^{\circ}<0$	$-3.9554<0$	$6.061\nless 0$
II	$\lvert\Delta S_a^{\circ}\rvert<S_g^{\circ}$	$3.9554 < 63.80$	$6.061 < 61.96$
III	$\lvert\Delta S_a^{\circ}\rvert> 10$	$3.9554 \ngtr 10$	$6.061 \ngtr 10$
IV	$-\Delta S_a^{\circ}<$ $12.2-0.0014\Delta H_a^{\circ}$	$3.9554 < 13.897$	$-6.061 < 9.048$

In the above table, the values of the standard entropy of adsorption are consistent with rule II and IV. The positive value of ΔS_a° of ethylene and butene violates rule I, which indicates that the adsorption of ethylene and butene deviates from ideal Langmuir adsorption behavior. In a survey of 129 cases, for kinetics of reactions catalyzed by solids by Boudart et al. (79), 41 cases showed positive values of ΔS_a°. Boudart regarded the third rule as a general guide line which might be always valid.

Furthermore, it is worth mentioning here that the above value of entropy change for ethylene and butene in a combined effect therefore it is not a pure effect of each component. From the present study it was not possible to obtain true values for entropy change for each component. However, within reasonable approximation, the values of adsorption equilibrium constants were found to comply with Boudart rules.

B. Discussion of Results

The catalytic disproportionation of olefins was first reported by Banks and Bailey (18) in 1964. In the case of propylene;

$$2\ C_3H_6 \rightleftharpoons C_2H_4 + C_4H_8\text{-}2 \quad \text{(5-50)}$$

Propylene — Disproportionation — Ethylene + 2-Butene

$$C_4H_8\text{-}2 \rightleftharpoons C_4H_8\text{-}1 \quad \text{(5-51)}$$

2-Butene — Isomerization — 1-Butene

$$C_3H_6 + C_4\text{-}H_8\text{-}2 + C_4\text{-}H_8\text{-}1 \rightleftharpoons \text{Unwanted byproducts}$$

WO_3, $Mo(CO)_6$, $W(CO)_6$ and Re_2O_7 on silica or alumina are the major catalysts used for disproportionation of olefins. The catalysts employed in the disproportionation reaction can also promote other types of reactions such as: olefin isomerization, olefin oligomerization, polymerization and hydrogenation. The best catalyst for the disproportionation should be able to promote the primary reaction and inhibit all possible secondary reactions. In order to do that, it is critical to understand the actual catalytic species for each reaction.

In this investigation, isomerization of 2-butene to 1-butene appeared to be independent of disproportionation activity, which indicated that the active sites were different for the two reactions. Isomerization was observed to increase as a function of temperature as shown in Figure (4-6). This suggested that the activation energy for isomerization is higher than that for disproportionation. These results are similar to those obtained on different alumina supported

catalysts (22, 25). For example, Bradshaw et al. (25) reported an increase in the rate of isomerization of 1-butene with a decrease in space velocity or an increase in temperature. Their results were obtained over a cobalt molybdate catalyst in the temperature range 122 - 245°C. On the other hand, Ogata and Kamiya (22) obtained similar results over a molybdena on alumina catalyst at low temperatures (0 to 50°C).

The hydrogenation of propylene to propane observed in this study was acoompanied by the dehydrogenation of 2-butene to form 1,3 butadiene. However, these reactions occurred at temperatures above 345°C. Polymerization and oligomerization could not be detected by the analytical technique employed in this study. Hydrogenation was reported by Banks and Bailey (18) to occur during the disproportionation of propylene over cobalt molybdate catalyst. Ogata and Kamiya (22) reported that during the disproportionation of propylene, the rate of polymerization and oligomerization increased with reaction temperature. Furthermore, the polymer formed caused a deactivation of active sites of the catalyst. Later, the authors (42) studied the disproportionation of propylene in the liquid phase. They concluded that the deactivation of the catalyst decreased in the presence of solvents since high hydrocarbons produced were transported from the catalyst surface to the free space of the reaction system.

Heterogeneous catalystic systems for disproportionation also readily promotes oligomerization of olefins, as

demonstrated by the reaction of 1-butene over CoO-MoO_3/γ-Al_2O_3 (81). Yamaguchi et al. (52) reported that the disproportionation of propylene and ethylene over WO_3/TiO_2 produced i-butene and propylene respectively. Both authors (52, 81) concluded that the reaction took place via carbene intermediate.

Several investigations have been reported in the literature aimed at improving the catalytic activity, selectivity and temperature dependence. Various methods of catalyst and support pretreatment were also evaluated. These include an alteration in the oxide to support ratio (41, 82), determination of activation temperature maxima and treatment with CO, H_2, chlorides, and various chelating ligands (43, 44, 50).

In this investigation the optimum conditions for catalyst activation was to calcine it in air at 600°C overnight followed by activation in a stream of dry nitrogen at 600°C for 12 hours. The activation carried out in a nitrogen atmosphere was accompanied by the evolution of water from the catalyst. The activity of the catalyst (WO_3 / γ-Al_2O_3) increased as a function of temperature of activation in the range 450-600 °C. This finding is in agreement with deVries and Pott (84). The authors (84) observed that the amount of water released from WO_3/ γ-Al_2O_3 upon activation increased with increasing activation temperature. They suggested that the activation process has

a high activation energy and the activity of the catalyst increased with liberation of water. We observed that the activation of the catalyst in dry air is just as effective as dry nitrogen which suggested that the activation is a dehydroxylation process as shown in equation (5-52).

Some disproportionation catalysts are characterized by an induction period during which the catalytic activity increased as a function of time, to reach a steady state value. This phenomena was observed on WO_3/SiO_2 catalyst (54,55) and on WO_3/Al_2O_3 (84).

In this study, the procedure was to cool the reactor from the activation temperature (600°C) to the desired temperature before propylene was introduced. A period allowed the nitrogen to be purged from the system by propylene. After this period, we did not observe an induction period over $WO_3/\gamma\text{-}Al_2O_3$. deVries et al. (84) reported that the break-in period over $WO_3/\gamma\text{-}Al_2O_3$ was about 1/2-2 hours, the period being shorter if the reaction temperature was higher. The authors concluded that during this period propylene interacted with the catalyst to form new active sites.

The catalytic activity of the heterogeneous catalysts containing tungsten or molybdenum oxides has a marked dependence on the nature of the support used (52). Ususally a higher opeating temperature (by about 200°C) is required for systems containing silica as support compared to those supported on γ-alumina (45). The literature indicates that a

that a combination of two oxides generate new acid sites (52). Therefore the sites in tungsten oxide, which are easily reduced would be dependent on the type of support for its activity. Yamaguchi et al. (52) investigated the effect of support on the activity of tungsten oxide catalysts for disproportionation and isomerization of olefins. They found that the rate of isomerization of 1-butene over a WO_3/TiO_2 catalyst increased as a function of tungsten oxide concentration. This increase was found to be in good agreement with the change in the acidity of the catalyst. Studies indicated that catalyst with increased protonic acidity were higher in isomerization activity (25).

In this investigation, no pretreatment of the catalyst was carried out. However, it was observed that selectivity towards disproportionation decreased with increase in temperature (150-390°C) and decreased in space time (1.06-17.88 g.cat-hr/g.mol). Figure (4-4 and 4-7).

The increase in temperature could activate isomerization sites which have higher activation energy. On the other hand, the higher space time will allow more of the 2-butene to be in contact with the isomerization catalytic sites. It was found that by a suitable choice of temperature and space time an optimum selectivity to ethylene and 2-butene can be obtained.

The selectivity of the WO_3/γ-alumina decreased as the tungsten oxide content increased as shown in Figure (4-3). Higher concentration of the oxide will create more active sites for disproportionation as well as isomerization. This

is demonstrated by the increase in conversion and decrease in selectivity. These findings support the results obtained by previous studies (41, 82). Korkhcf et al. (41) studied the effect of WO_3 content in a silica supported catalyst on initial rates for propylene disproportionation. Their results show that the activity of these catalysts increases with the increase in WO_3 content in the range 6-20%. Heckelsberg et al. (82) in a similar study found that a maximum activity was obtained from a catalyst containing 10 wt% WO_3/SiO_2.

The disproportionation activity of tungsten oxide supported on inorganic oxides like high surface area silica or alumina is well known (16, 37, 41, 43). However, the nature of interaction between the oxide and the carrier is not always understood and can differ in various systems. For the same oxide, the nature of active sites formed on the catalyst surface will depend on the type of supporting material used. The selectivity of disproportionation catalyst varies with the type of active sites available for reaction. There are many reports throughout the literature suggesting that the isomerization activity is favoured by the presence of acid sites (19, 25) . On the other hand, the combination of two oxides such as WO_3 and Al_2O_3 generates new acid sites (52).

Figures 4-1 and 4-2 show the effect of supporting material for a series of tungsten oxide catalysts on activity and selectivity for disproportionation as a function of temperature. The order of activity for disproportionation of propylene was: WO_3/ alumina > WO_3/Silica-alumina > WO_3/Silica

whereas the order for the isomerization was :

WO_3/Silica-alumina > WO_3/ γ-alumina > WO_3/ silica

The order of Catalytic activity is related to the formation of different disproportionation sites depending on the support used. Kerkhof et al. (41) studied the nature of interaction between carrier and oxide for WO_3/SiO_2 and WO_3/Al_2O_3 systems. They concluded that surface compounds are formed as well as on silica as on γ-alumina The interaction of alumina with tungsten oxide is stronger, resulting in better dispersion. In a subsequent investigation, Stork and Pott (45) concluded that in WO_3/γ-Al_2O_3, $Al_2(WO_4)_3$ is formed, whereas in WO_3/SiO_2, WO_3 does not react with the support. The authors verified their hypothesis using several techniques including phosphorescence spectroscopy, catalytic activity measurements and X-ray diffraction. They found a remarkable agreement between WO_3/γ-Al_2O_3 and $Al_2(WO_4)_3$, on one hand, and between WO_3/SiO_2 and WO_3 on the other.

Our results are in agreement with the findings of Stork and Pott (45) WO_3/γ-alumina was active at low temperatures 150-275 °C and the activity range found for this was similar to the one for $Al_2(WO_4)_3$. WO_3/SiO_2 was active at much higher temperature. In case of WO_3/Silica-alumina, it appears that both active sites were present, because this catalyst exhibited two regions of activity corresponding to both active sites. (Figures 4-1 and 4-2).

Selectivity is greatly affected by the supporting material used in the disproportionation catalysts (19, 20, 25, 52). Bradshaw et al. (25) reported that double bond

isomerization is proportional to the acidity of the catalyst and can be controlled by poisoning the catalyst with sodium ion. Yamaguchi et al. (52) showed that an increase in acidity resulted, on mixing tungsten oxide with other oxides. This increase was found to vary with the type of oxide used, and in the case of silica, only a slight increase in acidity was observed.

It is interesting to note that the results obtained in this study supports the results by others (19, 25, 52). The order of activity for isomerization of 2-butene to 1-butene is related to the order of acidity of the support used.

A catalyst dispersed on a carrier can exist in several forms. It may retain its chemical identity with the carrier acting as a dispersing agent, or it may dissolve in the carrier to give a solid solution or it may form a new stoichiometric compound with the carrier.

Catalytic experiments and physical measurements (86) have clearly shown that tungsten oxide retain its identity when dispersed on silica, with no indication of chemical reaction between the oxide and the support with alumina supported catalysts. It is generally accepted that the interaction of WO_3 with alumina is much stronger than silica.

The X-ray diffraction patterns was taken for the following samples: a catalyst before activation, a catalyst after activation, an active catalyst after reaction and a deactivated catalyst. The activity of the catalysts was proportional to $Al_2(WO_4)_3$ (Table-1)

The $Al_2(WO_4)_3$ cleavage plane (87, 88) has alternating Al^{+3} and W^{+6} sites. The atomic arrangement on the surface for hydrated (A) and dehydroxylated $Al_2(WO_4)_3$ (B) can be represented as follows:

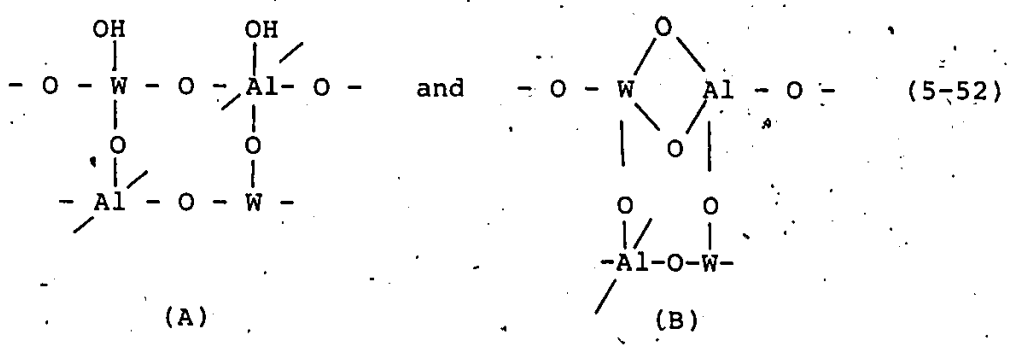

(5-52)

As mentioned before, activation is a dehydroxylation process. Therefore, the activated catalyst is best represented by structure (B) rather than structure (A).

C. Kinetics and Mechanism for Catalytic Disproportionation.

In the present study, the disproportionation of propylene has been investigated to establish the kinetic mechanism. Integral rate data obtained over an isothermal fixed bed reactor indicate that a dual-site mechanism is followed, involving the reaction of two adjacent chemisorbed molecules. The actual rate-controlling step involved a Langmuir-Hindshelwood type mechanism. The reaction can be visualized to take place as follows:

$$P + S \rightleftharpoons Ps \qquad \text{(adsorption)} \qquad (5\text{-}53)$$

$$2Ps \rightleftharpoons Es + Bs \qquad \text{(surface reaction)} \qquad (5\text{-}54)$$

$$Es \rightleftharpoons E + s \qquad \text{(desorption of Ethylene)} \qquad (5\text{-}55)$$

$$Bs \rightleftharpoons B + s \qquad \text{(desorption of Butene)} \qquad (5\text{-}56)$$

where P, E, B and s are propylene, ethylene, butene and the active site respectively. The surface reaction was found to be the rate controlling step in propylene disproportionation reaction and the following rate equation was derived.

$$r = \frac{-1}{2}\frac{d(P_p)}{dt} = k\,\frac{(P_p^2 - P_E P_B/K)}{(1+K_E P_E + K_B P_B + K_P P_P)^2} \qquad (5\text{-}57)$$

where k is the combined rate constant, K_P, K_E and K_B are the equilibrium adsorption constants for propylene, ethylene and butene respectively, and K is the thermodynamic equilibrium constant. The mechanism parameters and their temperature dependence were calculated from the experimental data using the non-linear regression technique.

Applying the initial rate assumption of near-zero partial pressures of products equation (5-57) reduces to:

$$ro = k\,(P_p)^2{}_0 / (1 + K_p(P_p)_o)^2 \qquad (5\text{-}58)$$

Most of the literature relating to disproportionation kinetics was based on initial rate data. Moffat and Clark (28) and Lewis and Willis (35) were successful in correlating their intial rate data for heterogeneously catalyzed disproportionation of propylene over cobalt molyodate on alumina catalysts with equation (2-28). Moffat and Clark (28) investigated the reaction between 121 to 205°C and pressure range of 1.36-5.44 atm, whereas Lewis and Wills (36) obtained their initial rate data in the same temperature range and pressures up to 9 atm. Davie et al. (33) also found that initial rate for disproportionation of proylene over $Mo(CO)_6/\gamma - Al_2O_3$ in the pressure range from 0.5×10^{-4} to 2.0×10^{-3} atm and tempratures between 17 to 77°C can be calculated from equation (5-58).

Begley and Wilson (32) found the Rideal model to apply to the disproportionation of propylene in the temperature range 217-457°C and pressures up to 62.3 atm. However, Moffat et al. (31) observed severe interface mass transfer effects for the same catalyst system used by Begley and Wilson (32).

Takahashi (39) obtained initial rates for the catalytic disproportionation of propylene in a static reactor for temperature up to 220°C and pressures in the range from 0.1 to 0.39

atm. He found the Langmuir-Hinshelwood model to hold over MoO_3/Al_2O_3 and WO_3/Al_2O_3. Although he assumed the adsorption of propylene over WO_3/AlO_2 the follow Freundlich equation, we suspect his data to be limited by mass transfer effects.

Recently, Luckner et al. (37) studied the disproportionation rection over a WO_3/SiO_2 catalyst in a differential bed reactor. Their experimental data collected at pressures up to 9 atm and temperature range 399 - 454°C could be correlated by equation (5-58). Hattikudur and Thodos (34) used a similar catalyst to study the kinetics of the same reaction between 343 to 454°C and pressure up to 66.7 atm. They found that both differential and integral rate data could be represented by the rate equation based on the dual-site mechanism.

The calculated apparent activation energy for propylene disproportionation over tungsten oxide on -alumina reported is 5.06 kcal/mol. Apparent activation energy for propylene disproportionation calculated by various investigators for WO_3/SiO_2, CoO - MoO_3/Al_2O_3 and $Mo(CO)_6/Al_2O_3$ were 18.6-59 (31, 32, 34, 37), 3.5-7.7 and 7.28 kcal/mol respectively.

The kinetic of propylene disproportionation over WO3/ γ-Al_2O_3 obtained in this study is in agreement with kinetic studies over other catalysts (28, 33, 34, 35, 37, 39). It can be concluded that the disproportionation of propylene is well interpreted kinetically be assuming that the rate is controlled by the surface reaction between adsorbed molecules on two neighboring active sites.

The results of this investigation has shown that the ratio of cis/trans-2-butene increased as a function of space time. It appears that the formation of cis-2-butene was favoured over trans-2-butene. The decrease in the mole fraction of 1-butene in the product analysis with the decrease in space time showed that only 2-butenes were favoured at short contact time. The ratio of ethylene to butenes approached unity as the space time increased. Experiments have shown that while 1-butene reacted over the catalyst (WO_3/γ-Al_2O_3) to give, ethyene, 2-butene, propylene and liquid products, ethylene was virtually inert towards this catalyst. These observations along with the rate model that was found to represent the data satisfactorily showed that the reaction proceeds through a "cyclobutane" intermediate. Applied to propylene the reaction can be visualized as follows:

$$H_2C{=}CH{-}CH_3 + H_2C{=}CH{-}CH_3 \rightleftharpoons H_2C\cdots CH{-}CH_3 \rightleftharpoons H_2C + CH{-}CH_3 \quad (5\text{-}59)$$
$$H_2C{=}CH{-}CH_3 \qquad H_2C\cdots CH{-}CH_3 \qquad H_2C \qquad CH{-}CH_3$$

$$H_3C{-}HC{=}CH{-}CH_3 \rightleftharpoons H_2C{=}CH{-}CH_2{-}CH_3 \quad (5\text{-}60)$$

2-Butene 1-Butene

The catalyst used in this study promoted isomerization to some degree. The presence of isomerized products such as 1-butene, could mask the real mechanism by reacting to give ethylene and propylene. For example; 1-butene could disproportionate to give ethylene and 3-hexene or could react with 2-butene to give propylene and 2-pentene.

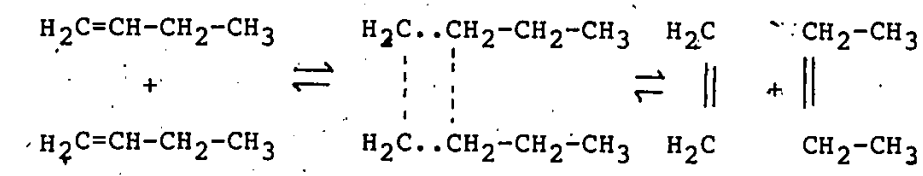

2 (1-Butene) (Ethylene)(2-Butene)

or

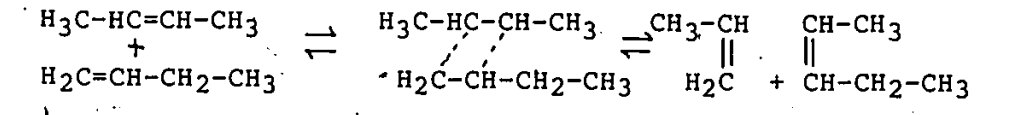

2-Butene + 1-Buten (propylene) (2-Pentene)

Therefore when the product distribution from propylene disproportionation is studied as a function of space time in order to arrive at a mechanism, it is better to use a selective catalyst or to study at such conditions where selectivity is maximum. Our results are in agreement with previous authors (25, 63, 24, 27, 19). Mol et al. (62), studying the disproportion of propylene, suggested a mechanism via a "cyclobutadiene" intermediate. This mechanism needs the transfer of four hyudrogen atoms from the olefin molecules to the catalyst surface. Experimental results of the present investigation have ruled out this mechanism (63, 94).

VII CONCLUSIONS AND RECOMMENDATIONS

The catalystic disproportionation of propylene was investigated over various supported tungsten oxide catalysts in an isothermal integral flow reactor between 150 and 490°C in the pressure range 3.041 to 7.124 atm and reciprocal of space velocity of 1.05 to 17.89 g.cat-hr/g.mol in order to establish the conditions for maximum conversion and yield, to derive a suitable rate equation and to propose a possible reaction mechanism:

Conclusions drawn from this investigation are:

(i) Unsupported tungsten oxide, -alumina, silica or silica-alumina have shown no activity for propylene disproportionation. However the activity and selectivity of supported tungsten oxide vary with the type of support.

(ii) WO_3 supported on silica-alumina catalysts consists of two types of active sites. One site is active at low temperature (160-275°C) and the other on at higher temperature (350-488°C).

(iv) The order of decrease in the selectivity as a function of temperature for various supported tungsten oxide catalysts was: slica-alumina > γ-alumina > silica.

(v) The activity a tungsten oxide catalyst supported on γ-alumina increased as the tungsten oxide concentration increased.

(vi) The activity of a 10wt% WO_3/γ-alumina increased with the increase in the temperature of activation. Maximum activity was obtained when the catalysts was activated in a stream of dry nitrogen at 600 °C for 12 hours.

(vii) The active component of the tungsten oxide catalysts supported on γ-alumina appeared to be $Al_2(WO_4)_3$ which was formed from the interaction of WO_3 with the support.

(viii) The selectivity decrease was related the rate of isomerization of 2-butene to 1-butene.

(ix) The rate of disproportionation of propylene over 10wt% WO_3/γ-alumina increased with increase of space time, temperature and pressure.

(x) The selectivity towards ethylene and 2-butene decreased as the temperature and space time increased.

(xi) Experimental data were found to be best correlated by a dual-site mechanism using Hougen-Watson approach based on Langmuir-Hinshelwood mechanisms where the rate is defined:

$$r = \frac{k\,(P_p^2 - P_E P_B / K)}{(1 + K_E P_E + K_B P_B + K_P P_P)^2}$$

where K_p, K_E, K_B, k are temperature dependent constants. The values of K_E, K_B and k increased with increased as the temperature increased from 180 - 300 °C, but K_p decreased.

(xii) The present data supports the four-center mechanism and a quasi-cyclobutane intermediate.

The following recommendations for further study are suggested by the results of this investigation.

(i) In order to obtain a better understanding of the formation of active sites, the effect of calcination and activation temperature and several ligands and poisons such as H_2, CO, H_2O and O_2 on the formation of active sites should be studied. Active sites should be monitored by analytical techniques such as X-ray diffiraction, Ramana spectroscopy and phosphorescence spectroscopy.

(ii) The nature of the active sites responsible for isomerization on a WO_3/γ-alumina should be investigated by studying the effect of adding several Group I-a and II-a metals.

(iii) It is recommended that disproportionation of radioactive propylene over a WO_3/γ-alumina catalyst be studied in order to gain insight into surface reaction mechanism as well as the delocalization of the double bond in propylene.

(iv) It is recommended that the catalytic disproportionation of propylene over a WO_3/SiO_2-Al_2O_3 be carried out in the temperature range (160-275 °C) and (350 - 490 °C), and more understanding of the kinetics, mechanism and active sites in the two temperature intervals.

VII. NOMENCLATURE

A	Component A
A	Area of a peak, cm^2
a_m	External particle surface area per unit mass, m^2/g.
a_v	External particle surface area per unit volume, m^2/cm^3.
a	Molecularity of a component A
B	Component B
C_P	Specific heat of a gas, cal./ g. mol.°C.
D_P	Diameter of particle, cm.
$D_{K,eff}$	Effective Knudsen diffusion coefficient, cm^2/s.
D_{AM}	Average diffusivity of component A, cm^2/s.
E	Effectiveness factor of the catalyst.
f	Chromatographic calibration factor.
F	Flow rate of the feed, g. mol/hr.
ΔF_A	Standard free energy of formation per mole of A, cal/g.mol
G_m	Molar velocity of gas flow based on the total cross-sectional area of the catalyst bed, g.mol/hr cm^2.
g_{mA}	Heat transfer due to heat of reaction per unit mass of catalyst, cal./hr g.
ΔH_A	Heat of reaction per mole of A reacted, cal./g.mol.
h_G	Heat transfer coefficient of the gas film.
I	Component I
j_D	Chilton-Colburn mass-transfer factor , dimensionless
j_H	Chilton-Colburn heat-transfer factor , dimensionless

K	Thermodynamic equilibrium constant.
K_{EB}	Equilibrium adsorption constant of ethylene and butene.
K_P	Equilibrium adsorpiton constant of propylene, atm^{-1}
K	Thermal conductivity of the gas. g.cal/sec.cm.°C
k_G	Mass transfer coefficient of the gas film.g.mol/sec.cm^2.atm.
k_S	Reaction rate constant combined with surface parameters.
k	Combined reaction rate constant. cm/sec
L	Molar concentration of active sites per unit mass. sites/g.
M	Molecular weight.
n	Number of moles.
P	Partial pressure (with subscript A,P,E,B, .. etc.), atm.
P_i	Partial pressure at the gas-solid interface.
P_r	Prandtl number, $C_p \mu/K$, dimensionless
P_f	Film pressure factor , dimensionless
Q	$(r_{mA} \Delta H / a_m C_p G_m)$
R	$r_{mA} / a_m \Phi G_m$
R	Gas constant , g.cal/g.mol.°K
R	Component R
Re	Reynolds number, $(D_p G_m / \mu)$ or $(G_m / a_v \Phi \mu)$, dimensionless
F	Average pore radius
r	Reaction rate (with subscript A, P, E, B) g.mol/hr.
r	Molecularity of component R
r_o	Initial rate , g.mol/hr.g.cat.
S	Component S

S	Selectivity of the catalyst for ethylene and 2-butene formation
s	Molecularity of component S
S_c	Schmidt number, $(\mu/\rho D_{AM})$, dimensionless
S_g°	Standard entropy , cal/g.mole -°C
T	Temperature, °C
T_{max}	Temperature where activity of the catalyst is maximum., °C
T_i	Temperature at the gas-solid interface , °C
V_g	Pore volume, cm^3/g.
V_i	Molar volume of a component, cm^3/mol.
W	Weight of the catalyst, gm.
X	Conversion of propylene
Y	Yield
Y_i	Mole faction at the interface
Y_{fA}	P_{fA}/Π
$\bar{z}$	Average Compressibility factor

Greek Symbols

β	Porosity of Catalyst , dimensionless
Δ	Finite increment or change of property
θ	Fractional coverage of catalyst surface by a certain component.
Θ	Parameter value
δ	Convergence limit

μ Viscosity, poises = g/cm.sec

Π Total pressure. atm.

ρ Density of gas. g/cm^3

ρ_p Density of the catalyst particle.

ϕ Shape factor, ration of actual external surface available for mass and heat transfer to the total external surface area, assumed to be 0.90 for irregular granules.

τ Tortuosity of catalyst, dimensionless

Subscripts

a Adsorption

av Average property

B Butene - 2

C Critical value

d Desorption

E Ethylene

f Properties at the average condition of the gas film.

i Properties at the gas-solid interface.

I Component I

j Component j

l Properties in the gas sample loop

P Propylene

r Reduced property

o Placed after a symbol means initial.

BIBLIOGRAPHY

1. Johnson, P.H., Hydrocarbon Processing, 4, 149 (1967).
2. Johnson, P.H., Chemical Week, July 23, 70 (1966).
3. Kenton, J.R., D.L. Crain and R.F. Kleinschmidt, U.S. Patent 3,491,163.
4. Hughes, W.B., Chemtech, 5 (8), 486 (1975).
5. Dixon, R.E., J.F. Hutto, R.T. Wilson and R.L. Banks, Oil and Gas J., 65 (4), 98 (1967).
6. Logan, R.S. and R.L. Banks, Oil Gas J., 66, 131 (1968).
7. Banks, R.L. and R.B. Reigier, Ind. & Eng. Chem., Prod. Res. Develop, 10, 46 (1971).
8. Heckelsberg, L.F., R.L. Banks and G.C. Bailey, Preprints, The Division of Petrol Chem, Am. Chem. Soc., San Francisco Meeting, April (1968).
9. Schneider, V. and P.K. Frolich, Ind. & Eng. Chem., 23, 1405 (1931).
10. Bailey, G.C., Catalysis Reviews, 3, 37 (1970).
11. Banks, R.L., Topics in Current Chemistry, 25, 39 (1972).
12. Mol, J.C., and Moulijn, "Adv. in Catal."; 24, 131 (1975).
13. Haines, R.J., and G.J. Leigh, Chem. Soc. Rev., 4, 155 (1975).
14. Banks, R.L. and L.F. Heckelsberg, Ind. & Eng. Chem., Prod. Res. & Develop., 14, 33 (1975).

15. Banks, R.L. and G.C. Bailey, Ind. & Eng. Chem., Prod. Res. & Develop., 10, 48 (1971).

16. Heckelsberg, L.F., R.L. Banks and G.C. Bailey, Ind. Eng. Chem., Prod. Res. & Develop., 7, 29 (1968).

17. Johnson, P.H., VII World Petrol Congress Proc., Mexico City, 5, 247 (1967).

18. Banks, R.L. and G.C. Bailey, Ind. & Eng. Chem., Proc. Res. & Develop., 3, 170 (1964).

19. Kobylinski, T.D. and H.E. Swift, J. of Catal., 26, 416 (1972).

20. Ibid, 33, 83 (1974).

21. Nakamura, R., H. Lida and E. Echigoya, Chem. Lett., 273 (1972).

22. Ogata, E. and Y. Kamiga, Ind. & Eng. Chem., Prod. Res. & Develop., 13 (4), 226 (1974).

23. Smith, J., W. Mowat, D.A. Whan and E.A.V. Ebsworth, Am. Chem. Soc., Dalton. Trans., 1743 (1974).

24. Banks, R.L. and G.C. Bailey, J. of Catal., 14, 276 (1969).

25. Bradshaw, C.P.C., E.J. Howmand L. Turner, J. of Catal, 7, 269 (1967).

26. Calderon, N., E.A. Ofstead, J.P. Ward, W.A. Judy and K.W. J. of the Am. Chem. Soc., 90, 4133 (1968).

27. Clark, A. and C. Cook, J. of Catal., 15, 420 (1969).

28. Moffat, A.J., and A. Clark, J. of Catal., 17, 264 (1970).

29. Woody, F.L., M.J. Lewis and G.B. Wills, J. of Catal., 14, 389 (1969).

30. Moffat, A.J., M.M. Johnson and A. Clark, J. of Catal., 18, 345 (1970).

31. Moffat, A.J., A. Clark and M.M. Johnson, J. of Cata., 22, 379 (1971).

32. Begley, J.W. and R.T. Wilson, J. of Catal., 9, 375 (1967).

33. Davie, E.S., D.A. Whan, and C. Kemball, J. of Catal., 24, 272 (1972).

34. Hattikudur, U.R. and G. Thodos, Chem. Reaction Eng. II, American Chemical Society, 80 (1974).

35. Lewis, M.J. and G.B. Wills, J. of Catal., 20, 182 (1972).

36. Ibid, 15, 140 (1969).

37. Luckner, R.C. and G.B. Wills, J. of Catal., 28, 83 (1973).

38. Luckner, R.C., G.E. McConchie, and G.B. Wills, J. of Catal., 28, 63 (1973).

39. Takahashi, T., Bull of the Japan Petrol Instit., 14, 40 (1972).

40. Engelhardt, J., Recueil Des. Travaux Chimiques Des Pays - Bas, 96, 13 (1977).

41. Kerkhof, F.P.J.M., R. Thomas and J.A. Moulijn, Recueil Des Travaux Chimiques Des Pays - Bas, 96, 121 (1977).

42. Ogata, E., T. Sadesawa, and Y. Kamiya, Bull of the Chem. Soc. of Japan, 49, 1317 (1976).

43. Pennella, F. and R.L. Banks, J. of Catal., 31, 304 (1973).

44. Pennella, F., R.B. Regier and R.L. Banks, J. of Catal., 34, 52 (1974).

45. Stork, W.H.J. and G.T. Pott, Recueil Des Travaux Chimiques Des Pays-Bas, 96, 105 (1977).

46. Stork, W.H.J., J.G.F. Coolegem and G.T. Pott, J. of Catal., 32, 497 (1974).

47. de Vries, J.L.K.F. and G.T. Pott, Recueil Des Travaux Chimiques Des Pays-Bas, 96, 96(1977).

48. Smith, J., R.F. Howe and D.A. Whan, J. of Catal., 34, 191 (1974).

49. Sadesawa, T., E. Ogata and Y. Kamiya, Bull. of the Chem. Soc. of Japan; 50, 998 (1977).

50. Sadesawa, T., E. Ogata and Y. Kimiya, Bull. of the Chem. Soc. of Japan, 52 (6), 1661 (1979).

51. Nakamura, R. and E. Echigoya, Bull. of the Japan Petrol Inst., 14, (2), 187 (1972).

52. Yamaguchi, T., Y. Tanaka and K. Tanabe, J. of Catal., 65, 442 (1980).

53. Gangwal, S.K. and G.B. Wills, J. of Catal., 52, 539 (1978).

54. Wills, G.B., J. Fathi-Kalajahi, S.K. Gangwal and S. Tang., Recueil Des Travaux Chimiques Des Pays-Bas, 96, 110 (1977).

55. Gangwal, S.K., J. Fathi-Kalajahl and G.B. Wills, Ind. & Eng. Chem., Prod. Res. and Develop., 16 (3), 237 (1977).

56. Gebret, E. and R.J. Ackerman, Inorg. Chem., 5, 136 (1966).

57. Giordana, N., J.C.J. Bart., A. Vaghi, A. Castellan., and G. Martinotti, J. of Catal., 38, 1(1975).

58. Thomas, R., J.A. Moulijn and F.P.J.M. Kerkhof, Recueil Des Travaux Des Pays-Bas, 96, 134 (1977).

59. Nassau, K., H.J. Levinsteim and G.M. Lalacono, J. of Phy. Chem. Solid, 26, 1805 (1965).

60. Thomas, R., J.A. Moulijn and F.P.J.M. Kerkhof, Recueil Des Travaux Des Pays-Bas, 96, 154 (1977).

61. Calderon, N., H.Y. Chen, and K.W. Scott, Tetrahedron Letters, 34, 3327 (1967).

62. Mol, J.C., J.A. Moulijn, and C. Boelhouwer, J. of Catal., 11, 87 (1968).

63. Crain, D.L., J. of Catal., 13, 110 (1969).

64. Mol, J.C., J.A. Moulijn and C. Boelhouwer, Chem. Commun., 633 (1968).

65. Hinshelwood, C.N., "The Kinetics of Chemical Change", Oxford Univ. Press, London, 207 (1926).

66. Taylor, H.S., J. of Phys. Chem., 30, 145 (1926).

67. Satterfield, C.N. and T.K. Sherwood, "The Role of Diffussion in Catalysis", Addison - Wesley Publishing Co., Inc., 31 (1963).

68. Thomas J.M. and W.J. Thomas: "Introduction to the Principles of Heterogeous Catalysis", Academic Press N.Y. 32 (1967).

69. Hougen, O.A., Ind. Eng. Chem., 53, 509 (1961).

70. Chilton, T.H. and A.P. Colburn, Ind. & Eng. Chem., 26, 1183 (1935).

71. Gramson, B.W., G. Thodos and O.A. Hougen, Trans. Am. Inst. Chem. Eng., 39, 1 (1943).

72. Wilke, C.R. and O.A. Hougen, Trans. Am. Inst. Chem. Eng., 61, 445 (1945).

73. Yoshida, F., O. Ramaswami and O.A. Hougen, AIChE.J., 8, 5 (1962).

74. Schwartz, C.E. and J.M. Smith, Ind. & Eng. Chem., 45, 1209 (1953).

75. Ergun, S., Chem. Eng. Prog., 48, 89 (1952).

76. Hougen, O.A. and K.M. Watson, "Chemical Process Principles", Part III, John Wiley and Sons, N.Y. (1947).

77. Yang, K.H. and O.A. Hougen, Chem. Eng. Prog., 46, 146 (1950).

78. Li, J.C.R., "Statistical Inference", II, Edwards Broth., Inc., Ann Arbor Michigan, 176 (1964).

79. Boudart, M., D.E. Mears and M.A. Vannice, "Comptes - rendu XXXVI e Congrès International de Chimie Industrielle", Industrie Chimique Belge, 32 (Special Issue), Part I, 281 (1967).

80. Handbook of Chemistry and Physics, CRC Press, Ohio, 53rd Edition D72 (1972-73).

81. Bawn, J., Proc. Chem. Soc., 165 (1962).

82. Heckelsberg, L.F., R.L. Banks and G.C. Bailey, Ind. & Eng. Chem., Prod. Res. and Develop., 7 (1), 29 (1968).

83. de Vries, J.L.K. and G.T. Pott, Recueil Des Travaux Des Pays-Bas, 96, 115 (1977).

84. Banks, R.L., G.C. Bailey, L.F. Heckelsberg and F. Pennella, Americal Meeting of the Catalysis Society (1969).

85. Biben, P. and G.T. Pott, J. of Catal., 30, 169 (1973).

86. Craig, D.C. and N.C. Stephenson, Acta. Cryst., B24, 1250 (1968).

87. de Boer, J.J., Acta. Cryst., B30, 1878 (1974).

88. Hougen, O.A. and K.M. Watson, Ind. & Eng. Chem., 35 (5), 529 (1943).

89. Corrigan, T.E., Chem. Eng., 199 (1955).

90. Laidler, K.J., "Chemical Kinetics", McGraw Hill Book Co., N.Y. 1965.

91. Cvetanovic, R.J. and Y. Amenomiya, Advances, in Catalysis, 17, 103-149 (1967).

92. Mol, T.C., Ph.D. Thesis, Univ. of Amsterdam (1971).

93. Mol, J.C., J.R. Visser and C. Boelhower, J. of Catal., 17, 114 (1970).

94. Missen, R.W., Trans. of Eng. Inst. of Canada, 6, #E3 Dec. (1963).

95. Emmett, P.H., "Catalysis", vol. 1, Reinhold Publ. Corp. N.Y., 339 (1954).

96. Rossini, F.D., et al., "Selected Values of Physical and Thermodynamic Properties of Hydrocarbons and Related Compounds," A.P.I. Research Project 44, Carnegie Press, Pittsburg, Pa., 1953.

97. Calderon, N., E.A. Ofstead, J.P. Ward, W.A. Judy and K.W. Scott, J. of the Am. Chem. Soc., 90, 4133 (1967).

98. Kittrell, J.R., "Advances in Chemical Engineering", 8, 97 (1970).

99. Langmuir, I., J. Am. Chem. Soc., 40, 1361 (1918).

IX APPENDICES

APPENDIX A

THERMODYNAMIC ASPECTS OF

PROPYLENE DISPROPORTIONATION

Equilibrium Constants

Equilibrium constants for this system were calculated by a procedure recently presented by Missen (94). Missen's technique is general for systems involving isomers in either the feed product or both.For system involving isomers in the products the equilibrium constant, K, is given by.

$$K = \Sigma K_j$$

where K_j is the equilibrium constant for reactant goint to the j^{th} isomer of products. This procedure is illustrated using the 573°K (300°C) data from Table (VIII-A).

Since the products contain both cis and trans-2-butene, two reactions are written as follows:

1. 2 Propylene⇌Ethylene + Cis-2-Butene
2. 2 Propylene⇌Ethylene + trans-2-butene.

From Table (VIII-A) the free energy for reaction 1 at 573°K is

$\Delta F = ((20.469 + 33.355) - 2\ (25.384))$

$= 3.045$ kcal/g.mol.

$$\ln K_1 = \frac{-\Delta G^o}{RT} = \frac{-(3045)}{1.987 \times 573} = -2.6737$$

K_1 at 573.16°K = 0.0689

For reaction 2

$\Delta G_f^o = ((20.469 + 32.754) - 2(25.384))$

$= 2.455$ kcal/g.mol

and $\ln K_2 = -\Delta G_f/RT$

$= -2455/(1.987)(573)$

$= -2.1556$

$K_2 = 0.1588$

The overall equilibrium constant, K, is given by the sum of K_1 and K_2

K at $573^oK = 0.1848$

and equilibrium conversion $X_{eq} = \frac{2\sqrt{k}}{1 + 2\sqrt{k}}$

X_{eq} at $573^oK = 46.23\%$

Equilibrium constants at 453^oK (180^oC), 483^oK (210^oC), and 523^oK (250^oC) were calculated by this procedure and the values obtained are:

K (180^oC) = 0.1670 $X_{eq} = 44.98\ \%$

K (210^oC) = 0.1715 $X_{eq} = 45.30\ \%$

K (250^oC) = 0.1775 $X_{eq} = 45.74\ \%$

TABLE -A-1

FREE ENERGY OF FORMATION DATA, kcal/g.mol

Temperature ^oK	298	453	483	523	573
Ethylene	16.282	18.353	18.981	19.633	20.469
Propylene	14.990	20.267	21.803	23.379	25.384
cis-2-Butene	15.740	24.725	27.325	29.979	33.344
trans-2-Butene	15.05	24.124	26.732	29.389	32.754

Data was taken from Rossini et al. (97).

APPENDIX B

CALIBRATION OF EQUIPMENT

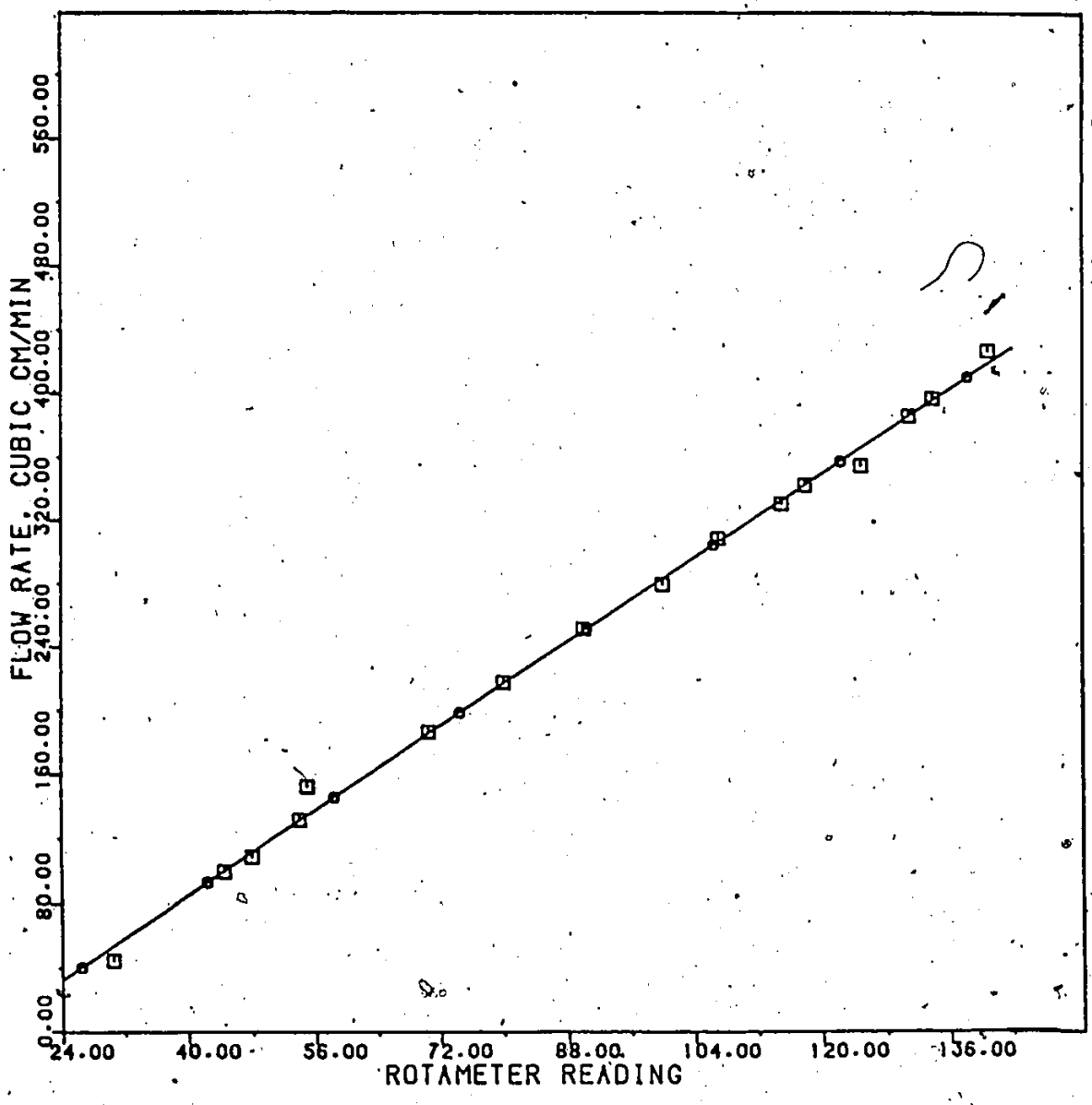

Figure 8-1. Calibration of Rotameter (R-4) at atmospheric pressure.

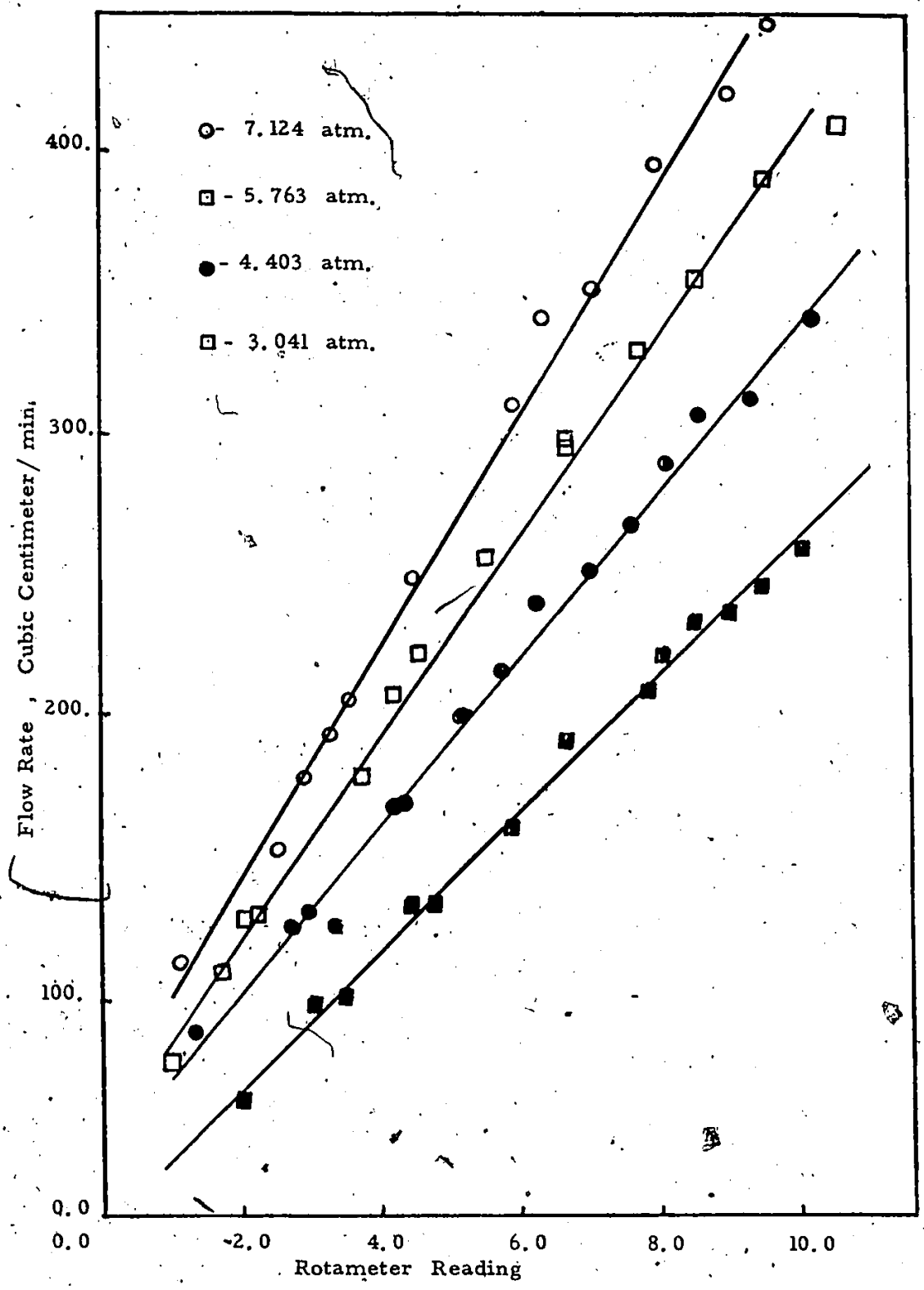

Figure 8-2 Calibration of Rotameter R (1) at Various Pressures.

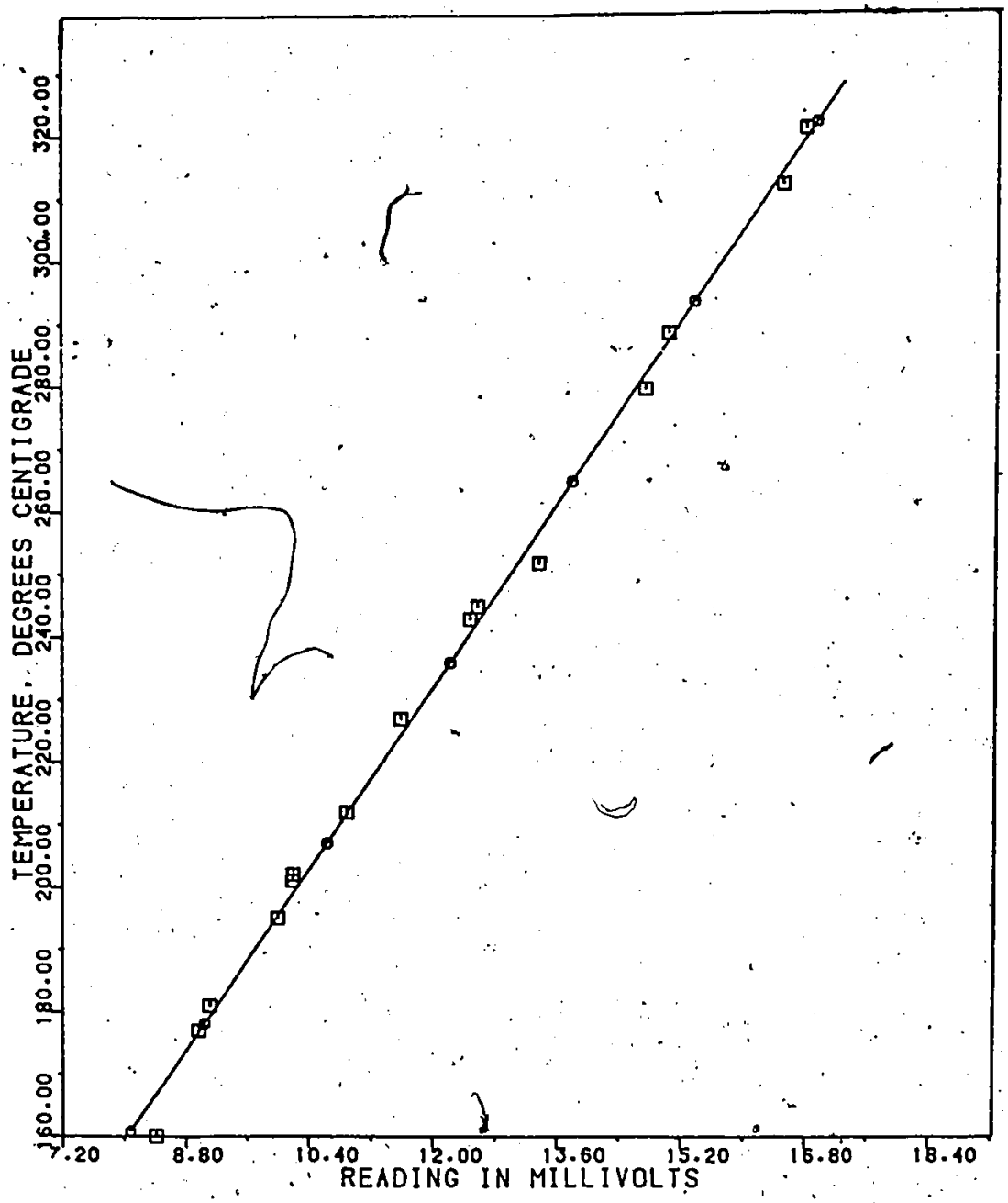

Figure 8-3 Calibration of the Thermocouple.

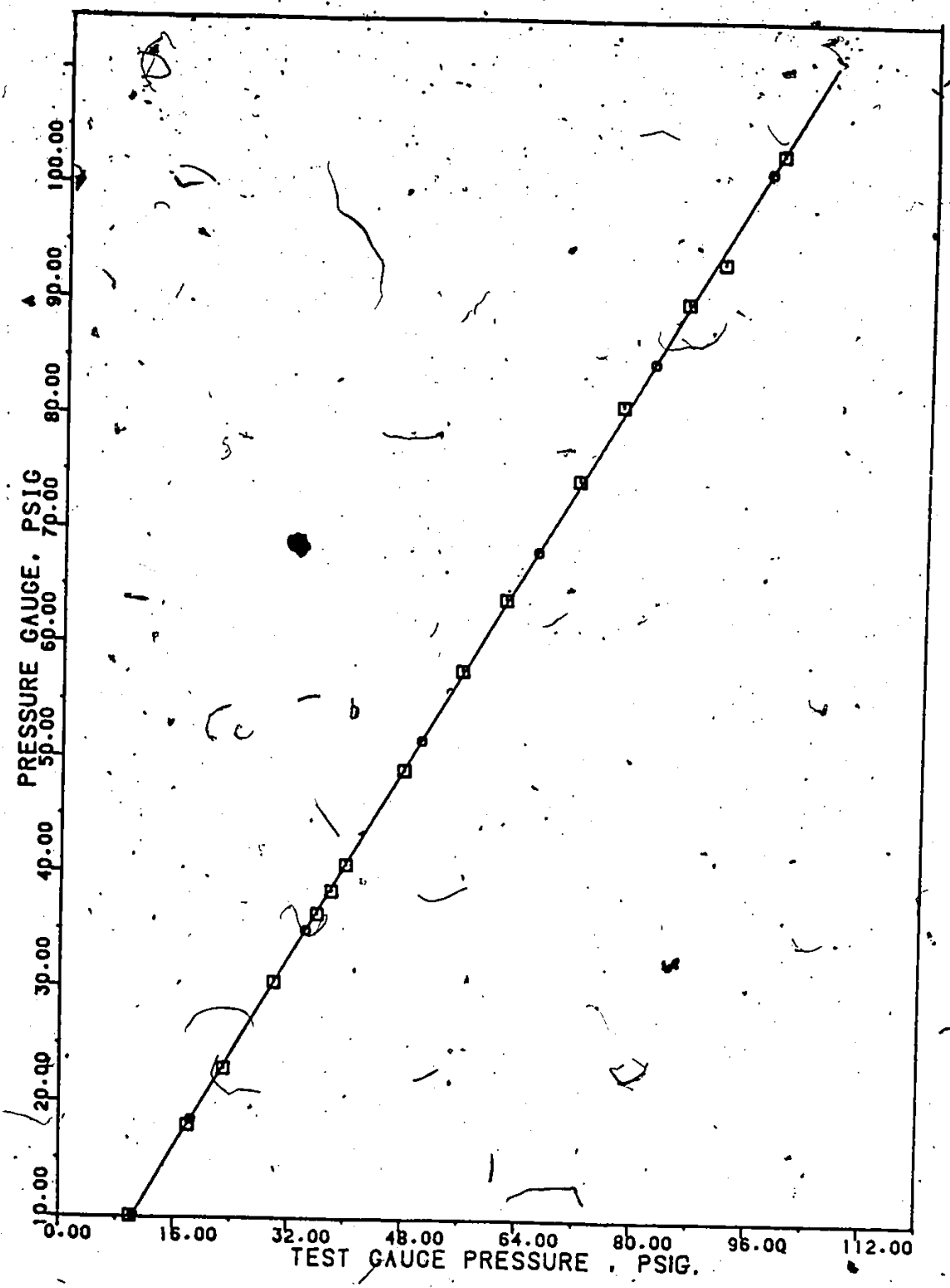

Figure 8-4 Calibration of Pressure Gauge.

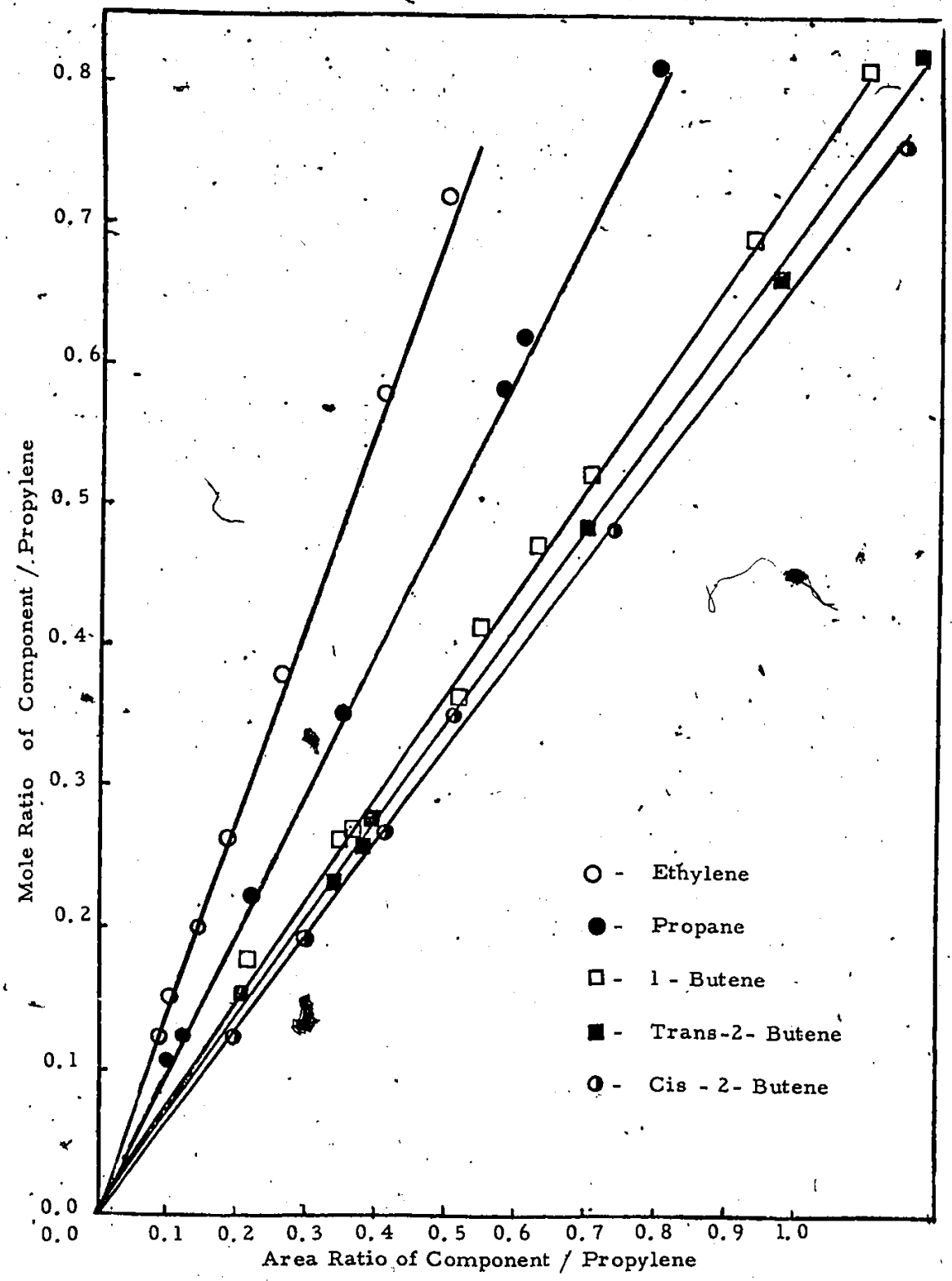

Figure 8-5 Chromatographic Calibration of Components

APPENDIX C

TABULATED EXPERIMENTAL DATA

TABLE C-1

Effect of W/F on Conversion of Propylene and Yield of Ethylene and Butene-2
Temperature: 180° C. Pressure: 3.041 atm.

Run No.	W/F g. cat-hr/g. mol	Mole Fraction in Product						Conversion X	Yield Y	Selectivity S (%)
		Ethylene	Propane	Propylene	1-Butene	t-2-Butene	c-2-Butene			
101	7.3978	0.1213	0.0060	0.8068	0.00	0.0474	0.0186	0.1880	0.1872	0.9961
102	7.8049	0.1276	0.0059	0.7889	0.00	0.0481	0.0195	0.1959	0.1952	0.9961
103	9.3600	0.1425	0.0059	0.7730	0.00	0.0552	0.0235	0.2220	0.2212	0.9960
104	10.5500	0.1566	0.0062	0.7492	0.00	0.0614	0.0265	0.2459	0.2446	0.9946
105	15.0081	0.1844	0.0070	0.6855	0.00	0.0792	0.0439	0.3100	0.3075	0.9917
106	3.5540	0.0679	0.0059	0.8903	0.00	0.0254	0.0105	0.1040	0.1038	0.9983
107	5.9080	0.1043	0.0058	0.8365	0.00	0.0391	0.0142	0.1581	0.1577	0.9973
108	13.5590	0.1676	0.0059	0.7133	0.00	0.0727	0.0405	0.2820	0.2807	0.9953
109	11.3670	0.1652	0.0060	0.7293	0.00	0.0702	0.0293	0.2659	0.2646	0.9952
110	2.4900	0.0491	0.0059	0.9191	0.00	0.0184	0.0075	0.0749	0.0749	1.00

TABLE C-1 (continued)

Temperature: 180°C Pressure: 4.403 atm

Run No.	W/F g. cat-hr/g. mol	Mole Fraction in Product						Conversion X	Yield Y	Selectivity S (%)
		Ethylene	Propane	Propylene	1-Butene	t-2-Butene	c-2-Butene			
111	6.5999	0.1353	0.0061	0.7819	0.0	0.0518	0.0249	0.2299	0.2199	0.9952
112	7.4217	0.1434	0.0061	0.7651	0.0	0.0570	0.0283	0.2299	0.2288	0.9952
113	8.9293	0.1611	0.0062	0.7422	0.0	0.0665	0.0241	0.2530	0.2517	0.9946
114	10.1464	0.1779	0.0061	0.7164	0.0	0.0749	0.0248	0.2790	0.2775	0.9948
115	6.9115	0.1330	0.0060	0.7759	0.0	0.0545	0.0306	0.2190	0.2180	0.9956
116	7.5833	0.1520	0.0060	0.7563	0.0	0.0653	0.0205	0.2388	0.2378	0.9956
117	10.6018	0.1787	0.0062	0.7094	0.0	0.0749	0.0308	0.2860	0.2845	0.9945
118	3.5500	0.0828	0.0060	0.8634	0.0	0.0308	0.0170	0.1311	0.1306	0.9966
119	11.5100	0.1864	0.0062	0.6977	0.0	0.0769	0.0329	0.2977	0.2961	0.9945
120	5.2980	0.1183	0.0058	0.8088	0.0	0.0448	0.0224	0.1860	0.1854	0.9968
121	13.2901	0.2034	0.0062	0.6707	0.0	0.0838	0.0359	0.3249	0.3231	0.9943
122	14.9600	0.2129	0.0062	0.6556	0.0	0.0878	0.0376	0.3401	0.3382	0.9943

TABLE C-1 (continued)

Temperature: 180°C Pressure: 5.763 atm.

Run No.	W/F g. cat-hr/g. mol	Mole Fraction in Product						Conversion X	Yield Y	Selectivity S (%)
		Ethylene	Propane	Propylene	1-Butene	t-2-Butene	c-2-Butene			
123	6.6630	0.1457	0.0059	0.7621	0.0	0.0582	0.0280	0.2330	0.2300	0.9957
124	7.4792	0.1632	0.0063	0.7422	0.0	0.0614	0.0269	0.2530	0.2515	0.9940
125	8.9566	0.1774	0.0062	0.7143	0.0	0.0709	0.0312	0.2811	0.2795	0.9944
126	10.1715	0.1840	0.0061	0.6905	0.0	0.0859	0.0334	0.3050	0.3033	0.9945
127	11.9184	0.1979	0.0062	0.6685	0.0	0.0854	0.0420	0.3272	0.3253	0.9944
128	3.1202	0.0824	0.0060	0.8614	0.0	0.0360	0.0142	0.1330	0.1326	0.9966
129	4.9721	0.1186	0.0057	0.8038	0.0	0.0499	0.0221	0.1910	0.1905	0.9973
130	5.8200	0.1098	0.0059	0.7800	0.0	0.0704	0.0339	0.2149	0.2140	0.9956
131	13.9100	0.2078	0.0058	0.6526	0.0	0.0896	0.0441	0.3431	0.3415	0.9954

TABLE C-1 (continued)

Temperature: 180°C Pressure: 7.124 atm

Run No.	W/F g. cat-hr/g. mol	Mole Fraction in Product						Conversion X	Yield Y	Selectivity S (%)
		Ethylene	Propane	Propylene	1-Butene	t-2-Butene	c-2-Butene			
132	7.6008	0.1327	0.0061	0.7274	0.0	0.0863	0.0476	0.2679	0.2665	0.9948
133	7.8136	0.1542	0.0060	0.7223	0.0	0.0805	0.0370	0.2730	0.2717	0.9951
134	10.2828	0.1574	0.0060	0.6748	0.0	0.1075	0.0543	0.3208	0.3192	0.9949
135	12.5979	0.1896	0.0064	0.6497	0.0	0.1067	0.0476	0.3461	0.3430	0.9937
136	8.3790	0.1611	0.0062	0.7114	0.0	0.0820	0.0393	0.2840	0.2825	0.9945
137	10.0550	0.1679	0.0066	0.6787	0.0	0.0981	0.0486	0.3169	0.3147	0.9928
138	14.0739	0.1910	0.0067	0.6338	0.0	0.1133	0.0552	0.3621	0.3595	0.9929
139	3.3297	0.0840	0.0063	0.8426	0.0	0.0453	0.0218	0.1520	0.1511	0.9944
140	5.5702	0.1198	0.0062	0.7735	0.0	0.0665	0.0340	0.2215	0.2203	0.9947
141	6.8100	0.1241	0.0060	0.7447	0.0	0.0807	0.0445	0.2505	0.2493	0.9954

TABLE C-2

Effect of W/F on Conversion of Propylene, Yield and selectivity to Ethylene

Temperature: 210°C Pressure: 3.041 atm.

Run No.	W/F g. cat-hr/g. mol	Mole Fraction in Product						Conversion X	Yield Y	Selectivity S (%)
		Ethylene	Propane	Propylene	1-Butene	t-2-Butene	c-2-Butene			
142	6.2500	0.1351	0.0065	0.7580	0.0092	0.0619	0.0294	0.2371	0.2264	0.9548
143	6.3980	0.1264	0.0061	0.7532	0.0094	0.0648	0.0402	0.2419	0.3314	0.0563
144	8.1990	0.1372	0.0065	0.7392	0.0099	0.0669	0.0403	0.2560	0.2444	0.9545
145	7.2000	0.1342	0.0061	0.7364	0.0098	0.0692	0.0444	0.2589	0.2477	0.9571
146	7.4965	0.1418	0.0063	0.7294	0.0129	0.0683	0.0413	0.2659	0.2514	0.9453
147	9.2410	0.1432	0.0063	0.7164	0.0144	0.0739	0.0458	0.2789	0.2629	0.9425
148	1.6984	0.1610	0.0066	0.6906	0.0170	0.0790	0.0457	0.3049	0.2858	0.9371
149	3.9039	0.0966	0.0063	0.8216	0.0073	0.0463	0.0219	0.1731	0.1647	0.9518
150	5.3200	0.1172	0.0062	0.7820	0.0094	0.0563	0.0289	0.2129	0.2028	0.9505
151	2.3500	0.0650	0.0062	0.8793	0.0037	0.0321	0.0131	0.1150	0.1108	0.9636
152	11.3984	0.1641	0.0067	0.6847	0.0173	0.0806	0.0466	0.3109	0.2013	0.9371
153	12.5000	0.1724	0.0062	0.6529	0.0225	0.0910	0.0549	0.3428	0.3183	0.9285

TABLE C-2 (continued)

Temperature: 210°C Pressure: 4.403 atm

Run No.	W/F g. cat-hr/g. mol	Mole Fraction in Product						Conversion X	Yield Y	Selectivity S (%)
		Ethylene	Propane	Propylene	1-Butene	t-2-Butene	c-2-Butene			
154	6.6585	0.1572	0.0061	0.7184	0.0149	0.0661	0.0374	0.2769	0.2606	0.9409
155	7.7939	0.1520	0.0062	0.6955	0.0188	0.0773	0.0502	0.3000	0.2795	0.9317
156	8.4063	0.1699	0.0064	0.6845	0.0200	0.0731	0.0460	0.3111	0.2891	0.9292
157	10.1396	0.1681	0.0065	0.6587	0.0239	0.0880	0.0547	0.3370	0.3109	0.9224
158	5.6700	0.1323	0.0059	0.7492	0.0071	0.0624	0.0432	0.2459	0.2378	0.9671
159	5.5700	0.1295	0.0061	0.7551	0.0084	0.0672	0.0437	0.2501	0.2403	0.9611
160	5.9200	0.1462	0.0060	0.7378	0.0101	0.0632	0.0373	0.2579	0.2466	0.9561
161	6.0150	0.1359	0.0058	0.7324	0.0110	0.0698	0.0451	0.2629	0.2508	0.9540
162	6.7471	0.1554	0.0061	0.7163	0.0138	0.0680	0.0404	0.2790	0.2638	0.9454
163	8.5120	0.1587	0.0060	0.6826	0.0195	0.0823	0.0509	0.3130	0.2919	0.9327
164	11.6498	0.1915	0.0074	0.6468	0.0296	0.0852	0.0495	0.3591	0.3262	0.9083
165	4.8671	0.1096	0.0061	0.7849	0.0103	0.0548	0.0343	0.2101	0.1988	0.9463
166	2.3100	0.0768	0.0063	0.8584	0.0041	0.0393	0.0150	0.1360	0.1311	0.9639

TABLE C-2 (Continued)

Temperature: 210 C Pressure: 5.763 atm

Run No.	W/F g. cat-hr/g. mol	Mole Fraction in Product						Conversion X	Yield Y	Selectivity S (%)
		Ethylene	Propane	Propylene	1-Butene	t-2-Butene	c-2-Butene			
167	5.6500	0.1399	0.0062	0.7254	0.0067	0.0728	0.0489	0.2699	0.2617	0.9695
168	6.0940	0.1357	0.0058	0.7144	0.0091	0.0814	0.0536	0.2810	0.2708	0.9637
169	7.1400	0.1467	0.0060	0.6915	0.0134	0.0871	0.0555	0.3041	0.2892	0.9513
170	9.6500	0.1639	0.0063	0.6478	0.0210	0.0997	0.0612	0.3480	0.3248	0.9334
171	5.5700	0.1527	0.0058	0.7161	0.0082	0.0727	0.0445	0.2793	0.2699	0.9664
172	6.6100	0.1535	0.0056	0.7015	0.0089	0.0798	0.0508	0.2939	0.2841	0.9663
173	7.2398	0.1859	0.0056	0.6746	0.0112	0.0771	0.0456	0.3211	0.3086	0.9612
174	8.5501	0.1726	0.0055	0.6648	0.0119	0.0885	0.0567	0.3309	0.3171	0.9604
175	4.3000	0.1274	0.0057	0.7649	0.0045	0.0597	0.0379	0.2301	0.2249	0.9773
176	5.2500	0.1342	0.0058	0.7453	0.0077	0.0653	0.0417	0.2499	0.2412	0.9652
177	5.9257	0.1412	0.0657	0.7372	0.0057	0.0694	0.0409	0.2581	0.2515	0.9744
178	5.6194	0.1467	0.0057	0.7275	0.0095	0.0685	0.0421	0.2678	0.2573	0.9609
179	6.9700	0.1589	0.0057	0.6945	0.0118	0.0788	0.0503	0.3010	0.2879	0.9567
180	9.2898	0.2053	0.0061	0.5578	0.0192	0.0682	0.0434	0.3379	0.3169	0.9380
181	3.9500	0.1161	0.0056	0.7778	0.0053	0.0581	0.0369	0.2170	0.2112	0.9731
182	2.4500	0.0939	0.0059	0.8366	0.0049	0.0294	0.0294	0.1580	0.1527	0.9663

TABLE C-2 (Continued)

Temperature: 210°C Pressure: 7.124 atm

	Temperature °C	Mole Fraction in Product						Conversion X	Yield Y	Selectivity X (%)
		Ethylene	Propane	Propylene	1-Butne	t-2-Butene	c-2-Butene			
183	5.5098	0.1521	0.0059	0.7095	0.0106	0.0749	0.0470	0.2859	0.2740	0.9585
184	6.9387	0.1634	0.0061	0.6855	0.0129	0.0818	0.0503	0.3100	0.2955	0.9532
185	8.3542	0.1761	0.0063	0.6607	0.0182	0.0864	0.0523	0.3350	0.3148	0.9397
186	8.5411	0.1847	0.0067	0.6449	0.0205	0.0867	0.0565	0.3509	0.3279	0.9343
187	11.9051	0.1959	0.0069	0.6151	0.0258	0.0917	0.0646	0.3809	0.3522	0.9246
188	6.7495	0.1634	0.0062	0.6896	0.0093	0.0809	0.0506	0.3059	0.2949	0.9638
189	7.8062	0.1778	0.0064	0.6567	0.0106	0.0888	0.0543	0.3390	0.3209	0.9464
190	10.427	0.1897	0.0069	0.6308	0.0211	0.0941	0.0575	0.3651	0.3412	0.9346
191	2.5152	0.0951	0.0063	0.8197	0.0069	0.0445	0.0276	0.1750	0.1671	0.9549
192	3.8300	0.1228	0.0060	0.7710	0.0083	0.0569	0.0349	0.2240	0.2147	0.9583
193	1.6200	0.0663	0.0063	0.8724	0.0048	0.0310	0.0192	0.1219	0.1165	0.9553

TABLE C-3

Effect of W/F on Conversion of Propylene, Yield and selectivity to Ethylene and Butene-2
Temperature: 250°C Pressure: 3.041 atm

Run No.	W/F g. cat-hr/g. mol	Mole Fraction in Product						Conversion X	Yield Y	Selectivity S (%)
		Ethylene	Propane	Propylene	1-Butene	t-2-Butene	c-2-Butene			
194	5.4000	0.1335	0.0073	0.7304	0.0290	0.2460	0.1310	0.2649	0.2333	0.8809
195	6.1700	0.1331	0.0073	0.7173	0.0274	0.0699	0.0450	0.2780	0.2480	0.8920
196	7.1499	0.1650	0.0073	0.6925	0.0285	0.0698	0.0370	0.3031	0.2718	0.8968
197	8.7788	0.1476	0.0078	0.6786	0.0336	0.0805	0.5180	0.3169	0.2799	0.8832
198	9.3200	0.1574	0.0083	0.6678	0.0354	0.0811	0.0499	0.3278	0.2800	0.8800
199	3.0500	0.0946	0.0069	0.8083	0.0135	0.0474	0.0293	0.1865	0.1713	0.9186
200	4.4300	0.1169	0.0067	0.7594	0.0220	0.0592	0.0357	0.2357	0.2119	0.8989
201	1.6000	0.0569	0.0072	0.8783	0.0119	0.0282	0.0175	0.1160	0.1026	0.8843
202	5.5250	0.1289	0.0070	0.7396	0.0280	0.0629	0.0335	0.2550	0.2253	0.8816
203	9.8000	0.1667	0.0079	0.6489	0.0375	0.0859	0.0529	0.3469	0.3056	0.8811
204	14.8772	0.1782	0.0090	0.6110	0.0573	0.0935	0.0509	0.3850	0.3225	0.8379

TABLE C-3 (continued)

Temperture: 250°C Pressure 4.403 atm

Run No.	W/F g. cat-hr/g. mol	Mole Fraction in Product						Conversion X	Yield Y	Selectivity S (%)
		Ethylene	Propane	Propylene	1-Butene	t-2-Butene	c-2-Butene			
205	5.7446	0.1464	0.0072	0.7048	0.0322	0.0671	0.0423	0.2906	0.2559	0.8951
206	8.0508	0.1670	0.0078	0.6617	0.0315	0.0789	0.0531	0.3350	0.2990	0.9373
207	4.7500	0.1352	0.0065	0.7303	0.0149	0.0680	0.0452	0.2650	0.2484	0.9273
208	5.7703	0.1390	0.0067	0.7204	0.0179	0.0702	0.0451	0.2749	0.2549	0.9189
209	5.5300	0.1317	0.0066	0.7114	0.0210	0.0789	0.0504	0.2840	0.2610	0.9216
210	5.4923	0.1446	0.0067	0.7026	0.0208	0.0718	0.0535	0.2929	0.2695	0.9041
211	6.8200	0.1421	0.0067	0.6820	0.0278	0.0851	0.0563	0.3136	0.2830	0.9024
212	7.9739	0.1600	0.0072	0.6547	0.0280	0.0922	0.0580	0.3411	0.3101	0.9091
213	1.7403	0.0692	0.0070	0.8586	0.0104	0.0323	0.0225	0.1358	0.1240	0.9132
214	2.7949	0.1039	0.0067	0.7887	0.0145	010509	0.0353	0.2062	0.1900	0.9217
215	9.8973	0.1556	0.0080	0.6359	0.0396	0.0971	0.0637	0.3599	0.3165	0.8792
216	9.6124	0.1672	0.0077	0.6388	0.2932	0.0964	0.0605	0.3570	0.3242	0.9080

Table C-3 (continued)

Temperature: 250°C Pressure: 5.763 atm

Run No.	W/F g. cat-hr/g. mol	Mole Fraction in Product						Conversion X	Yield Y	Selectivity S (%)
		Ethylene	Propane	Propylene	1-Butene	t-2-Butene	c-2-Butene			
217	5.9000	0.1624	0.0079	0.6846	0.0250	0.0755	0.0447	0.3101	0.2826	0.9086
218	0.4974	0.1559	0.0078	0.6537	0.0321	0.0915	0.0590	0.3420	0.3064	0.8957
219	8.0900	0.1765	0.0085	0.6462	0.0313	0.0861	0.0515	0.3412	0.3139	0.8981
220	12.3621	0.1721	0.0092	0.5991	0.0449	0.1069	0.0679	0.2970	0.3469	0.8737
221	4.1532	0.1372	0.0078	0.7289	0.0288	0.0630	0.0342	0.2684	0.2345	0.8802
222	4.9497	0.1387	0.0072	0.7087	0.0324	0.0668	0.0562	0.2867	0.2517	0.8778
223	5.4991	0.1457	0.0078	0.6836	0.0	0.0744	0.0535	0.3120	0.2736	0.8769
224	8.1876	0.1317	0.0075	0.6469	0.0375	0.1054	0.0717	0.3489	0.3082	0.8832
225	10.4079	0.1756	0.0080	0.6160	0.0388	0.0983	0.0645	0.3780	0.3372	0.8874
226	3.0108	0.1186	0.0078	0.7720	0.0215	0.0508	0.0292	0.2230	0.1987	0.8909
227	1.8700	0.0942	0.0079	0.8286	0.0132	0.0372	0.0190	0.1660	0.1503	0.9055

TABLE C-3 (continued)

Temperature: 250°C Pressure: 7.124 atm

Run No.	W/F g. cat-hr/g. mol	Mole Fraction in Product						Conversion X	Yield Y	Selectivity S (%)
		Ethylene	Propane	Propylene	1-Butene	t-2-Butene	c-2-Butene			
228	6.9131	0.1649	0.0071	0.6647	0.0291	0.0822	0.0518	0.3309	0.2989	0.9032
229	6.5233	0.1764	0.0075	0.6548	0.0318	0.0800	0.0490	0.3409	0.3059	0.8973
230	8.2913	0.1779	0.0077	0.6269	0.0319	0.0944	0.0609	0.3690	0.3332	0.9029
231	8.8033	0.1874	0.0082	0.6230	0.0382	0.0885	0.0542	0.3729	0.3306	0.8865
232	13.6175	0.1849	0.0089	0.5852	0.0467	0.1063	0.0679	0.4110	0.3592	0.8738
233	5.1389	0.1585	0.0069	0.7005	0.0148	0.0780	0.0406	0.2950	0.2778	0.9418
234	5.9744	0.1609	0.0069	0.6835	0.0178	0.0798	0.0509	0.3121	0.2918	0.9350
235	6.1556	0.1635	0.0069	0.7855	0.0193	0.0803	0.0545	0.3200	0.2983	0.9318
236	7.2162	0.1739	0.0070	0.6508	0.0240	0.0860	0.0581	0.3450	0.3180	0.9221
237	8.7965	0.1825	0.0072	0.6359	0.0267	0.0897	0.0579	0.3500	0.3302	0.9173
238	9.5780	0.1879	0.0079	0.6189	0.0300	0.0929	0.0619	0.3770	0.3426	0.9089
239	12.5100	0.1989	0.0086	0.5921	0.0411	0.0984	0.0601	0.4040	0.3582	0.8865
240	2.4600	0.1115	0.0072	0.7939	0.0087	0.0493	0.0294	0.2009	0.1902	0.9466
241	3.4807	0.1353	0.0068	0.7434	0.0126	0.0632	0.986	0.2518	0.2371	0.9518

TABLE C-4

Effect of W/F on Conversion of Propylene, Yield and selectivity to Ethylene and Butene - 2

Temperature: 300°C Pressure: 3.041 atm

Run No.	W/F g. cat-hr/g. mol	Mole Fraction in Product						Conversion X	Yield Y	Selectivity S (%)
		Ethylene	Propane	Propylene	1-Butene	t-2-Butene	c-2-Butene			
242	2.9199	0.1295	0.0066	0.7720	0.0097	0.0556	0.0266	0.2225	0.2117	0.9494
243	3.6801	0.1404	0.0067	0.7422	0.0164	0.0627	0.0317	0.2533	0.2347	0.9276
244	4.3300	0.1491	0.0076	0.7223	0.0219	0.0648	0.0342	0.2729	0.2482	0.9091
245	5.0100	0.1532	0.0075	0.7024	0.0296	0.0716	0.0356	0.2930	0.2604	0.8888
246	5.9265	0.1647	0.0083	0.6796	0.0342	0.0731	0.0401	0.3159	0.2779	0.8795
247	8.4100	0.1743	0.0097	0.6378	0.0478	0.0853	0.0451	0.3580	0.3047	0.8511
248	3.7369	0.1302	0.0075	0.7412	0.0251	0.0626	0.0333	0.2539	0.2262	0.8903
249	1.7200	0.0990	0.0069	0.8336	0.0067	0.0415	0.0124	0.1610	0.1528	0.9488
250	1.0550	0.0660	0.0070	0.8783	0.0052	0.0296	0.0134	0.1159	0.1095	0.9439
251	8.9870	0.1811	0.0096	0.6232	0.0497	0.0887	0.0445	0.3720	0.3168	0.8516
252	17.8900	0.1986	0.0117	0.5653	0.0676	0.1011	0.0556	0.4310	0.3554	0.8246

TABLE C-4 (continued)

Temperature: 300°C Pressure: 4.403 atm

Run No.	W/F g. cat-hr/g. mol	Mole Fraction in Product						Conversion X	Yield Y	Selectivity S (%)
		Ethylene	Propane	Propylene	1-Butene	t-2-Butene	c-2-Butene			
253	5.3500	0.1778	0.0097	0.6697	0.0365	0.0707	0.0358	0.3256	0.2843	0.8719
254	5.4000	0.1670	0.0102	0.6688	0.0390	0.0739	0.0401	0.3265	0.2820	0.8627
255	3.9784	0.1547	0.0069	0.7164	0.0145	0.0707	0.0367	0.2789	0.2621	0.9398
256	4.6400	0.1596	0.0072	0.7055	0.0212	0.0702	0.0363	0.2899	0.2661	0.9178
257	4.7500	0.1610	0.0067	0.6856	0.0289	0.0753	0.0427	0.3100	0.2792	0.9004
258	7.1000	0.1825	0.0085	0.6354	0.0445	0.0878	0.0450	0.3599	0.3140	0.8745
259	4.1815	0.1406	0.0070	0.7105	0.0115	0.0829	0.0477	0.2852	0.2712	0.9511
260	8.5300	0.1318	0.0069	0.6914	0.0263	0.0903	0.0532	0.3041	0.2753	0.9054
261	8.5300	0.1646	0.0085	0.6170	0.0442	0.1056	0.0606	0.3789	0.3303	0.8715
262	2.2600	0.1263	0.0072	0.7744	0.0118	0.0534	0.0269	0.2206	0.2067	0.9369
263	1.3106	0.0882	0.0076	0.8444	0.0069	0.0348	0.0181	0.1501	0.1410	0.9398
264	10.1531	0.1810	0.0137	0.5991	0.0705	0.0871	0.0485	0.3969	0.3166	0.7977
265	14.4313	0.1677	0.0122	0.5696	0.0721	0.1108	0.0666	0.4267	0.3452	0.8089

TABLE C-4 (continued)

Temperature: 300°C Pressure: 5,763 atm

Run No.	W/F g. cat-hr/g. mol	Mole Fraction in Product						Conversion X	Yield Y	Selectivity S (%)
		Ethylene	Propane	Propylene	1-Butene	t-2-Butene	c-2-Butene			
266	5.4082	0.1677	0.0080	0.6608	0.0391	0.0813	0.0430	0.3349	0.2921	0.8721
267	5.6105	0.1636	0.0089	0.6568	0.0416	0.0804	0.0488	0.3389	0.2927	0.8636
268	9.2300	0.1419	0.0103	0.6070	0.0566	0.1068	0.0773	0.3889	0.3261	0.8384
269	13.2265	0.1229	0.0110	0.5729	0.0784	0.1342	0.0822	0.4251	0.3393	0.7984
270	4.3500	0.1412	0.0066	0.6876	0.1986	0.0899	0.0547	0.3071	0.2858	0.9278
271	1.6707	0.1064	0.0073	0.7998	0.0139	0.0533	0.0192	0.1949	0.1788	0.9172
272	2.7600	0.1415	0.0071	0.7422	0.0205	0.0800	0.0047	0.2529	0.2264	0.8945
273	2.1200	0.1236	0.0071	0.7741	0.0214	0.0698	0.0041	0.2209	0.1976	0.8945
274	5.8700	0.1668	0.0094	0.6498	0.0425	0.0819	0.0498	0.3459	0.2984	0.8524

TABLE C-4 (continued)

Temperature: 300 C Pressure: 7.124 atm

Run No.	W/F g. cat-hr/g. mol	Mole Fraction in Product						Conversion X	Yield Y	Selectivity S (%)
		Ethylene	Propane	Propylene	1-Butene	t-2-Butene	c-2-Butene			
275	9.0346	0.1934	0.0118	0.6041	0.0598	0.0857	0.0453	0.3919	0.3243	0.8273
276	6.7000	0.1779	0.0097	0.6349	0.0411	0.0876	0.0493	0.3610	0.3149	0.8724
277	10.2000	0.1478	0.0099	0.5932	0.0595	0.11860	0.0710	0.4030	0.3374	0.8373
278	10.1629	0.1432	0.0093	0.5863	0.0545	0.1142	010924	0.4099	0.3500	0.8534
279	12.9000	0.1372	0.0104	0.5735	0.0681	0.1318	0.0783	0.4228	0.3472	0.8212
280	17.8871	0.1188	0.0123	0.5504	0.0897	0.1410	0.0878	0.4459	0.3476	0.7793
281	7.7500	0.1752	0.0135	0.6190	0.0199	0.1143	0.0579	0.3769	0.3473	0.9222
282	10.6000	0.1978	0.0083	0.5927	0.0317	0.1115	0.0586	0.4041	0.3679	0.9105
283	6.7285	0.1775	0.0076	0.6339	0.0285	0.1000	0.0526	0.3621	0.3301	0.9116
284	12.3937	0.1951	0.0085	0.5743	0.0435	0.1146	0.0640	0.4219	0.3736	0.8855
285	2.7600	0.1332	0.0067	0.7562	0.0222	0.0666	0.031	0.2550	0.2300	0.9056
286	4.3910	0.1511	0.0064	0.6816	0.0304	0.0882	0.0424	0.3140	0.2814	0.8969
287	1.6699	0.1145	0.0069	0.7964	0.0143	0.0460	0.0223	0.1990	0.1829	0.9190
288	3.2100	0.1475	0.0067	0.7131	0.0245	0.0737	0.0344	0.2822	0.2556	0.9056

TABLE C-5

Effect of Temperature on Conversion of Propylene, Yield and selectivity to Ethylene and Butene - 2 for Disproportionation Over Tungsten Oxide on γ - Alumina Catalyst

Pressure: 4.403 atm W/F: 7.88 g. cat-hr/g. mol.

Temperature °C	Mole Fraction in Product						Conversion X	Yield Y	Selectivity S (%)
	Ethylene	Propane	Propylene	1-Butene	t-2-Butene	c-2-Butene			
150	0.0575	0.0065	0.8969	0.0	0.0281	0.0109	0.0973	0.0966	0.9929
155	0.0766	0.0066	0.8609	0.0	0.0375	0.0184	0.1335	0.1325	0.9927
175	0.1223	0.0067	0.7848	0.0	0.0564	0.02880	0.2102	0.2086	0.9924
184	0.1365	0.0068	0.7468	0.0066	0.0687	0.0347	0.2484	0.2399	0.9659
191	0.1526	0.0070	0.7232	0.0079	0.0729	0.0364	0.2722	0.2619	0.9623
197	0.1584	0.0069	0.7046	0.0108	0.0786	0.0407	0.2908	0.2776	0.9547
207	0.1767	0.0072	0.6825	0.0127	0.0788	0.0420	0.3130	0.2975	0.9505
219	0.1828	0.0072	0.6539	0.0177	0.0892	0.0491	0.3418	0.2870	0.9396
236	0.1988	0.0075	0.6329	0.0235	0.0885	0.0487	0.3629	0.3360	0.9258
246	0.1934	0.0074	0.6150	0.0269	0.0980	0.0588	0.3810	0.3507	0.9204
252	0.2023	0.0075	0.6225	0.0264	0.0883	0.0530	0.3735	0.3436	0.9200
259	0.1969	0.0076	0.6077	0.0303	0.0954	0.0621	0.3884	0.3545	0.9126
271	0.2077	0.0082	0.6030	0.0333	0.0954	0.0525	0.3931	0.3555	0.9044
286	0.2037	0.0082	0.5939	0.0394	0.0985	0.5633	0.4023	0.3585	0.8911
298	0.2109	0.0087	0.5860	0.0433	0.0895	0.0615	0.4102	0.3619	0.8823
329	0.2081	0.0112	0.5429	0.0679	0.1004	0.0695	0.4536	0.3780	0.8333
354	0.2172	0.0140	0.5434	0.0701	0.066	0.0686	0.4531	0.3725	0.8220
379	0.2011	0.0170	0.5329	0.0834	0.0940	0.0715	0.4636	0.3666	0.7907
402	0.2050	0.0208	0.5486	0.0759	0.0793	0.0702	0.4478	0.3545	0.7917

TABLE C-6

Effect of Temperature on Conversion of Propylene Yield and Selectivity to Ethylene and Butene - 2 for Disproportionation over Tungsten Oxide Supported on Silica - Alumina Catalyst

Pressure: 4.403 atm W/F: 7.88 g. cat-hr/g. mol

Temperature °C	Mole Fraction in Product						Conversion X	Yield Y	Selectivity S (%)
	Ethylene	Propane	Propylene	1-Butene	t-2-Butene	c-2-Butene			
364	0.0549	0.0114	0.7993	0.0426	0.0512	0.0405	0.1955	0.1465	0.7496
329	0.0562	0.0083	0.8572	0.0177	0.0353	0.0253	0.1372	0.1167	0.8508
294	0.1937	0.0104	0.6245	0.0367	0.0751	0.0595	0.3715	0.3283	0.8838
265	0.1839	0.0069	0.6433	0.0295	0.0784	0.0579	0.3526	0.3203	0.9084
238	0.1661	0.0063	0.6815	0.0155	0.0760	0.0545	0.3141	0.2967	0.9445
202	0.1127	0.0058	0.7916	0.0042	0.0465	0.0390	0.2032	0.1982	0.9756
191	0.1150	0.0083	0.7917	0.0040	0.0487	0.0323	0.2031	0.1959	0.9677
207	0.1278	0.0079	0.7597	0.0063	0.0597	0.0386	0.2354	0.2260	0.9603
223	0.1621	0.0077	0.7055	0.0073	010714	0.0459	0.2899	0.2794	0.9639
234	0.1853	0.0074	0.6521	0.0102	0.0899	0.0549	0.3437	0.3303	0.9609
235	0.2080	0.0074	0.6196	0.01315	0.0970	0.0549	0.3764	0.3599	0.9561
265	0.2081	0.0074	0.6036	0.0152	0.1033	0.0624	0.3925	0.3736	0.9523
264	0.2160	0.0075	0.5999	0.0160	0.1021	0.0584	0.3962	0.3766	0.9505
273	0.2068	0.0075	0.6032	0.0168	0.1019	0.0636	0.3929	0.3724	0.9479
278	0.2047	0.0080	0.6142	0.0192	0.0937	0.0602	0.3818	0.3586	0.9393
300	0.1970	0.0087	0.6117	0.0248	0.0967	0.0611	0.3843	0.3548	0.9233
318	0.1864	0.0098	0.6345	0.0254	0.0844	0.0595	0.3614	0.3303	0.9139
331	0.1062	0.0109	0.7788	0.0191	0.0478	0.0372	0.2162	0.1912	0.8842
339	0.0550	0.0123	0.8885	0.0149	0.0201	0.0092	0.1058	0.0843	0.7964

TABLE C-6 (Continued)

Pressure: 4.403 atm W/F: 7.88 g. cat-hr/g. mole

Temperature °C	Mole Fraction in Product						Conversion X	Yield Y	Selectivity S (%)
	Ethylene	Propane	Propylene	1-Butene	t-2-Butene	c-2-Butene			
291	0.2216	0.0074	0.5611	0.0482	0.0976	0.0641	0.4352	0.3833	0.8807
247	0,1876	0.0060	0.6467	0.0221	0.0817	0.0558	0.3490	0.3250	0.9313
230	0.1523	0.0057	0.7096	0.0128	0.0682	0.0515	0.2858	0.2719	0.9512
218	0.1367	0.0057	0.7503	0.0084	0.0584	0.0404	0.2448	0.2356	0.9624
207	0.1231	0.0057	0.7686	0.0068	0.0544	0.0415	0.2265	0.2190	0.9668
197	0.1008	0.0053	0.8152	0.0036	0.0417	0.0334	0.1795	0.1759	0.9800
131	0.0804	0.0052	0.8543	0.0	0.0333	0.0268	0.1406	0.1406	1.00
170	0.0605	0.0053	0.8918	0.0	0.0230	0.0194	0.1029	0.1029	1.0
160	0.0477	0.0051	0.9198	0.0	0.0171	0.0103	0.0751	0.0751	1.00
296	0.1849	0.0070	0.6438	0.0286	0.0789	0.0568	0.3531	0.3213	0.9100
315	0.1341	0.0082	0.7266	0.0245	0.0609	0.9058	0.2687	0.2408	0.8963
320	0.0630	0.0085	0.8518	0.0160	0.0354	0.0245	0.1427	0.1229	0.8613
350	0.0392	0.0132	0.8949	0.0162	0.0224	0.0141	0.0993	0.0757	0.7625
340	0.0361	0.0101	0.8766	0.0225	0.0292	0.0255	0.1171	0.0904	0.7716
368	0.0530	0.0152	0.8036	0.0383	0.0489	0.0409	0.1912	0.1429	0.7473
488	0.1598	0.0348	0.5525	0.0867	0.0761	0.0423	0.4439	0.2782	0.6267
465	0.1390	0.0279	0.5767	0.0999	0.0747	0.0406	0.4196	0.2545	0.6066
447	0.1285	0.0196	0.5965	0.1067	0.0754	0.0483	0.3997	0.2523	0.6311
403	0.1136	0.0163	0.6518	0.0951	0.0690	0.0541	0.3417	0.2367	0.6928

TABLE C-7

Effect of Temperature on Conversion of Propylene, Yield and selectivity to Ethylene and Butene-2 for Disproportionation over Tungsten Oxide Supported on Silica Catalyst

Pressure: 4.403 atm W/F: 7.88 g. cat-hr/g. mol

Temperature °C	Mole Fraction in Product						Conversion X	Yield Y	Selectivity S (%)
	Ethylene	Propane	Propylene	1-Butene	t-2-Butene	c-2-Butene			
270	0.0022	0.0047	0.9931	0.0	0.0	0.0	0.0022	0.0022	1.00
280	0.0031	0.0047	0.9922	0.0	0.0	0.0	0.0031	0.0031	1.00
290	0.00400	0.0048	0.9912	0.0	0.0	0.0	0.0040	0.0040	1.00
300	0.0049	0.0048	0.9903	0.0	0.0	0.0	0.0049	0.0048	1.00
310	0.0068	0.0248	0.883	0.0	0.0	0.0	0.0069	0.0068	1.00
320	0.0092	0.0046	0.9862	0.0	0.0	0.0	0.0092	0.0091	1.00
331	0.0120	0.0049	0.9832	0.0	0.0	0.0	0.0119	0.0119	1.00
340	0.0234	0.0047	0.671	0.0	0.0	0.0	0.0282	0.0282	1.00
352	0.0329	0.0048	0.9547	0.0	0.0075	0.0	0.0405	0.0405	1.00
366	0.0436	0.0048	0.9332	0.0044	0.0116	0.0024	0.0620	0.0570	0.9294
380	0.0662	0.0048	0.8908	0.0088	0.0176	0.0117	0.1044	0.0956	0.9153
390	0.0780	0.0047	0.8669	0.0112	0.0228	0.0162	0.1283	0.1171	0.9124
400	0.1072	0.0049	0.821	0.0157	0.0299	0.0213	0.1741	0.1583	0.9095
416	0.1419	0.0048	0.7553	0.0236	0.0422	0.0321	0.2398	0.3162	0.9017
432	0.1928	0.0050	0.6782	0.0307	0.0537	0.0396	0.3172	0.2859	0.9014
450	0.2182	0.0050	0.6214	0.0367	0.0676	0.0512	0.3746	0.3369	0.8993
460	0.2524	0.0051	0.5784	0.0412	0.0678	0.0551	0.4178	0.3752	0.898
470	0.2792	0.0052	0.5527	0.0430	0.0679	0.0519	0.4437	0.3990	0.8992
480	0.2852	0.0068	0.5378	0.0443	0.0725	0.0533	0.4587	0.4110	0.8962
494	0.2916	0.0073	0.5198	0.0478	0.0753	0.0582	0.4769	0.4252	0.8915

TABLE C-8

Effect of Tungsten Oxide Concentration on Conversion Yield and Selectivity for Propylene Disproportionation on γ - Alumina Supported Catalysts.

Temperature: 290 C Pressure: 4.403 atm W/F = 10 g. cat-hr/g. mol

Run No.	WO_3 Concentration %	Mole Fraction in Product						Conversion X	Yield Y	Selectivity S (%)
		Ethylene	Propane	Propylene	1-Butene	t-2-Butene	c-2-Butene			
293	5	0.0799	0.0053	0.8568	0.0111	0.0288	0.0182	0.1379	0.1268	0.9196
294	10	0.2037	0.0083	0.5939	0.0394	0.0985	0.0563	0.4023	0.3581	0.8901
295	15	0.1526	0.0060	0.5428	0.0522	0.1327	0.11381	0.4537	0.3991	0.8796

TABLE C-9

Effect of Time On Stream on Conversion of Propylene
for Disproportionation Over Tungsten Oxide on γ-Alumina Catalyst
Temperature: 180 C Pressure: 4.403 Atm W/F: 7.88 g. cat-hr/g. mol

Time Sec.	Mole Fraction in Product						Conversion X
	Ethylene	Propane	Propylene	1-Butene	t-2-Butene	c-2-Butene	
0.0	0.1230	0.0057	0.7353	0.0	0.0802	0.0558	0.2599
10	0.1559	0.0062	0.7316	0.0	0.0722	0.0341	0.2636
36	0.1353	0.0061	0.7519	0.0	0.0669	0.0397	0.2432
50	0.1421	0.0061	0.7540	0.0	0.0661	0.0316	0.2411
85	0.1386	0.0062	0.7549	0.0	0.0680	0.0322	0.240
113	0.1398	0.0062	0.7581	0.0	0.0644	0.0314	0.2369
145	0.1324	0.0061	0.7546	0.0	0.0661	0.0409	0.2405
193	0.1364	0.0062	0.7635	0.0	0.0629	0.0308	0.2315
219	0.1321	0.0061	0.7659	0.0	0.0648	0.0311	0.2291
248	0.1328	0.0061	0.7700	0.0	0.0608	0.0303	0.2201
356	0.1287	0.0062	0.7880	0.0	0.0480	0.02912	0.2069

TABLE C-9 (continued)

Temperature: 210°C Pressure: 4.403 atm W/F: 7.88 g. cat-hr/g. mol

Time Sec.	Mole Fraction in Product						Conversion X
	Ethylene	Propane	Propylene	1-Butene	t-2-Butene	c-2-Butene	
0	0.1788	0.0063	0.6625	0.0121	0.0888	0.0517	0.3332
16	0.1747	0.0064	0.6833	0.0080	0.0857	0.0417	0.3122
32	0.1749	0.0064	0.6831	0.0080	0.0857	0.0417	0.3124
57	0.1497	0.0060	0.6895	0.0078	0.0909	0.0559	0.3060
76	0.1666	0.0062	0.6855	0.0066	0.0836	0.0513	0.3100
106	0.1516	0.0060	0.6936	0.0059	0.0886	0.0540	0.3018
134	0.1666	0.0060	0.6916	0.0028	0.0837	0.0491	0.3039
163	0.1509	0.0059	0.6980	0.0040	0.0863	0.0546	0.2974
217	0.1637	0.0060	0.6963	0.0022	0.0821	0.0493	0.2991
247	0.1503	0.0059	0.7000	0.0037	0.0857	0.0542	0.2953
285	0.1607	0.0061	0.7047	0.00	0.0796	0.0486	0.2906
310	0.1523	0.0054	0.6994	0.0	0.0872	0.0551	0.2960
336	0.1595	0.0061	0.7170	0.0	0.0785	0.0386	0.2783

TABLE C-9 (continued)

Temperature: 250°C Pressure: 4.403 atm W/F: 7.88 g. cat-hr/g. mol

Time Sec.	Mole Fraction in Product						Conversion X
	Ethylene	Propane	Propylene	1-Butene	t-2-Butene	c-2-Butene	
0	0.1754	0.0083	0.6401	0.0389	0.0871	0.0462	0.3558
25	0.1787	0.0075	0.6539	0.0310	0.0814	0.0474	0.3419
42	0.1717	0.0070	0.6549	0.0234	0.0851	0.0481	0.3438
60	0.1789	0.0073	0.6613	0.02434	0.0845	0.0480	0.3343
73	0.1721	0.0068	0.6632	0.0216	0.0821	0.0531	0.3324
94	0.1801	0.0062	0.6601	0.0212	0.0831	0.0462	0.3353
110	0.1713	0.0067	0.6684	0.0185	0.0833	0.0516	0.3272
134	0.1779	0.0065	0.6652	0.0236	0.0832	0.0425	0.3303
178	0.1696	0.0061	0.6682	0.0202	0.0871	0.0475	0.3268
210	0.1665	0.0067	0.6769	0.0137	0.0788	0.512	0.3189
285	0.1161	0.0064	0.6757	0.0169	0.0123	0.0967	0.3231
330	0.1665	0.0062	0.6849	0.0218	0.0759	0.0416	0.3106

TABLE C-9 (continued)

Temperature: 300°C Pressure: 4.403 atm W/F: 7.88 g. cat-hr/g. mol

Time Sec.	Mole Fraction in Product						Conversion X
	Ethylene	Propane	Propylene	1-Butene	t-2-Butene	c-2-Butene	
0	0.1975	0.0100	0.0582	0.9587	0.0957	0.0559	0.4142
15	0.1836	0.0104	0.6043	0.0504	0.0959	0.0559	0.3918
32	0.1668	0.0088	0.6157	0.0505	0.0987	0.0595	0.3803
53	0.1378	0.0116	0.6007	0.07097	0.1129	0.0660	0.3954
75	0.1463	0.0086	0.6246	0.0429	0.0959	0.0817	0.3713
109	0.1310	0.0081	0.6144	0.0514	0.1182	0.0769	0.3816
122	0.1330	0.0085	0.6373	0.0494	0.0960	0.0762	0.3586
153	0.1183	0.0083	0.6333	0.0496	0.1157	0.0748	0.3626
165	0.1044	0.0077	0.6317	0.0520	0.1145	0.0897	0.3642
174	0.1234	0.0090	0.6323	0.0577	0.1025	0.0751	0.3636
190	0.0968	0.0076	0.6463	0.0537	0.1147	0.0808	0.3495
205	0.1163	0.0085	0.6422	0.0554	0.1074	0.0702	0.3536
228	0.1023	0.0080	0.6595	0.0491	0.1127	0.0784	0.3565
242	0.12641	0.0081	0.6525	0.0482	0.0949	0.0699	0.3433
257	0.1044	0.0077	0.6462	0.0442	0.1028	0.0949	0.3497
273	0.1044	0.0077	0.6462	0.0442	0.1027	0.0672	0.3438
292	0.0979	0.0082	0.6748	0.0476	0.0985	0.0729	0.3208
305	0.1013	0.0078	0.6958	0.0424	0.0925	0.0602	0.2997
325	0.0901	0.0078	0.7056	0.0412	0.0869	0.0684	0.2899
347	0.1558	0.0070	0.7010	0.0289	0.0675	0.0398	0.2944
354	0.1575	0.0069	0.7048	0.0258	0.0629	0.0421	0.2906

TABLE C-10

Effect of Flow Rate on Conversion for Propylene

Temperature: 300°C Pressure: 4.403 atm W/F: 10 g. cat-hr/g. mol

Run No.	Flow Rate Mole/hr.	Mole Fraction in Product						Conversion X
		Ethylene	Propane	Propylene	1-Butene	t-2-Butene	c-2-Butene	
300	0.400	0.1359	0.0096	0.5877	0.0620	0.1228	0.0820	0.4085
301	0.500	0.1629	0.0102	0.5971	0.059	0.1022	0.0681	0.3990
302	0.18442	0.0114	0.5822	0.0628	0.0973	0.0618	0.600	0.4140
303	0.1494	0.0073	0.5791	0.0422	0.1349	0.0872	0.700	0.4171

TABLE C-11

Effect of Particle Size on Conversion for Propylene Disproportionation over a Tungsten Oxide on γ - Alumina

Temperature: 300°C Pressure: 4.403 atm W/F: 10 g. cat-hr/g. mol

Run No.	Particle Size μ	Mole Fraction in Product						Conversion X
		Ethylene	Propane	Propylene	1-Butene	t-2-Butene	c-2-Butene	
304	0.340	0.150	0.0096	0.5840	0.0633	0.1125	0.0806	0.4121
305	0.720	0.1424	0.0089	0.6050	0.0518	0.1083	0.0835	0.3911
306	0.478	0.1810	0.0137	0.5991	0.0705	0.0872	0.0485	0.3970
307	1.240	0.1308	0.0097	0.6177	0.0596	0.1061	0.0762	0.3783
308	1.500	0.0839	0.0094	0.7308	0.0429	0.0796	0.0535	0.3645
309	0.630	0.1629	0.0102	0.5972	0.0594	0.1022	0.0681	0.3989
310	0.630	0.1844	0.0114	0.5822	0.0628	0.0974	0.0618	0.4140

APPENDIX D

SAMPLE CALCULATION AND MATERIAL BALANCE

For each run, product distribution was checked by injecting a constant volume of the product into a gas chromatograph for analysis. From the recorded chromatographic analysis of a sample, the peak area and retention time were obtained for each component in the sample. These data plus the detector calibration factors were used to calculate the mole fraction of the six components: ethylene, propane, propylene, 1-butene, trans-2-butene and cis-2-butene.

A computer program was used to calculate: mole fraction of components, conversion, selectivity, yield, molar ratio of ethylene to butenes, material balance based on atomic carbon, and material balance based on atomic hydrogen. A Sample calculation of how the program works is illustrated in the following example

For each calculation, the weight of the catalyst, flowrate of propylene, pressure of reaction, temperature, detector calibration factors of components, and area of peaks for the components were fed into the computer. The data used in this example was taken from run #280.

Component	Area	Area Ratio	Molar Ratio	Mole fraction
Ethylene	2705	0.24066	0.21579	0.1188
propane	223	0.01984	0.02234	0.0123
propylene	11240	1.000	1.000	0.5504
1-Butene	1744	0.15516	0.16293	0.0897
trans-2-Butene	2795	0.24867	0.25612	0.1410
cis-2-Butene	1586	0.14110	0.15948	0.0878

$MR(i) = AR(i) * DCF(i)$

$$X(i) = \frac{MR(i)1}{1 + MR(1) + MR(2) + MR(4) + MR(5) + MR(6)}$$

where MR (i) = Molar ratio of component to that of propylene

AR(i) = Area ratio of component to that of propylene

DCF(i) = Detector Calibration factor for a component

X(i) = Mole fraction of a componene

$$\text{Conversion} = \frac{MR(1) + MR(2) + MR(4) + MR(5) + MR(6) - 0.00648}{1 + MR(1) + MR(2) + MR(4) + MR(5) + MR(6)}$$

$$\text{Conversion} = 1 - \frac{\text{moles of propylene out of the reactor}}{\text{moles of propylene fed into the reactor}}$$

$$\text{Conversion} = \frac{0.21579 + 0.02234 + 0.16293 + 0.25612 + 0.15948 - 0.00648}{1 + 0.21579 + 0.02234 + 0.16293 + 0.25618 + 0.15948}$$

$$= 0.4459$$

$$\text{Selectivity} = \frac{X(1) + X(5) + X(6)}{\text{Conversion}}$$

$$= \frac{0.1188 + 0.1410 + 0.0878}{0.4459}$$

$$= 0.7793$$

Yield Conversion x Selectivity

$$= 0.4459 \times 0.7793 = 0.3476$$

$$\text{Molar Ratio of Ethylene to butenes} = \frac{X(1)}{X(4) + X(5) + X(6)}$$

$$\frac{0.1188}{0.0897 + 0.1410 + 0.0878} = 0.3730$$

Material Balance Based on Atomic Carbon

Component	In Feed Mole/hr.	in Product moles/hr.
Ethylene	0	0.1624
Propane	0.0078	0.0144
Propylene	1.2234	0.6933
1-butene	0	0.1104
trans-2-butene	0	0.1652
cis-2-butene	0	0.0908
Total	1.2312	1.2365

$$\% \text{ Deviation} = \left(\frac{1.2312 - 1.2365}{1.2312}\right) \times 100 = 0.43\%$$

Material Balance Based on Atomic hydrogen

Component	In Feed Mole/hr.	In Product Moles/hr.
Ethylene	0	0.3248
Propane	0.0208	0.0384
Propylene	2.4444	1.3866
1-Butene	0	0.2208
trans-2-Butene	0	0.3304
cis-2-butene	0	0.1816
Total	2.4652	2.4826

$$\%\text{Deviation} \quad \left(\frac{2.4652 - 2.4826}{2.4652}\right) \times 100 = 0.706\%$$

APPENDIX - E Effect of Internal Diffusion

APPENDIX - F External Resistance to Mass and Heat Transfer

1 Drop in Partial Pressure from Ambient Stream to Catalyst Surface

2 Temperature Drop from Catalyst to Ambient Stream

E Effect of Internal Diffusion

a) Molecular Diffusion

The effect of molecular diffusion (film diffusion) was tested by measuring the effect of feed rate on conversion, while keeping the space time constant. The experimental results for molecular diffusion are represented in Figure (5-2) and given in Appendix (C). The consistancy of conversion indicates that molecular diffusion is not significant in the catalytic disproportionation of propylene when the flow rate is higher than 0.4 g. mole/hr.

b) Knudsen Diffusion and Effectiveness Factor

The experimental results for Knudsen diffusion are shown in Figure (5-3) and the data are given in Appendix (C). An estimate of Knudsen diffusion and Effectiveness factor for γ-alumina supported tungsten oxide catalyst used in this investigation is calculated for run #280. Using a modified Theile method and given as follows:

(i) Calculation of molecular weight of gas mixture:

Component	Inlet mole fraction	Outlet mole fraction	Average mole fraction
C_2H_2	0.00	0.1188	0.0594
C_3H_8	0.0065	0.0123	0.0094
C_3H_6	0.9935	0.5504	0.7719
$1\text{-}C_4H_8$	0.00	0.0897	0.0448
$trans\text{-}2\text{-}C_4H_8$	0.00	0.1410	0.0705
$cis\text{-}2\text{-}C_4H_8$	0.00	0.0878	0.0439

M_{av} = 43.5 g/g. mole

(ii) calculation of Knudsen diffusion coefficient, $D_{K,eff}$

$$D_{K,eff} = 19400 \frac{\beta^2}{T S_g \rho_p} \sqrt{\frac{T}{M}}$$

where:

T = 300°C = 573° = K

β = 0.4 Porosity of the catalyst

T = tortuosity = 5.0

S_g = surface area of the catalyst 1.46×10^6 cm^2/g

ρ_p = particle density = 1.664 g/cm^3

M = molecular weight of the gaseous mixture = 43.5 g/g. mole

The tortuosity is an emperical factor related to pore geometry and its value must be estimated. The value of the tortuosity is conservatively assumed to be 5.0.

$$D_{K,eff} = 19400 \times \frac{(0.4)^2}{5.0 \times 1.46 \times 10^6 \times 1.664} \sqrt{\frac{573}{43.5}}$$

$$= 9.27 \times 10^{-4} \text{ cm}^2/\text{sec.}$$

(iii) Calculation of reaction rate

$$r = X.\frac{F}{W} = 0.4459 \times \frac{0.0559}{3600} \times 1.664$$

$$= 1.1525 \times 10^{-5} \text{ g. mole/sec-cm}^3 \text{ of catalyst}$$

(iv) Calculation of reactant concentration C.

$$C = \frac{273}{573 \times 22400} = 2.127 \times 10^{-5} \text{ g. mole/cm}^3 \text{ of catalyst}$$

(v) Calculation of dimensionless modulus ϕ

$$\phi = \frac{R^2 r}{D_{K,eff} C}$$

where

R, particle radius = 0.0243 cm

$$\phi = \frac{(0.0243)^2 \times 1.1525 \times 10^{-5}}{9.27 \times 10^{-4} \times 2.127 \times 10^{-5}} = 0.346$$

Calculation of Effectiveness factor, E

E = 1.0 From Figure 3-7 of reference (67).

Therefore the experimental and calculated results show that pore diffusion resistance is negligible.

F External Resistance to Mass and Heat Transfer

1. Drop in Partial Pressure from Catalyst to Ambient Stream.

The data for estimation of external diffusion from #252. The conditions which apply to this evaluation are:

Temperature = 300°C

W/F = 17.89 g. cat-hr/g. mole

Pressure = 3.041 atm.

Weight of the Catalyst = 7.3355 gram

	Inlet Composision		Outlet Composition	
	Flow g.mole/hr	mole fraction Yi	Flow g.mole/hr.	mole fraction Yi
C_2H_4	0	0	0.0812	0.1986
C_3H_8	0.0026	0.0065	0.0048	0.0117
C_3H_6	0.4074	0.9935	0.2311	0.5653
$1\text{-}C_4H_8$	0	0	0.0276	0.0676
$trans\text{-}2\text{-}C_4H_8$	0	0	0.0413	0.1011
$cis\text{-}2\text{-}C_4H_8$	0	0	0.0227	0.0556
	0.4100	1.0000	0.4087	1.0000

a) Calculation based on the Yoshida et al.(73).

(i) Calculation of dimension R_j

R_j = molal reaction rate of component j per unit per unit mass of catalyst

= ((moles in) - (moles out)) per hour of component j/weight of catalyst.

a_m = specific surface area 1.46×10^6 cm^2/g

G_m = molal mass velocity of feed based on total cross-section area of catalyst bed in g.moles/hr. cm^2

$$= \frac{0.4100}{\pi/4\ (0.988)^2} = 0.5348 \text{ g. mole/hr. cm}^2$$

(ii) Calculation of particle pressure drop $\Delta Pj/Pj$

= mole fraction of component j at interface

$$Yi = ((Y_j)_{in} + (Y_j)_{out})\ /2$$

The results are tabulated as follows where Figure 2 of Yoshida et al. Plots of $\Delta P_j/P_j$ versus R/Y_j was referred.

Component	$(Y_i)_{av}$	r_{mj}	$R_j \times 10^8$	$R_j/Y_j \times 10^6$	$(\Delta P_j/P_j)_{max}$
C_2H_4	0.0993	0.0812	1.5752	0.1586	less than 0.0001 atm
C_3H_8	0.0091	0.0022	0.0427	0.0470	
C_3H_6	0.7794	0.1763	3.4200	0.0439	
$1\text{-}C_4H_8$	0.0338	0.0276	0.5354	0.1584	
$trans\text{-}2\text{-}C_4H_8$	0.0506	0.0413	0.8012	0.1585	
$cis\text{-}2\text{-}C_4H_8$	0.0278	0.0227	0.4042	0.1453	

Calculation of pressure drop of propylene using the equation

$$\Delta y_p = \frac{\Delta P_p}{P_p} = R(J_D)^{-1} y_{f_p} (S_c)^{2/3}$$

Calculation of j_D

$Re = Gm/a_v \phi \mu$

Component	$(y_j)_{av}$	T_c °K	P_c atm	$\mu_c \times 10^4$ pois	M gm
C_2H_4	0.0993	282	50	1.68	28.05
C_3H_8	0.0091	269.8	41.9	1.42	44.09
C_3H_6	0.7794	365	45.6	1.48	42.08
$1\text{-}C_4H_8$	0.0338	420	39.7	1.35	56.1
$trans\text{-}2\text{-}C_4H_8$	0.0506	428.6	40.5	1.33	56.1
$cis\text{-}2\text{-}C_4H_8$	0.0278	435.6	41.5	1.34	56.1

$\mu' = \Sigma \mu_j Y_j = 42.3$ $\qquad p'_r = \frac{P}{P_c} = \frac{3.041}{45.} = 0.0669$

$T'_c = \Sigma T_{cj} Y_j = 363.8$

$T'_r = \frac{573}{368.8} = 1.5750$

$P'_c = \Sigma P_{cj} Y_j = 45.4$

$\mu_c = \Sigma \mu_{cj} Y_j = 1.4834 \times 10^{-4}$ pois.

a_v = external surface area of catalyst/unit volume of catalyst

$= 1.46 \times 10^6 \times 1.664 = 2.4296 \times 10^6$ cm^2/cm^3

From chemical Process Principles Chart by Hougen et al.

Figure 262A find μ'_r knowing P'_r and T'_r

$\mu = \mu'_r \times \mu'_c = 0.72 \times 1.4845 \times 10^{-4}$

$= 1.069 \times 10^{-4}$ pois

$$Re = \frac{G_m}{a_v \phi \mu} = \frac{0.5348}{2.4295 \times 0.9 \times 1.069} \times 10^{-2} = 2.688 \times 10^{-3}$$

$j_D = 0.84\ (Re)^{-0.51} = 17.1885$

(ii) Calculation Schmidt number, Sc

Diffusivity of Propylene in various gases is calculated using Gilliland equation

$$D_{P-j} = 0.0043 \frac{T^{2/3}}{P(v_p^{1/3} + v_j^{1/3})^2} \left(\frac{1}{M_p} + \frac{1}{M_j}\right)^{\frac{1}{2}}$$

Components	M	V_j	$(Y_j)_{av}$	D_{p-j}
C_2H_4	28.05	44.4	0.0930	0.0828
C_3H_8	44.09	74.0	0.0091	0.0614
C_3H_6	42.08	66.6	0.7794	--
$1\text{-}C_4H_8$	56.1	88.8	0.0338	0.0546
$trans\text{-}2\text{-}C_4H_8$	56.1	88.8	0.0506	0.0546
$cis\text{-}2\text{-}C_4H_8$	56.1	88.8	0.0278	0.0546

$$D_{p-j} = 0.0043 \frac{(573)^{3/2}}{3.041\ ((66.6)^{1/3} - (V_j)^{1/3})^2} \cdot \left(\frac{1}{42.08} + \frac{1}{Mj}\right)^{\frac{1}{2}}$$

$$D_{p-mix} = \frac{1-y_j}{\Sigma Y_j/D_{p-j}} = \frac{1 - 0.7794}{3.3364} = 0.066\ cm^2/sec.$$

$$\rho = \frac{DM'}{RT} = \frac{3.041 \times 42.3}{82.05 \times 573} = 2.736 \times 10^{-3}\ g/cm^3$$

$$(Sc)_p = \frac{\mu}{\rho D_{p-mix}} = \frac{1.069 \times 10^{-4}}{0.066 \times 2.736 \times 10^{-3}} = 5.92 \times 10^{-1}$$

$$(Sc)_p^{2/3} = 0.705$$

R_p = ((moles) in (moles) out)/$G_m\ \phi\ a_m$

$= (0.4074 - 0.2311) / 0.5348 \times 0.9 \times 1.46 \times 10^{-6}$

$= 3.42 \times 10^{-8}$

Let the reaction be represented as follows

$$2\ C_3H_6 \rightleftharpoons C_2H_4 + C_4H_8$$

then $y_{f_p} = 1 + y_p \frac{(2-2)}{2} = 1.0$

$$\left(\frac{\Delta P}{P}\right)_p = R\,(j_D)^{-1}\; y_{f_p}\; (Sc)^{2/3}_p$$

$$= (3.42 \times 10^{-8})\; (17.1885)^{-1}\; (0.705)\; \frac{3.041}{0.7794}$$

$$= 5.46 \times 10^{-9} \text{ atm}$$

2 - Temperature Drop from Catalyst to Ambient Stream

The data estimation of temperature drop form catalyst particle to ambient stream are obtained from run #252. The calculation is based on the method of Yoshida etal.(73). Figure (4) of their paper was used to determine ΔT versus Q.

$$Q = \frac{r_{m_A} \quad \Delta H_A}{a_m \ \Phi \ C_p \ G_m}$$

ΔH_A = molar heat of reaction of component A

C_p = molar heat capacity at constant pressure of the gas stream which is calculated as follows:

Component	Mole faction				
j	in	out	average	$(C_p)j$	$(C_p)_j Y_j$
C_2H_4	0	0.1986	0.0993	16.581	1.6465
C_3H_8	0.0065	0.0117	0.0091	29.91	0.2722
C_3H_6	0.9935	0.5653	0.7794	24.878	19.4686
$1\text{-}C_4H_8$	0	0.0676	0.0338	31.55	1.0664
$trans\text{-}2\text{-}C_4H_8$	0	0.0506	0.0506	33.608	1.7006
$Cis\text{-}2\text{-}C_4H_8$	0	0.0556	0.0278	33.987	0.9448

Component	Mole Fraction Y_j in	out	average	Hj (at 300°C) KCal/g. mole $(H)_j$	$(H)_j Y_j$
C_2H_4	0	0.1986	0.0993	10.745	1.067
C_3H_8	0.0065	0.0117	0.0091	-28.380	-0.258
C_3H_6	0.9935	0.5654	0.7794	2.1995	+1.714
$1\text{-}C_4H_8$	0	0.0676	0.0338	-3.430	-0.115
$trans\text{-}2\text{-}C_4H_8$	0	0.1011	0.0506	-6.0992	-0.309
$cis\text{-}2\text{-}C_vH_8$	0	0.0556	0.0278	-5.512	-0.142

$C_j = \Sigma\ (C_p)_j\ Y_j$

$= 25.099$

$G_m = \frac{0.4100}{0.7666} = 0.5349$ g. mol/hr. cm^2

$\phi = 0.9$.

$a_m = 146 \times 10^6$ cm^2 1 g.

$(r_m)_p = 0.43102 \times 0.1363 = 0.0588$ g. mol/hr. g. of cat.

$(\Delta H)_p$ at 300°C = 1.957 cal/g. mol

$Q = 0.0538 \times 1957/146 \times 10^4 \times 0.9 \times 25.099 \times 0.5349$

$Q = 6.544 \times 10^{-6}$

Since Figure 4 of Yoshida et al. (73) ΔT 0.1°C, the catalyst surfact temperature effect can therefore be neglected.

APPENDIX G

INITIAL REACTION RATE DATA

TABLE - G-1

INITIAL REACTION RATE DATA AT VARIOUS TEMPERATURES

Pressure	Initial Reaction Rate x 10^2 (mole /hr. g.catalyst)			
atm	180°C	210°C	250°C	300°C
3.041	1.645	2.794	3.871	4.885
4.403	2.170	3.429	4.792	5.482
5.763	2.504	3.952	4.974	6.302
7.124	2.734	4.145	5.337	6.711

APPENDIX H

CALCULATED VALUES OF SPACE TIME (W/F)

The effect of W/F on conversion (X) was studied in the experimental range 180 - 300°C and at pressures between 3.041 to 7.124 atm.

The following is a sample tabulation of the deviation between calculated (from the integrated rate equation, mechanism 12) and experimental versus X relations. It is based on data obtained at 250°C and initial pressure of propylene of 3.041 atm. The values of k, K_P and K_{EB} were obtained from Table 5.

$k = 0.05474$

$K_P = 0.43860$

$K_{EB} = 2.4200$

$K = 0.1775$

A computer program subsititues these values in the integrated rate equation of the dual site mechanism and compares (W/F) calculated to (W/F) experimental.

$$\% \text{ deviation} = \frac{(W/F)_{exp.} - (W/F)_{cal.}}{(W/F)_{exp.}}$$

Conversion	$(W/F)_{exp.}$	$(W/F)_{cal.}$	%Deviation
0.2649	5.400	5.520	2.216
0.2780	6.170	6.057	-1.838
0.3031	7.150	7.230	1.125
0.3170	8.779	7.987	-9.022
0.3279	9.320	8.646	-7.232
0.1865	3.050	3.078	0.909
0.2357	4.430	4.476	1.043
0.1160	1.600	1.605	0.287
0.2556	5.525	5.165	-6.509
0.3469	9.80	9.965	1.681
0.3850	14.877	13.628	-8.395

Average Deviation = 2.34%